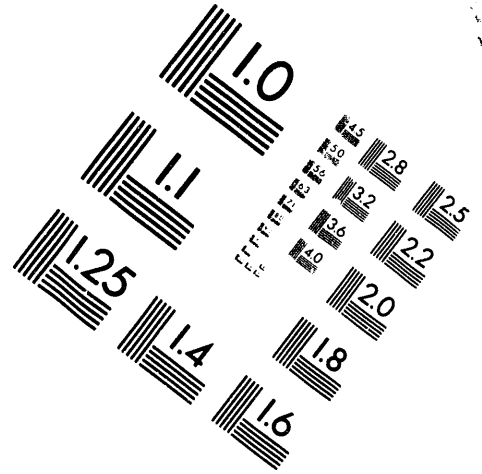
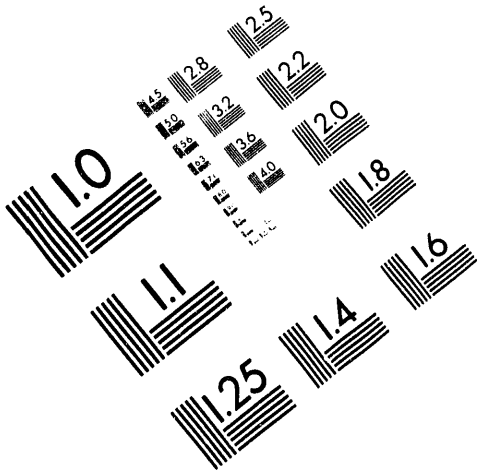




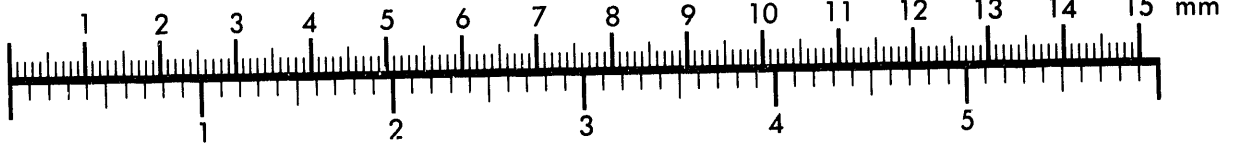
AIM

Association for Information and Image Management

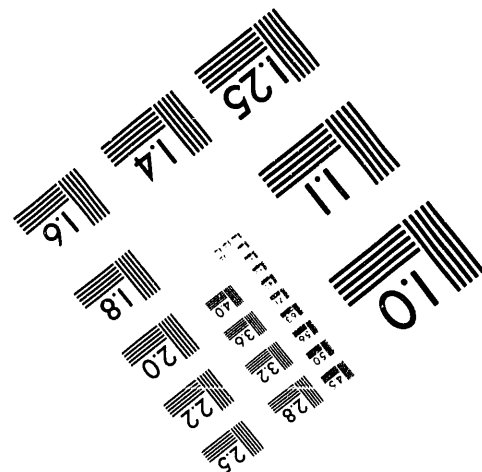
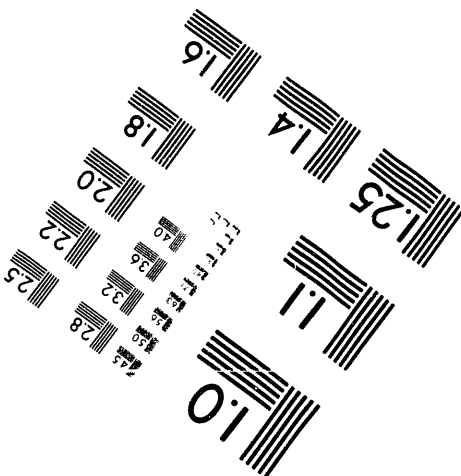
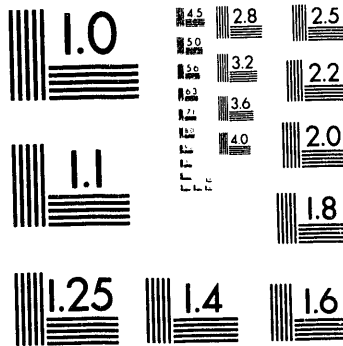
1100 Wayne Avenue, Suite 1100
Silver Spring, Maryland 20910
301/587-8202



Centimeter



Inches



MANUFACTURED TO AIM STANDARDS
BY APPLIED IMAGE, INC.

1 of 2

STRATEGY PLAN

A METHODOLOGY TO DEFINE THE FLOW RATE
AND PRESSURE REQUIREMENTS FOR TRANSFER
OF DOUBLE-SHELL TANK WASTE SLURRIES

J. A. Bamberger
L. M. Liljegren

April 1993

Prepared for
the U.S. Department of Energy
under Contract DE-AC06-76RLO 1830

Pacific Northwest Laboratory
Richland, Washington 99352

MASTER

SUMMARY

This document presents an analysis of the pressure drop and flow rate requirements for transport of double-shell tank slurries. Experiments to characterize the transport of double-shell tank slurries through piping networks and to resuspend materials that settle during pump outages are proposed. Reported values of physical properties of double-shell tank slurries were analyzed to evaluate the flow regimes that are likely to occur during transport. The results of these evaluations indicate that the slurry will be pseudohomogeneous during transport and that the slurry rheology is sufficiently non-Newtonian to affect both the pressure drop achieved during transport and the critical Reynolds number. Because existing correlations to predict the pressure drop during turbulent transport of non-Newtonian fluids have not been verified for use with double-shell tank slurries, Newtonian and non-Newtonian fluid experiments to characterize flow through smooth and corroded pipes are recommended. The non-Newtonian experiments should be performed using slurries that contain particles of a size similar to those in double-shell tank slurries and be performed in similarly sized pipes. The transport data collected in the non-Newtonian experiment will be used to determine whether a non-Newtonian correlation developed by Hanks (1978) adequately describes the experimental results.

Currently, the slurries are expected to flow in a pseudohomogeneous fashion. To verify this prediction, it is recommended that the degree of stratification be monitored. If significant stratification is detected during the non-Newtonian experiments or if later analyses of waste characteristics suggest that wastes containing larger particles will be transported in the lines, the strategy plan recommends that additional experiments be performed. These additional experiments would determine the minimum deposit velocity for settling and determine the pressure drop in stratified flows.

Analysis of waste properties indicate that double-shell slurries do not crystallize or gel permanently to form permanent solids when settled. They may, however, form cohesive masses that can be eroded by fluid action.

It is anticipated that settled solids can be flushed out with fluid flowing at a sufficiently large velocity. In addition, it is recommended that an experiment should be performed in which noncrystalizing slurries that have been allowed to settle naturally in the line are resuspended. The pressure drop required to resuspend a naturally settling plug will be compared to the pressure drop predicted on the basis of correlations determined in the standardized plug experiments. Resuspension will be visually monitored during both types of tests. If the correlations are found to correctly predict the pressure drop in the second experiment, the correlations will be considered valid and will be useful in predicting resuspension requirements in the transport lines. If the results do not agree, the proposed models of resuspension will be reevaluated on the basis of both the numerical results obtained and differences in the qualitative mechanisms observed during the two sets of experiments. If differences are identified, new experiments that incorporate these differences would be proposed.

The evaluations of the flow regime also indicate that plugging is unlikely during normal transport. However, settling and plugging are possible if pump outages occur. In these circumstances, total vertical plugs and partial horizontal plugs are expected. Plugs that occur may be either dilatant (i.e., closely packed plugs with low shear strengths but some penetration resistance) or cohesive (i.e., loosely packed but exhibiting a shear strength and low penetration resistance). The strategy plan recommends that experiments be performed to determine the pressure required to remove standardized cohesive and dilatant plugs from partial horizontal and complete vertical plugs.

CONTENTS

SUMMARY	iii
NOMENCLATURE	xi
1.0 INTRODUCTION	1.1
1.1 BACKGROUND	1.1
1.2 OBJECTIVES OF TRANSPORT AND RESUSPENSION INVESTIGATION . . .	1.4
1.3 TEST STRATEGY PLAN ORGANIZATION	1.8
2.0 CONCLUSIONS AND RECOMMENDATIONS	2.1
2.1 CONCLUSIONS	2.1
2.2 RECOMMENDATIONS	2.1
2.2.1 Transport Experiments	2.2
2.2.2 Resuspension Experiments	2.3
3.0 BACKGROUND DATA AND THEORY	3.1
3.1 SLURRY CHARACTERIZATION	3.1
3.1.1 Shear Stress Response	3.1
3.1.2 Types of Flow Patterns	3.4
3.1.3 Analyzing Slurry Flow	3.10
3.1.4 Double-Shell Tank Slurries	3.10
3.1.5 Transport of Other Wastes	3.21
3.2 NEWTONIAN FLUID FLOW	3.22
3.2.1 Energy Balance in Pipe Flows	3.22
3.2.2 Prediction of Pressure Losses for Flow of Newtonian Fluid in a Circular Pipe	3.26
3.2.3 Loss Coefficients	3.31
3.3 NON-NEWTONIAN FLUID FLOW	3.34

3.3.1	Transitional Reynolds Number for a Yield Pseudoplastic Fluid	3.40
3.3.2	Friction Factor in the Turbulent Flow of a Yield Pseudoplastic Fluid	3.42
3.3.3	Applying Hanks' Model	3.43
3.4	PLUGGING AND RESUSPENSION	3.47
3.4.1	Plugging Scenarios	3.47
3.4.2	Resuspension Scenarios	3.50
3.4.3	Resuspension of Vertical Plugs	3.53
3.4.4	Resuspension of Horizontal Partial Plugs	3.60
3.4.5	Summary of Resuspension Mechanisms	3.67
3.5	REVIEW OF TESTING TO DATE	3.67
3.5.1	Transport Experiment Review	3.67
3.5.2	Resuspension and Plugging Experiment Review	3.71
4.0	NEWTONIAN AND NON-NEWTONIAN TRANSPORT EXPERIMENTS	4.1
4.1	OBJECTIVES	4.1
4.1.1	Newtonian Flow Experiments	4.2
4.1.2	Non-Newtonian Flow Experiments	4.3
4.2	EQUIPMENT AND SIMULANT DESCRIPTION	4.4
4.2.1	Equipment Description	4.5
4.2.2	Fluids Used in Testing	4.13
4.3	TEST APPROACH	4.16
4.4	DATA ANALYSIS APPROACH	4.18
4.5	PROJECTED RESULTS	4.19
4.6	LIMITATIONS	4.21
5.0	RESUSPENSION AND PLUGGING EXPERIMENTS	5.1
5.1	OBJECTIVES	5.1

5.2	EQUIPMENT AND SIMULANT DESCRIPTION	5.1
5.3	TEST APPROACH	5.5
5.3.1	Resuspension of Standard Plugs	5.5
5.3.2	Resuspension of Naturally Settled Plugs	5.9
5.4	DATA ANALYSIS APPROACH	5.10
5.5	PROJECTED RESULTS	5.12
5.6	LIMITATIONS	5.13
6.0	PLUGGING AND LEAK DETECTION	6.1
6.1	OBJECTIVES	6.1
6.2	LEAK AND PLUG DETECTION	6.1
6.2.1	Evaluation of Methods to Detect Leaks	6.2
6.2.2	Methods Ranking	6.4
6.3	UNPLUGGING	6.4
6.3.1	Methods Evaluation	6.4
6.3.2	Methods Ranking and Limitations	6.5
6.3.3	Recommendations	6.6
7.0	REFERENCES	7.1
	APPENDIX - SAMPLE CALCULATION	A.1

FIGURES

1.1	Double-Shell Tank Waste Treatment, Storage, and Disposal Paths	1.2
1.2	Slurry Transport Flow Chart	1.7
1.3	Resuspension Flow Chart	1.9
3.1	Rheograms for Time-Independent Fluids	3.2
3.2	Viscosity Versus Shear Rate for Time-Independent Fluids	3.4
3.3	Heterogeneous Slurry Flow Patterns	3.5
3.4	Variation in Pressure Drop Versus Velocity	3.7
3.5	Flow Pattern Map	3.9
3.6	Comparison of Predictions of Minimum Transport Velocity, V_{m2} ; 0.25-mm Sand in Water at 0.01 Volume Fraction Solids	3.13
3.7a	Flow Rate Required to Achieve Symmetric Suspension in Water	3.17
3.7b	Flow Rate Required to Achieve Symmetric Suspension in Water	3.17
3.7c	Flow Rate Required to Achieve Symmetric Suspension of Particles in Tank 101-AZ Waste for 2-in. Diameter Pipe	3.18
3.7d	Flow Rate Required to Achieve Symmetric Suspension of Particles in Tank 101-AZ Waste for 3-in. Diameter Pipe	3.18
3.8	Typical Pipeline Section	3.23
3.9	Pipe Flow Developing Region	3.26
3.10	Moody Diagram	3.29
3.11	Typical Expansion Loop	3.33
3.12	Friction Factor Versus Hedstrom Number and Reynolds Number	3.37
3.13	Viscosity of the Centrifuged Supernate from DST 101-AZ	3.39
3.14	Example of Vertical Plug	3.48
3.15	Wall Shear Stress τ_0 Required to Entrain a Particle of Diameter D into the Air	3.51
3.16	Vertical Plug Resuspension Mechanisms	3.54

3.17	Mechanisms for the Erosion of Partial Plugs in Horizontal Pipes	3.61
3.18	Necessary Conditions for Turbulent Suspension	3.64
4.1	Example of Pressure Tap Installation	4.12
4.2	Predicted Newtonian Experiment Results	4.20
4.3	Predicted Non-Newtonian Experiment Results for $n_{\text{experimental}} = 0.6$	4.22
4.4	Predicted Non-Newtonian Experiment Results for $n_{\text{experimental}} = 0.9$	4.22
5.1	Pump Selection Example	5.3
5.2	Anticipated Resuspension Scenario for Plug Resuspension	5.7
6.1	Method to Locate Leak	6.3
6.2	Method to Locate Plug	6.3

TABLES

2.1	Prediction of Experimentally Determined Loss Coefficients	2.3
2.2	Resuspension of Horizontal Plugs	2.4
2.3	Resuspension of Vertical Plugs	2.5
3.1	Core Sample Properties Taken from Tank 103-AN	3.16
3.2	Some Fitting Loss Coefficients in Turbulent Flow	3.33
3.3	Hedstrom Number Range for DST Wastes and Simulants	3.38
3.4	Procedure for Applying Hanks' Model	3.44
3.5	Accuracy of the Pressure Transducers Used to Measure the Friction Factor in Fully Developed Flow of Water in 3-in. Pipe at 20 gal/min	3.69
3.6	Accuracy of the Pressure Transducers Used to Measure the Friction Factor for 80% Glycerol Flowing through a 3-in. Pipe at 89.3 gal/min	3.69
4.1	Uncertainty for Newtonian Pipe Flow Experiments	4.10
4.2	Range of Reynolds Numbers Achieved Using Proposed Newtonian Fluids	4.13
4.3	The Hedstrom Numbers and Reynolds Numbers for the Two Recommended Non-Newtonian Test Fluids	4.15
5.1	Proposed Resuspension Test Cases	5.8
5.2	Cohesive Vertical Plugs	5.14
5.3	Dilatant Vertical Plugs	5.14
5.4	Cohesive Horizontal Plugs	5.14
5.5	Dilatant Horizontal Plugs	5.14
A.1	Anticipated Accuracy for Newtonian Pipe Flow	A.5
A.2	Anticipated Accuracy in Non-Newtonian Flow	A.7
A.3	Anticipated Accuracy for the Measurement of Loss Coefficients for Elbows	A.10

NOMENCLATURE

A	area, cross-sectional area (L^2)
a	pipe radius (L), square duct height (L)
A_u	unplugged cross-sectional area of pipe (L^2)
B	coefficient empirically derived by Hanks
C_1	proportionality constant
C_b	solids volume fraction
C_t	concentration at maximum packing density
D	pipe diameter (L)
d	particle diameter (L)
D_H	hydraulic diameter (L)
dP	pressure drop (M/LT^2), pressure exerted across plug (M/LT^2)
dP_{ent}	excess pressure drop caused by flow development and turbulent friction at pipe entrance (M/LT^2)
dP_{err}	differential pressure transducer measurement accuracy
dP_{excess}	excess pressure drop caused by flow development and turbulent friction (M/LT^2)
$\left. \frac{dP}{H} \right _{measured}$	pressure gradient exerted on plug
dP_{loss}	irreversible pressure loss due to friction (M/LT^2)
$\left. \frac{dP}{dx} \right _{loss}$	irreversible pressure gradient (M/L^2T^2)
DSS	double-shell tank slurry
DST	double-shell tank
dV/dr	shear rate in r direction (T^{-1})
dV/dy	shear rate in y direction (T^{-1})
F	force (ML/T^2)
f	Darcy friction factor
f_c	friction factor at critical Reynolds number
g	acceleration of gravity (L/T^2)
g_c	gravity acceleration constant (ML/T^2)
H	height of plug (L)
h_b	depth of solids bed (L)
He	Hedstrom number $(\rho D^2/\tau_y)(\tau_y/K)^{2/n}$
h_u	height of unplugged portion of duct (L)

HWVP	Hanford Waste Vitrification Plant
K	consistency index ($M/L T^{2-n}$), loss coefficient
K1,K2,K3	constants of unknown value of order one
k	Von Karman's constant used to predict mixing length
L	mixing length, pipe length (L)
m	mass flow rate (M/T)
n	flow behavior index
N_b	bulk resuspension parameter
NCAW	neutralized current acid waste
NCRW	neutralized cladding removal waste
N_e	erosion resuspension parameter
N_g	gravitational resuspension parameter
N_s	settling velocity parameter
N_{te}	turbulent eddy erosion parameter
N_y	yield resuspension parameter
P	pressure (M/LT^2)
P_B	normal dispersive "Bagnold" force at bed surface
PUREX	plutonium and uranium extraction
Q	volumetric flow rate (L^3/T)
R	dimensionless parameter used to apply Hanks' model [Equation (3.37)]
R_c	critical Reynolds number
Re	Reynolds number, $\rho VD/\mu$
Re_c	critical Reynolds number at transition from laminar to turbulent flow
Re_{m1}	Reynolds number for the transition from asymmetric to symmetric suspension
Re_{m2}	Reynolds number at V_{m2}
Re_p	pseudoplastic Reynolds number
rms	root mean square
s	density ratio, ρ_s/ρ_1
u^*	friction velocity (L/T)
V	fluid velocity (L/T)
\bar{V}	bulk mean velocity (L/T)
v'	characteristic velocity fluctuation that is on the order of the friction velocity u^* near the bed wall (L/T)
V_m	mixture velocity (L/T)

V_{m1}	transition velocity between symmetric and asymmetric slurry suspension (L/T)
V_{m2}	critical deposit velocity (L/T)
V_{m3}	velocity between stationary and moving bed (L/T)
V_{m4}	lower bound for stationary bed motion (L/T)
V_{mu}	velocity in unplugged portion of the pipe (L/T)
V_s	particle settling velocity (L/T)
Z	elevation of the pipe section (L)

Greek Letters

α	dynamic friction coefficient for bed, kinetic energy flux coefficient
ϵ	pipe roughness (L)
ϵ/D	pipe relative roughness
η	dimensionless shear rate
λ	dimensionless mixing length
μ	viscosity (M/LT)
μ_m	mixture viscosity (M/LT)
μ_a	apparent viscosity (M/LT)
ν	kinematic viscosity (L ² /T)
ξ	dimensionless pipe radius
ξ_o	unsheared dimensionless pipe radius
ξ_{oc}	unsheared dimensionless pipe radius at critical Reynolds number
ρ	mixture density, fluid density (M/L ³)
ρ_m	mixture density (M/L ³)
ρ_l	liquid density (M/L ³)
ρ_s	slurry or solids density (M/L ³)
σ	average distance between particle surfaces (L)
τ	shear stress (M/LT ²)
τ_b	shear stress on bed (M/LT ²)
τ_s	shear stress of plug (M/LT ²)
τ_w	shear stress at fluid surface (M/LT ²)
τ_y	yield stress (M/LT ²)
ψ	function defined in Equation (3.31)
ϕ	turbulence damping function, function depending on bed solids concentration f(s)

1.0 INTRODUCTION

1.1 BACKGROUND

Double-shell tanks (DSTs) at Hanford are used to store liquid and sludge wastes (transuranic, high-level, and low-level). These wastes will be retrieved and processed into immobile waste forms that will be suitable for disposal. A flow diagram outlining proposed treatment strategies is presented in Figure 1.1. Double-shell tank wastes originate from varying sources including the single-shell tanks, the canyon reprocessing facility analytical laboratories, and decontamination operations. The evaporator facility is used to control double-shell tank waste volume. Double-shell tank wastes are processed in the waste pretreatment facility where they are separated into high level and low level waste fractions and returned to double-shell tanks. The low level waste is processed in the grout treatment facility; the high level waste is to be processed in the Hanford Waste Vitrification Plant.

The waste treatment strategies can only be performed safely by ensuring that the pressure drop that occurs during transport is limited to a safe level and by minimizing the probability of plugging of the line. In the event of pump failure, some degree of settling is expected; therefore, methods of resuspension must be identified. Thus, proper design requires the ability to predict the pressure losses that occur during transport of waste and the degree of settling that may occur during transport. In addition, accurate predictions of the pressure and flow rates required to resuspend material that settles during pump outages is needed to properly size the pumps in the transport lines.

The waste chemical and physical properties of the seven waste types vary considerably. Current plans call for transporting two distinct waste types; these are cladding removal waste, from N-Reactor fuel, and current acid waste, from the plutonium and uranium extraction (PUREX) process. Both wastes are neutralized with sodium hydroxide during processing prior to storage in the double-shell tanks. In addition, waste treatment plans require that pretreated wastes be transported in pipes when they are returned to the double-shell

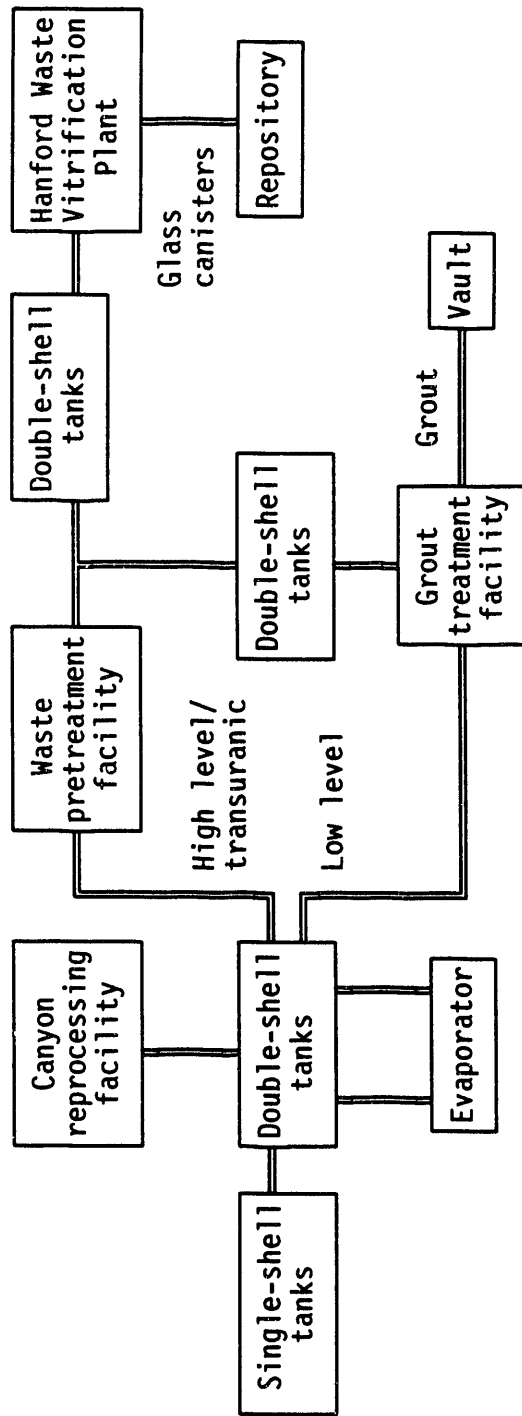


FIGURE 1.1. Double-Shell Tank Waste Treatment, Storage, and Disposal Paths

tanks. Rheological information describing the characteristics of both untreated and pretreated wastes is required for proper design of the transport lines. Some information on the rheology of untreated neutralized current acid waste (NCAW) and neutralized cladding removal waste (NCRW) is available; the rheology of the pretreated wastes is not yet known.

Laboratory studies have been conducted to characterize the physical and chemical properties of actual wastes and waste simulants. In May 1986, Scheele and McCarthy compared the properties of waste from double-shell tank 105-AW with NCRW simulant. Both the waste and the simulant were yield pseudoplastic; however, the actual waste properties of yield stress (9.6 Pa versus 0.0363 Pa) and viscosity (176 cP versus 2.1 cP) were much higher than those of the simulant. In September 1986 Fow, Scheele, McCarthy, Thornton, Heath, and Scott characterized waste from double-shell tank 103-SY. Each of the waste samples were evaluated at two temperatures and at two concentrations (as taken from the tank and at a 1:1 dilution with water). All waste samples were termed non-Newtonian; one was characterized as yield pseudoplastic; the other samples were classified as pseudoplastic or dilatant. Fow et al.'s information was used to recommend the level of dilution required to reduce the apparent viscosity to a level that would allow the slurry to be pumped without excess pressure drop and to predict the critical Reynolds number for transition to turbulence. In 1986 Scheele and McCarthy recommended that the slurries be transported in the turbulent regime to reduce the likelihood of settling.

Although only limited measurements of double-shell tank wastes have been made, the data show that the undiluted waste is non-Newtonian and can contain significant quantities of solids. In addition, the waste properties vary considerably from tank to tank. Furthermore, there is some evidence that slurries containing washed solids exhibit non-Newtonian behavior, as noted by Peterson, Scheele and Tingey in 1989 at concentrations where those containing untreated solids do not, as noted by Gray, Peterson, Scheele, and Tingey in 1990.

Liquid and sludge waste in double-shell tanks will be retrieved and transferred to existing or new facilities before the wastes are solidified. Retrieval and transport may involve transferring slurries up to 7 miles, if

transfer occurs between tank farms. In addition to transport, resuspending the waste must be considered because slurry transfer pump outages may occur as a part of routine operation. When pumping is stopped, the particulate in the slurry may settle, changing the slurry from pseudohomogeneous to heterogenous. With no flow, plugging of the pipeline may occur. Pumps must be sized to allow resuspension of the slurry without appreciable particulate loss in pipeline components. In 1988 Peterson and Powell investigated slurry transport and resuspension with inconclusive results. As a consequence, this strategy plan is being developed to provide closure to the issue of slurry transport and resuspension.

1.2 OBJECTIVES OF TRANSPORT AND RESUSPENSION INVESTIGATION

The objectives of this analysis, being performed by Pacific Northwest Laboratory^(a) are to 1) determine whether the pressure drop during transport of double-shell tank slurries can be predicted on the basis of currently available information, 2) to evaluate the likelihood of settling during normal transport, and 3) to determine whether the pressure drop and flow rate required to resuspend settled solids could be predicted using available correlations. These objectives were achieved by 1) examining the plans for transport of double-shell tank slurries, 2) obtaining information describing the physical and rheological properties of the wastes, 3) evaluating the degree of stratification that is likely during normal operation on the basis of published correlations, 4) evaluating the importance of non-Newtonian rheology of the waste, and 5) evaluating published theories of resuspension to determine their applicability to the current problem.

Analyses to date indicate that

1. Some slurries are non-Newtonian; others are not. The pressure losses that occur during the transport of Newtonian slurries can be predicted using the Moody diagram. Correlations for the pressure drop in non-Newtonian slurries have been proposed (Hanks 1978) but have not been shown to be applicable to all fluids. Thus, the correlations for the

(a) Operated for the U.S. Department of Energy by Battelle Memorial Institute under Contract DE-AC06-76RLO 1830.

friction factor in non-Newtonian fluids must either be verified or developed experimentally.

2. Minimal diameter stratification is expected when untreated NCAW or NCRW slurries are transported at flow rates between 65 and 100 gpm through 2-in. and 3-in. pipes. The degree of stratification expected when slurries containing washed or pretreated slurries are transported was not analyzed because the size and density information for these particles is not available. Preliminary information from Gray, Peterson, Scheele, and Tingey in 1990 suggests that washed solids exhibit greater settling velocities than unwashed solids and would be more highly stratified during transport.
3. Information describing the pressure drop and flow rate required to resuspend small cohesive particles that form plugs does not exist. Information describing resuspension of noncohesive particles that form dilatant plugs exists; however, it has been collected using much larger particles than those of interest. Consequently, these results cannot be applied with confidence to the current problem. A strategy plan for future work has been developed to provide the information required for design of the transport lines.

The objective of the transport and resuspension strategy plan is to provide a concise methodology to guide the analytical, computational, and experimental efforts being proposed to bound the issues of Newtonian and non-Newtonian slurry transport and slurry resuspension applicable to double-shell tank waste. The strategy plan methodology balances the need for analytical, computational, and experimental research with the end result. Realizing that subsequent research is based on initial plan results, a critical path based on the most probable outcome of the prior steps is outlined. Decision points and rational for making the decisions are included with these analyses.

This transport and resuspension research plan has been designed to provide the types of information required by Westinghouse Hanford to permit them to develop a pipeline design and pipeline operating strategy to ensure that successful pipeline operation can be conducted. The research objectives are 1) to provide data required for operation of waste transfer piping systems during continuous waste transport and during resuspension after an outage; 2) to recommend whether or not existing correlations fit the data; and 3) to provide methods to detect formation of flow blockages and leaks.

These objectives will be met through a series of analytical, computational, and experimental investigations using Newtonian and non-

Newtonian fluids. Both Newtonian and non-Newtonian experiments are proposed to investigate slurry transport. The flow chart defining the experimental investigation is shown in Figure 1.2.

The scope of the Newtonian fluid experiments is based on using two fluids to

- determine friction factors and loss coefficients for specified loop components in laminar through turbulent flow regimes
- produce an estimate of pipe roughness factor, ϵ/D , for 2-in. diameter and 3-in. diameter smooth (new) and corroded (old) pipe in laminar through turbulent flow regimes.

The Newtonian data will be used to confirm system operation by comparison of data from components already well characterized with literature values for two pipe relative roughness values and to provide additional Newtonian data at two pipe relative roughness values for friction factor versus Reynolds number and Hedstrom number correlation. Hanks' model does not account for variations in pipe relative roughness. By providing data at two pipe relative roughness values the effect of this parameter can be observed.

The scope of the non-Newtonian fluid experiments based on using two fluids is to

- determine friction factors and loss coefficients for specified loop components in laminar through turbulent range
- determine maximum and minimum acceptable operating flow rates for transporting waste, based on planned operating conditions
- compare experimental data with that predicted by Hanks' model to evaluate whether the Hanks model (1978) adequately represents our data at the specified pipe relative roughness.

Hanks' model predicts critical Reynolds number and friction factor in turbulent region for pseudohomogeneous fluids. If the non-Newtonian data in the laminar regime agrees with Govier and Aziz's (1972) correlation, the simulant can be described by a pseudohomogeneous model, and it is expected that turbulent flow regimes and Hanks' model should apply in turbulent flow. If Hanks' model does not agree with the data collected in turbulent flow, then

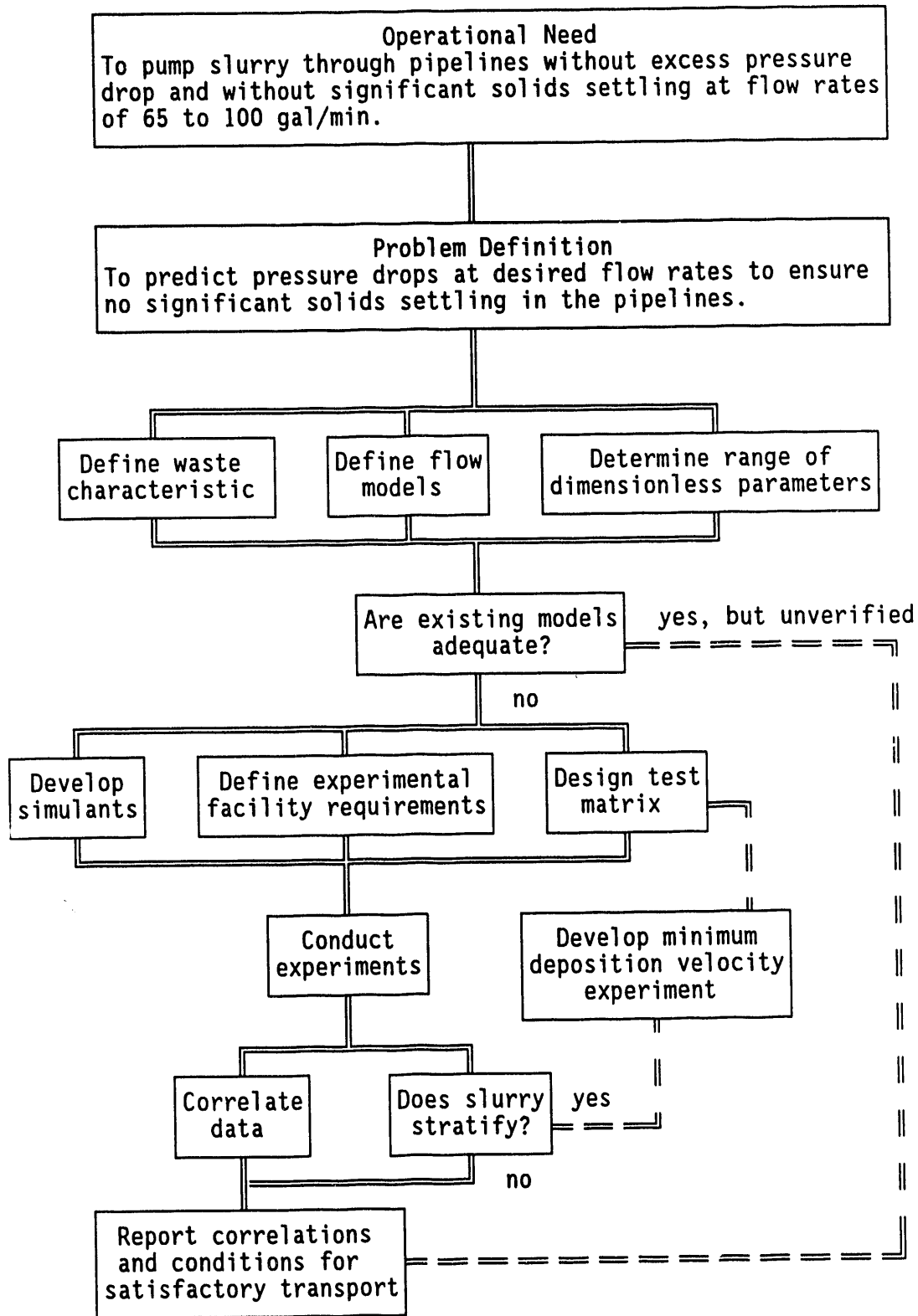


FIGURE 1.2. Slurry Transport Flow Chart

changing the coefficient term B would be investigated. If this change is not adequate, applying another pseudohomogeneous model would be recommended.

If the data in the laminar region does not agree with the laminar flow correlation that appears in Govier and Aziz (1972), then the simulant is not pseudohomogeneous in the laminar regime. Therefore, one would not necessarily expect Hanks' model to apply in the turbulent regime. However, because of the enhanced ability of fluid to resuspend particles in the turbulent regime, it is possible the simulant behavior may have changed to pseudohomogeneous and Hanks' model could still apply or be modified as specified above. If the turbulent data does not fit a pseudohomogeneous model and stratification is detected, a heterogeneous flow model would be recommended.

Only non-Newtonian experiments are recommended to investigate resuspension. The scope of the resuspension experiments is to

- investigate the applicability of resuspension mechanisms to quantify excess pressure required for resuspension
- determine the flow rates and the excess pressures required to resuspend standardized cohesive and dilatant horizontal (partial) and vertical (full) plugs
- propose methods to identify the occurrence of settling and plugging in real time and to locate the region in which settling or plugging has occurred.

The flow chart defining the resuspension investigation is presented in Figure 1.3.

1.3 TEST STRATEGY PLAN ORGANIZATION

This strategy plan is organized to present the results of this analysis; also it is organized as if it were the final report which results from conducting the analyses, computer modeling, and experimentation outlined in the strategy plan to address the experiment objectives. This type of presentation fulfills two separate goals. First it structures the strategy plan to present a logical concise argument for each step of evaluation and to postulate anticipated results. Second it provides results and correlations in the predicted final format. This method of presentation will enable

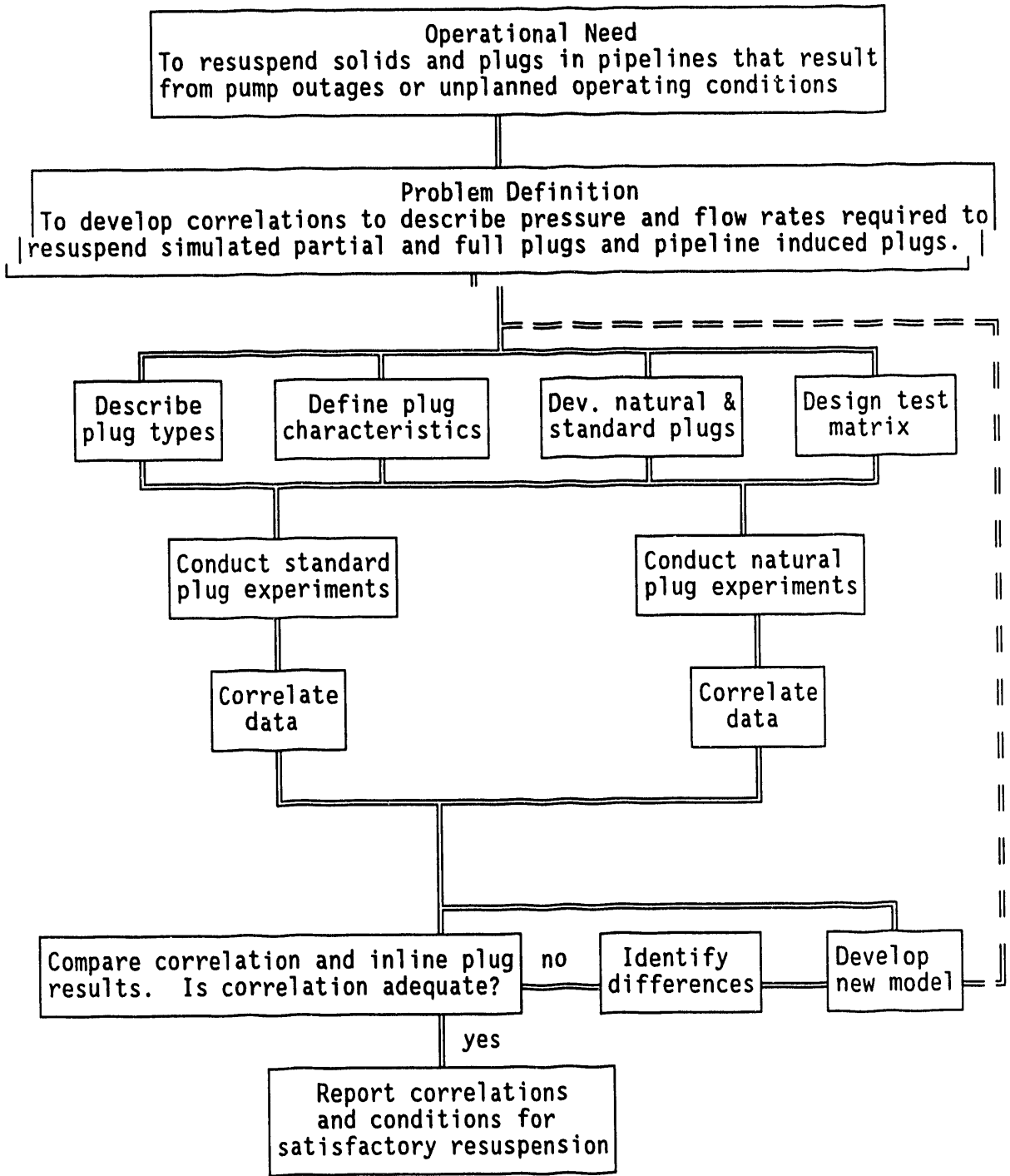


FIGURE 1.3. Resuspension Flow Chart

Westinghouse Hanford to evaluate the type of information to be received and to assess the information's usefulness to process applications.

The strategy plan critical path includes three experimental activities and one instrumentation development activity. These activities are 1) a Newtonian pressure drop experiment (Figure 1.2), 2) a non-Newtonian pressure drop experiment (Figure 1.2), 3) a resuspension experiment (Figure 1.3), and 4) a literature search of experimental methods and instrumentation to detect settling and plugging. Anticipated conclusions and recommendations resulting from these activities are listed in Section 2.0. In Section 3.0 background data from past activities at Hanford and transport and resuspension theory and correlations presented in the literature are analyzed to provide the background required to describe slurry transport. In Sections 4.0 through 6.0, each of the activities is defined including analysis objectives, equipment description, test approach, data analysis approach, and projected results and limitations. Sensitivity analyses for the experimental activities are summarized in the Appendix.

2.0 CONCLUSIONS AND RECOMMENDATIONS

Double-shell tank waste transfer activities were investigated analytically. Based on the analyses, it is proposed that two double-shell tank waste transfer activities be investigated experimentally: transport of Newtonian and non-Newtonian fluids through pipeline components and resuspension of solids settled in horizontal and vertical pipeline sections. Conclusions from the analytical investigations are listed in Section 2.1. Recommendations for transport and resuspension experiments and anticipated experimental results are listed in Section 2.2.

2.1 CONCLUSIONS

The results of this analytical investigation indicate that:

- Some double-shell tank wastes exhibit significant degrees of non-Newtonian behavior that will affect the pressure drop achieved during transport.
- Correlations to predict pressure drop in non-Newtonian fluids have been proposed but have not been shown to be applicable to all fluids. Thus, correlations for the friction factor in non-Newtonian fluids must be verified.
- Negligible stratification is expected during normal transport of double-shell tank wastes; this suggests that plugging is unlikely during normal transport.
- There is a need to predict the pumping requirements to unplug lines if solids settle as a result of pump outages.

2.2 RECOMMENDATIONS(a)

As a result of the analytic investigations, two types of experiments are proposed to investigate Newtonian and non-Newtonian slurry transport and to investigate slurry resuspension. From the analytic investigations, predictions of the types and magnitudes of anticipated experimental results and their uncertainty intervals are estimated.

-
- (a) This document is a strategy plan. The results presented under recommendations are those predicted analytically prior to conducting the actual experiments. All uncertainty intervals reported in this strategy plan represent the expected resolution of the measurement rather than the expected range in which the measured value will fall.

2.2.1 Transport Experiments

Transport experiments are recommended to be conducted with Newtonian fluids to verify system operation and to characterize pipe roughness.

- Experiments are proposed in the laminar and turbulent Reynolds number regimes to characterize flow through smooth pipes. The friction factor versus Reynolds number data will match the Moody diagram predictions for some value of relative roughness with a root mean square (rms) deviation of less than $\pm 8\%$.
- Experiments are proposed in the laminar and turbulent Reynolds number regimes to characterize the average pipe relative roughness. The average relative roughnesses (ϵ/D) for the 2-in. diameter smooth and corroded pipes and the 3-in. diameter smooth and corroded pipes are predicted to be $0.09\% \pm 8\%$, $2.4\% \pm 8\%$, $0.06\% \pm 8\%$, and $1.6\% \pm 8\%$, respectively. The corresponding equivalent roughness would be 0.00015 ft for the smooth pipe and 0.004 ft for the corroded pipe.
- Predictions of the loss coefficients calculated for the pipeline components in the turbulent flow regime are listed in Table 2.1. The loss coefficient uncertainty intervals are anticipated to be $\pm 8\%$.

Upon successful completion of the Newtonian fluid experiments, non-Newtonian fluid experiments are recommended to be conducted to determine friction factor (f), Hedstrom number (He), Reynolds number (Re), and flow behavior index (n) relationships, and to determine whether Hanks' model adequately represents the non-Newtonian data.

- Non-Newtonian fluid experiments are recommended to be conducted with the smooth 2-in. and 3-in. diameter pipe in the laminar and turbulent Reynolds number regimes to determine pressure losses within the pipe. The data should show that Hanks' model can be used to represent this data within $\pm 10\%$.
- Non-Newtonian fluid experiments are recommended to be conducted with the corroded 2-in. and 3-in. diameter pipe in the laminar and turbulent Reynolds number regimes to determine pressure losses within the pipe. The data should show that Hanks' model does not represent this data within $\pm 10\%$ because Hanks' model does not account for pipe roughness effects.
- Based on the anticipated results listed above, Hanks' model should be applicable for only smooth pipe data and should be extrapolated to apply to corroded pipe only with extreme caution.
- It is anticipated that Hanks' theory would not be reliable to use for predicting the critical Reynolds number within $\pm 20\%$.

TABLE 2.1. Prediction of Experimentally Determined Loss Coefficients

<u>Loop Component</u>	<u>Loss Coefficient</u> $K = dP / (1/2 \rho V^2)$	
	<u>Newtonian</u>	<u>non-Newtonian</u>
Expansion loop	10 \pm 5%	20 \pm 10%
Pipe jumper	5 \pm 5%	10 \pm 10%
Elbow	0.9 \pm 5%	1.1 \pm 10%
Pittsburgh brass ball valve	5 \pm 5%	10 \pm 10%
PUREX connector configuration	10 \pm 5%	15 \pm 10%

- The anticipated loss coefficients calculated for the pipe components in the turbulent flow regime are listed in Table 2.1. The loss coefficient uncertainty intervals are anticipated to be \pm 10%.

2.2.2 Resuspension Experiments

It is recommended that resuspension experiments be conducted with two non-Newtonian slurries to determine the excess pressure required to dislodge horizontal and vertical cohesive and dilatant plugs. Estimates of these anticipated pressures are summarized in Tables 2.2 and 2.3.

TABLE 2.2. Resuspension of Horizontal Plugs

N_e , Erosion Parameter		
<u>Plug Characteristics</u>	<u>$N_e = f \rho v^2 / 8 \tau_s$</u>	<u>$dP/L)_{\text{measured}} = 8 N_e \tau_s / 2 D$</u>
Cohesive 1 ($\tau = 1.5$ kPa)	1.2 $\pm 10\%$	95 kPa/m $\pm 15\%$
	1.1 $\pm 10\%$	83 kPa/m $\pm 15\%$
Cohesive 2 ($\tau = 4$ kPa)	1.3 $\pm 10\%$	240 kPa/m $\pm 15\%$
	1.2 $\pm 10\%$	257 kPa/m $\pm 15\%$
N_{te} , Turbulent Eddy Erosion Parameter		
	<u>$N_{te} = f v^2 / 8 v_s^2$</u>	<u>$dP/L)_{\text{measured}} = 8 N_{te} v_s^2 \rho / 2 D$</u>
Dilatant 1 ($d = 8 \mu\text{m}$)	1.1 $\pm 15\%$	0.12 Pa/m $\pm 15\%$
	1.3 $\pm 15\%$	0.13 Pa/m $\pm 15\%$
Dilatant 2 ($d = 60 \mu\text{m}$)	1.2 $\pm 15\%$	12 Pa/m $\pm 15\%$
	1.1 $\pm 15\%$	12 Pa/m $\pm 15\%$

TABLE 2.3. Resuspension of Vertical Plugs

<u>Plug Characteristics</u>	<u>N_g, Gravitational Parameter</u>	
	<u>$N_g = dP/C_b(s - 1)\rho g H$</u>	<u>dP/H)_{measured}</u>
Dilatant 1	1.5 ±10%	15 kPa/m ±10%
	1.4 ±10%	14 kPa/m ±10%
Dilatant 2	1.6 ±10%	16 kPa/m ±10%
	1.7 ±10%	17 kPa/m ±10%
	<u>N_s, Settling Parameter</u>	
	<u>$N_s = V/V_s$</u>	<u>dP/H)^(a)_{measured}</u>
Cohesive 1	1.5 ±10%	To be determined
	1.5 ±10%	To be determined
Cohesive 2	1.6 ±10%	To be determined
	1.4 ±10%	To be determined

(a) Pressure cannot be estimated at this date. It requires a better estimate of the plug properties than is currently possible. The value would be less than those seen for dilatant plugs.

3.0 BACKGROUND DATA AND THEORY

In this section, literature, theory, experimental data, and correlations are analyzed. Slurry characteristics are defined in Section 3.1. In Sections 3.2 and 3.3 the factors that lead to pressure changes in the flow of single-phase Newtonian and two-phase non-Newtonian slurry flows and engineering methods to predict pressure changes in both types of pipe flows are described. Resuspension mechanisms are discussed in Section 3.4 and prior experimental efforts are analyzed in Section 3.5.

3.1 SLURRY CHARACTERIZATION

Slurries can be characterized by their response to shear stress and by their flow patterns. Physical properties of double-shell tank slurries and simulants are analyzed to characterize their rheology and flow patterns under a range of transport conditions.

3.1.1 Shear Stress Response

Fluids are classified according to their response to shear stresses. A shear stress is defined as:

$$\tau = \frac{F}{A} \quad (3.1)$$

where τ = shear stress (M/LT²)
F = force (ML/T²)
A = area (L²).

For Newtonian fluids in laminar flow:

$$\tau = \mu \left(\frac{dV}{dr} \right) \quad (3.2)$$

where μ = viscosity (M/LT)
 dV/dr = shear rate in r direction (T⁻¹).

The viscosity, μ , is a proportionality constant that is independent of shear rate and is affected only by pressure and temperature for a Newtonian fluid. A plot of shear stress versus rate of shear in the laminar flow regime is known as a rheogram (Figure 3.1). The slope of the curve is constant for a Newtonian fluid.

All fluids that display rheograms that are not linear through the origin are considered to be non-Newtonian. Non-Newtonian fluids are usually classified as time-independent, time-dependent, or viscoelastic fluids.

The rheological behavior of a yield pseudoplastic fluid can be represented by the following equation:

$$\tau = \tau_y + K \left(\frac{dV}{dy}\right)^n \quad (3.3)$$

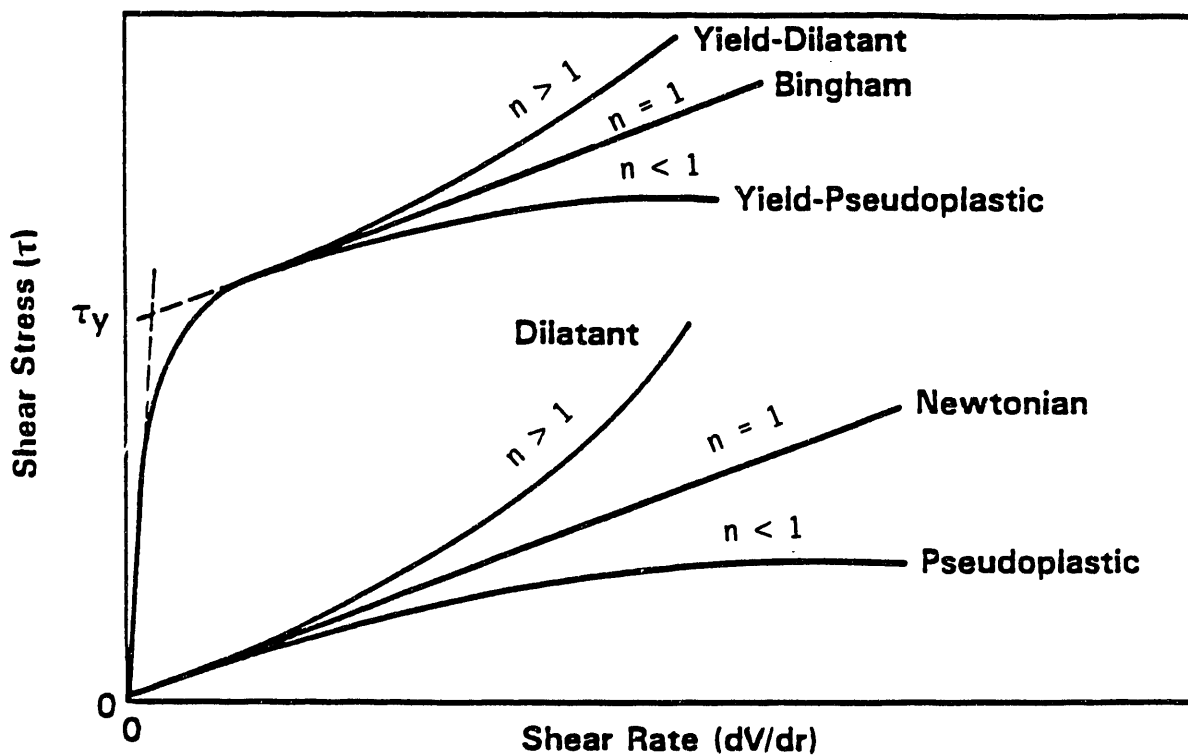


FIGURE 3.1. Rheograms for Time-Independent Fluids

where K = consistency index (M/L T²⁻ⁿ)
 dV/dy = shear rate in y direction (T⁻¹)
 n = flow behavior index.

The yield-power law model defined by Equation (3.3) reduces to the Bingham plastic model when $n = 1$, the power law model when $\tau_y = 0$, and the Newtonian model when $\tau_y = 0$ and $n = 1$.

Because the bulk of the available mixing data is based on Newtonian fluids, it is convenient to define an apparent viscosity, μ_a , as follows:

$$\mu_a = \frac{\tau}{\left(\frac{dV}{dy}\right)} = \frac{\tau_y + K \left(\frac{dV}{dy}\right)^n}{\left(\frac{dV}{dy}\right)} \quad (3.4)$$

The apparent viscosity for non-Newtonian fluids is a function of the shear rate.

Rheograms for classical time-independent, non-Newtonian fluids are shown in Figure 3.1. The relationship between apparent viscosity and shear rate for these fluids is described by Figure 3.2. The "apparent viscosity" of a non-Newtonian fluid is a function of shear rate but otherwise can be considered analogous to the Newtonian viscosity for Newtonian fluids.

Non-Newtonian fluids are typically classified as fluids with yield stresses, τ_y , and fluids without yield stresses. These classifications are further defined as fluids that decrease in viscosity with increasing applied shear rate (pseudoplastic or yield pseudoplastic, if the slurry has a yield stress), and fluids that increase in viscosity with increasing applied shear rate (dilatant or yield dilatant).

Fluids with flow behavior indices greater than one have stress versus strain-rate curves that are "concave upward", as seen in Figure 3.1. Fluids that exhibit this concave upward trend are said to be dilatant. Fluids with flow behavior indices less than one have stress versus strain rate curves that are "concave downward", as seen in Figure 3.1. Fluids that exhibit this concave downward trend are said to be pseudoplastic.

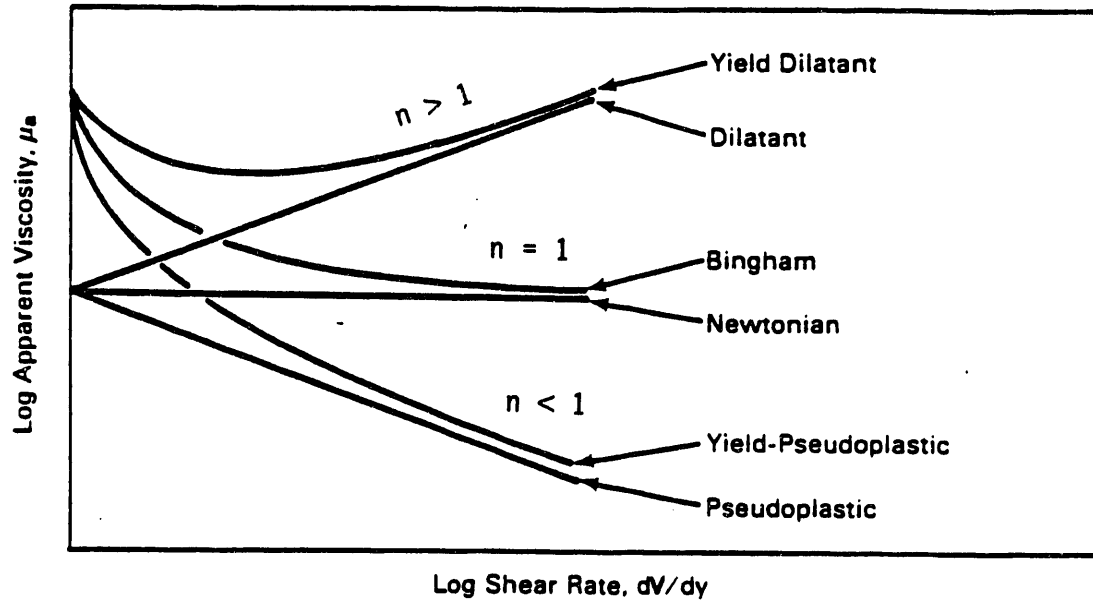


FIGURE 3.2. Viscosity Versus Shear Rate for Time-Independent Fluids

Slurries containing particles that are capable of close packing, such as sands, often exhibit dilatant characteristics at some concentration of solids. These types of fluids generally settle in a close pack configuration and the settled solids do not generally exhibit cohesive behavior. In contrast, slurries containing colloidal particles, such as clay, often exhibit pseudoplastic behaviors. These slurries frequently exhibit gelling and high shear strengths. When allowed to settle, these slurries often form extremely loose packed beds with high water content. It is possible for these loose packed beds to be highly rigid despite the low solids content. The settled solids from these materials are often termed "cohesive".

3.1.2 Types of Flow Patterns

The flow behavior of mixtures containing both solid and liquid constituents, referred to as slurries, is more complicated than that of single-phase mixtures. Factors that may affect slurry behavior significantly and that must be considered in selecting appropriate methods of flow analyses include the size, shape, and mass of the particles, and the relative concentration of the solids. All of these factors can affect the degree of

suspension of particles in the fluid and the velocity difference between the particle and liquid phases. Because the degree of suspension strongly affects the total pressure drop in the flow, factors affecting the degree of suspension will be discussed here.

Slurries containing large or dense particles are often observed to stratify, leading to the existence of a bed of solid particles in the lower region of the pipe, as shown in Figure 3.3. Slurries in which the solids are unevenly distributed, such as those in which a bed of particles forms in the lower portion of a horizontal pipe, exhibit pressure loss characteristics that differ from slurries in which particles are uniformly distributed throughout the pipe. The exact degree of suspension is affected by particle size, but is also strongly affected by the degree of turbulence in the fluid, the relative densities of the liquid and solid, the concentration of solids in the slurry, and the mean fluid velocity. Early attempts to classify slurry flows focused on particle size only. This is somewhat simplistic, but resulted

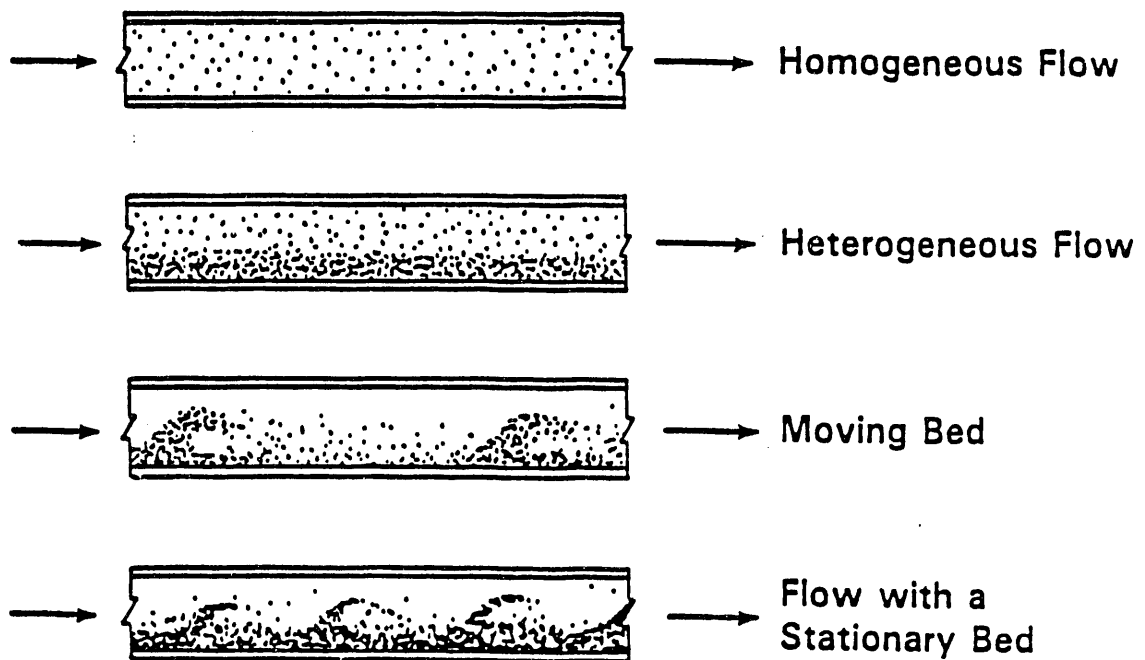


FIGURE 3.3. Heterogeneous Slurry Flow Patterns

in some general rules based on size classification for the degree of suspension achieved in typical industrial designs (Govier and Aziz 1972). These classifications are:

1. Ultrafine particles. Particles with diameters less than $10\ \mu\text{m}$ are almost always fully suspended when solid/liquid slurries are transported in industrial settings. Gravitational effects are negligible and do not lead to stratification of the solids (see homogeneous flow in Figure 3.3).
2. Fine particles. Particles with diameters between $10\ \mu\text{m}$ and $100\ \mu\text{m}$ are fully suspended in most industrial transport lines. However, the effect of gravity is sufficiently great to cause concentration gradients. The magnitude of these concentration gradients depends on the ability of the fluid to lift and distribute the particles. In general, concentration gradients are smaller in high velocity turbulent flows than in low velocity laminar flows (see heterogeneous flow in Figure 3.3).
3. Medium-sized particles. Particles with diameters larger than $100\ \mu\text{m}$ but less than $1000\ \mu\text{m}$ require high velocities for full suspension. At low velocities they will form a moving bed of particles (see moving bed in Figure 3.3).
4. Coarse and ultracoarse particles. Particles with diameters larger than $1000\ \mu\text{m}$ but less than $10,000\ \mu\text{m}$ are seldom suspended in the normal operating range of industrial pipe flows. These particles generally form a bed in the lower portion of the pipe. Particles larger in diameter than $10,000\ \mu\text{m}$ are almost never suspended at normal industrial velocities. These particles may be transported in the form of a sliding bed at the bottom of a pipe (see stationary bed in Figure 3.3).

Analyses of double-shell tank slurries (DSS) indicate that most particles in the slurries fall in the fine and ultrafine range. A small fraction of the particles may be medium-sized; occasional coarse particles may also be present. In May 1986, while characterizing zirflex decladding sludge, Scheele and McCarthy reported the average diameter of solid particles in actual NCRW to be $8.65\ \mu\text{m}$; the maximum diameter was $47\ \mu\text{m}$. The presence of high concentrations of small particles is often sufficient to cause suspension of small numbers of medium and coarse particles; thus, techniques used to analyze the motion of slurries containing fine and ultrafine particles are expected to be applicable to double-shell tank slurries.

As previously described, ultrafine particles are uniformly suspended throughout the fluid in almost any flow situation of industrial significance.

However, the degree of suspension of fine and medium-sized particles may vary and is strongly affected by the flow velocity, turbulence, and concentration of particles. When the mean solids loading is sufficient to allow bed formation, the pressure drop versus mixture velocity will vary, as shown in Figure 3.4. The mixture velocity in the figure is defined such that

$$\dot{m} = \rho_m V_m A \quad (3.5)$$

where \dot{m} = the mass flow rate of slurry (M/T)
 ρ_m = the mixture density (M/L³)
 V_m = mixture velocity (L/T)
 A = unblocked pipe area (L²).

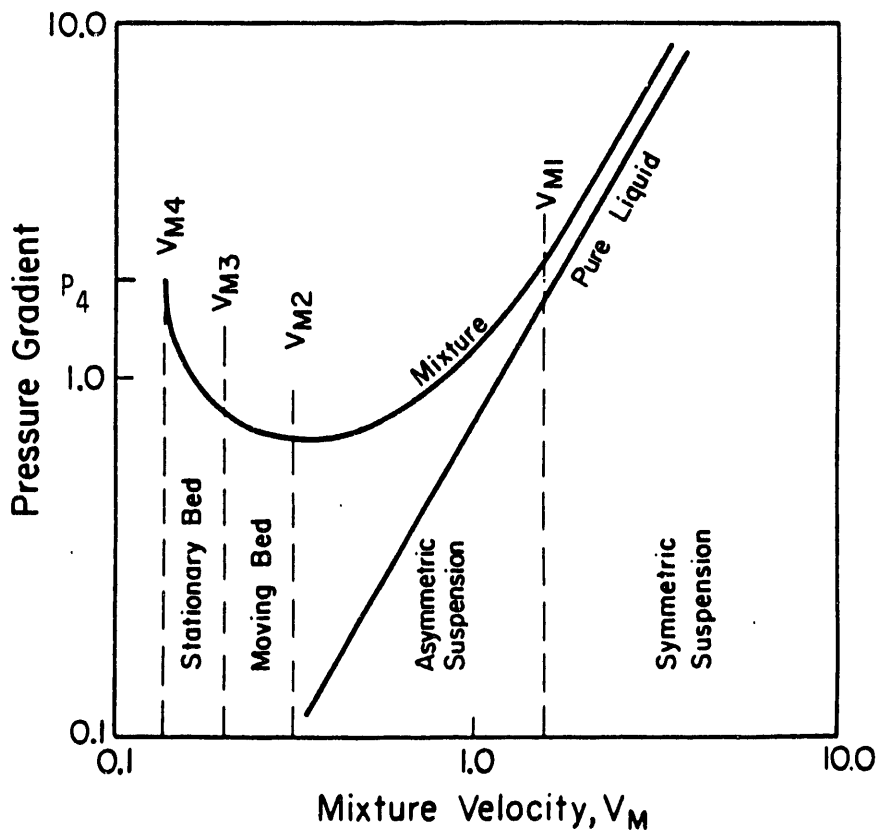


FIGURE 3.4. Variation in Pressure Drop Versus Velocity

A slurry containing fine or medium-sized particles may exhibit the following flow patterns:

1. Fully suspended, symmetrically distributed particle phase. At sufficiently high velocities, the random forces exerted by the fluid on the particles may lift the particles against gravity. The particle concentration will cease to vary with elevation in the pipe, but may vary with pipe radius. $V \geq V_{m1}$ in Figure 3.4 (see homogeneous flow in Figure 3.3).
2. Fully suspended, asymmetrically distributed particle phase. As velocity decreases, turbulence forces and other fluid forces are insufficient to completely overcome the effects of gravity. Particles may still be completely suspended, but higher concentrations of particles will exist in the lower pipe regions. $V_{m2} \leq V \leq V_{m1}$ in Figure 3.4 (see heterogeneous flow in Figure 3.3).
3. Moving bed motion. Further reductions of the velocity cause the fluid forces to decrease to a level where particles are suspended infrequently. A sliding layer of particles forms in the lower portion of the pipe. $V_{m3} \leq V \leq V_{m2}$ in Figure 3.4 (see moving bed in Figure 3.3).
4. Stationary bed motion. At sufficiently low velocities, the layer of particles in contact with the lower pipe wall ceases to move. Some particles in the upper layer of the bed are lifted and transported with the liquid, but generally in this regime solids transport is low. $V_{m4} \leq V \leq V_{m3}$ in Figure 3.4 (see flow in a stationary bed in Figure 3.3).

As the velocity is reduced below V_{m4} , the solids settle rapidly and in the absence of an abnormally high applied pressure gradient, the pipe will block.

Factors affecting the relative magnitudes of the four transition velocities are not well understood. Factors such as particle diameter and pipe diameter can affect the values of each transition velocity, in manners that differ qualitatively. Newitt et al. (1955) proposed that the effect of mean particle diameter and mixture velocity on the flow regime could be described by a flow regime map, Figure 3.5. However, it will be shown that correlations predicting the two transition velocities V_{m1} and V_{m2} appearing in the literature produce predictions that differ significantly in magnitude. Consequently, maps such as those proposed by Newitt should be interpreted as providing qualitative rather than quantitative information. In any case, all

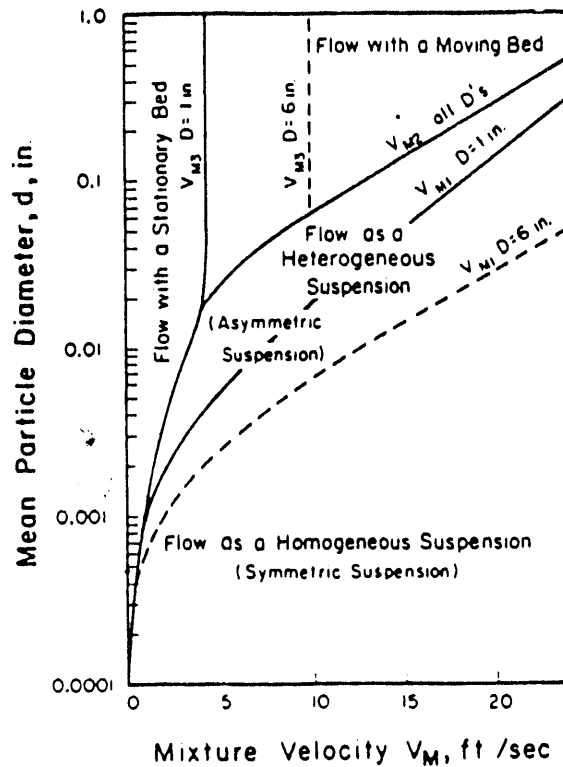


FIGURE 3.5. Flow Pattern Map (Newitt et al. 1955)

transition curves collapse to a single curve at small particle diameters such as those found in double-shell wastes. Thus, it is not possible to determine the distance between each transition velocity for wastes containing extremely small particles from these maps.

The flow pattern achieved has significant effects on pressure losses in slurry flows. In general, effective friction factors, $f = \frac{D}{\frac{1}{2} \rho V^2} \frac{dP}{L}$, are smallest in the symmetrically suspended flow configurations. The variation of the friction factor results in pressure losses that first decrease with increasing mixture velocity and then increase with increasing mixture velocity. Stationary bed motion exhibits extremely high friction factors. A qualitative illustration of the typical variation in the pressure gradient with velocity may be seen in Figure 3.4, which was taken from Govier and Aziz (1972). In the stationary bed regime, the pressure gradient required to overcome friction decreases with mixture velocity. Once the slurry is fully suspended, the

pressure gradient increases with mixture velocity. The behavior in the fully suspended region resembles that seen in single-phase flow where the pressure gradient increases monotonically with fluid velocity.

3.1.3 Analyzing Slurry Flow

The flow pattern achieved by a particular slurry affects the methods that may be used to analyze the flow and predict the pressure drop. In the stationary bed and sliding bed regimes, the particle's velocity differs markedly from the mean liquid velocity. In these two regimes, analyses require the use of individual transport equations to predict the behavior of each phase. Techniques of this sort are discussed at length by Soo (1987) and Wallis (1969).

In principle, general multiphase flow analyses may be used to analyze the motion of slurries in any of the flow classifications. However, full multiphase flow analysis of complex mixtures is computationally intensive. In addition, Wallis (1969) notes that full multiphase flow techniques in which transport equations are applied to each phase can produce accurate predictions for the pressure losses in flows only when the physical processes describing transfer of mass, momentum, and energy between phases is well understood; in many cases, these processes are understood only approximately. As a result, methods that treat a symmetrically suspended slurry as a pseudohomogeneous mixture can produce equally accurate results with great reduction in computational effort. It is often possible to model symmetrically suspended slurries as pseudohomogeneous mixtures, provided that an appropriate rheological model is selected (see Section 3.1.1). Pseudohomogeneous techniques may not be applied to slurries in the sliding bed or stationary bed regime.

3.1.4 Double-Shell Tank Slurries

It is clear that the degree of suspension of a particular slurry must be assessed before an appropriate analysis method is selected. The size of the particles in the double-shell tank slurries suggests that the mixture will flow either in the symmetrically or asymmetrically suspended regimes during

normal operation. Methods to predict the degree of suspension of solids in the slurry are discussed by Govier and Aziz (1972).

Predicting the transition to turbulence is thought to be important for ensuring the particulate suspension. A number of workers consider the existence of turbulence to be a necessary condition for maintaining suspension (Durrand 1953, Wasp 1977). However, this does not appear to be strictly true. Thomas (1979) observed that the critical deposit velocity, V_{m2} , could fall in the laminar, transitional, or turbulent flow region. Thus, turbulence does not appear either necessary or sufficient to ensure particle suspension. Thomas' experimental results suggest that the critical deposit velocity (below which a bed forms) occurs in laminar flow when pipes are small or when the viscosity of the liquid in the slurry is high. The critical deposit velocity may occur well into the turbulent region if low viscosity slurries are transported in large pipes. Thomas stated that the data collected were insufficient to warrant an exact correlation, but suggests while flow remains laminar the critical deposit velocity, V_{m2} , varies as:

$$V_{m2} \sim \rho g C_t (s - 1) \phi D^2 / \mu \quad (3.6)$$

where V_{m2} = critical deposit velocity (L/T)

g = acceleration of gravity (L/T²)

C_t = concentration at maximum packing density

s = density ratio

ϕ = function that depends on the solids concentration bed $f(s)$.
(Thomas does not provide the form of the function ϕ .)

The critical deposit velocity, V_{m2} , may be expressed in terms of the Reynolds number, Re_{m2} , as

$$Re_{m2} = \frac{\rho V_{m2} D}{\mu} = C_1 \left(\frac{\rho^2 g D^3}{\mu^2} \right) C_t (s - 1) \phi \quad \text{when } Re_{m2} = Re_c \quad (3.7)$$

where Re_{m2} = Reynolds number at V_{m2}

C_1 = proportionality constant. Thomas did not suggest a value for the constant of proportionality, C_1 .

When flow is turbulent, the critical deposit velocity was lower than that predicted on the basis of the suggested laminar flow relation. In this case, Thomas suggested that it could be predicted using:

$$V_{m2} = (8.7) [g \mu (s - 1) / \rho]^{0.37} (D \rho / \mu)^{0.11} \quad (3.8)$$

or in terms of Reynolds number as:

$$Re_{m2} = \frac{\rho V_{m2} D}{\mu} = (8.7) \rho^2 \left[\frac{g D^3}{\mu^2 (s - 1)} \right]^{0.37} \quad (3.9)$$

Thus, the suspension is enhanced by the onset of turbulence.

The effect of particle size on these relations was not studied by Thomas because all measurements were performed using silica sand with an average diameter of 150 μm . Tests were performed in pipes with diameters of 9.41 mm, 18.9 mm, and 105 mm. Experiments of the critical deposit velocity for smaller particles have not been reported. However, the critical deposit velocity would be expected to be much smaller for 10 μm diameter particles, such as those found in double-shell tank wastes, than for 150 μm particles, such as those studied by Thomas (1979).

Correlations for the prediction of the minimum transport velocity, V_{m2} that appear in the literature do not produce consistent predictions. Wicks (1965) compared predictions for the minimum transport velocity required to suspend 250 μm sand in water at a concentration of 0.01 of sand by volume. In Figure 3.6, predictions for the minimum transport velocity based on correlations by Zandi and Govatos (1967) and Sinclair have been added to the original figure from Wicks. It is clear that the correlations produce significantly different predictions for minimum transport velocity. Consequently, it is not possible to predict the minimum transport velocity with any degree of precision. Precise determination of the minimum transport velocity does not appear to be important to the transport of double-shell tank wastes.

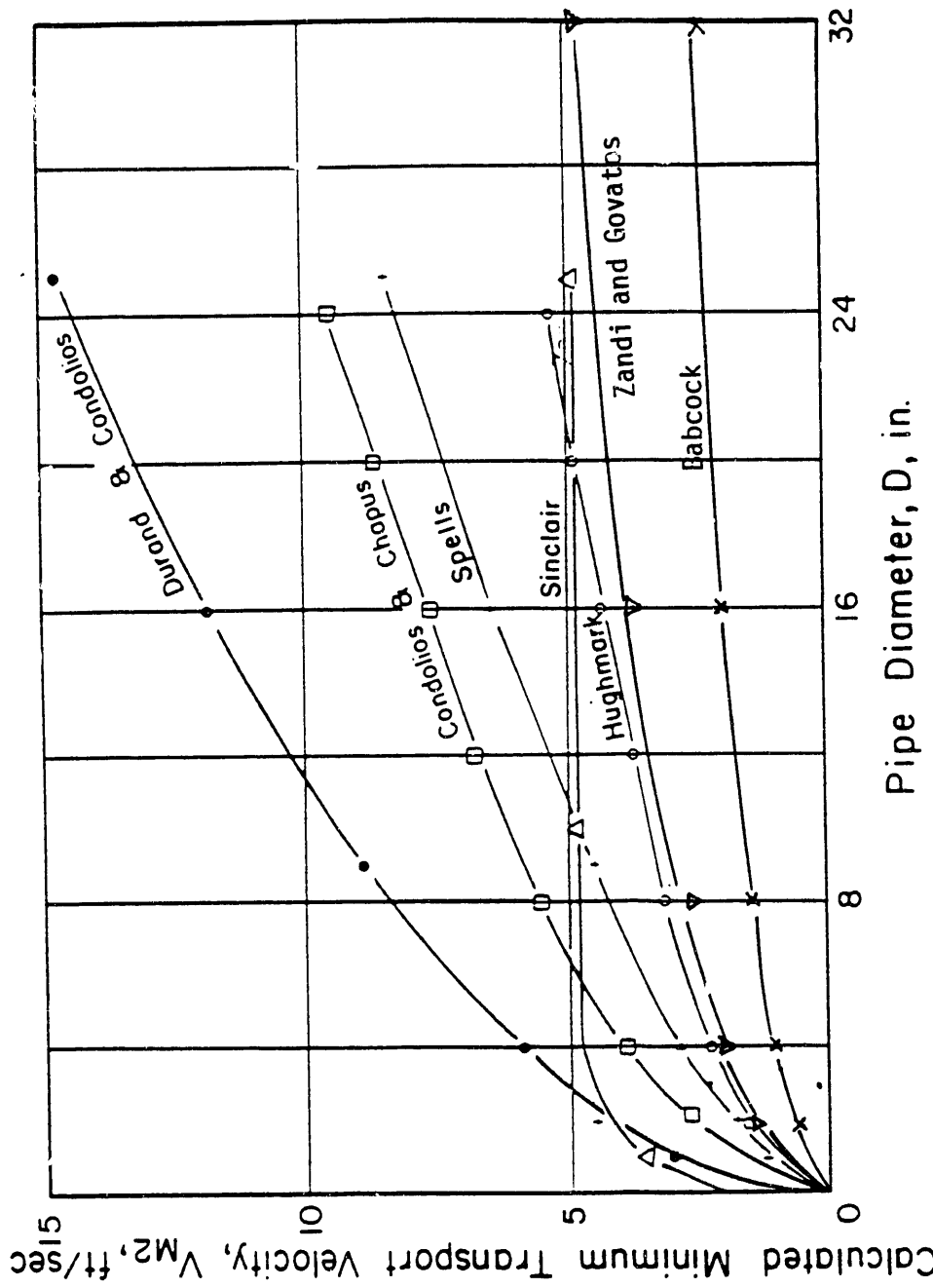


FIGURE 3.6. Comparison of Predictions of Minimum Transport Velocity, V_{m2} ; 0.25-mm Sand in Water at 0.01 Volume Fraction Solids

Because double-shell tank wastes are extremely fine, it is considered likely that they would be transported in symmetric suspension. The velocity for transition from symmetric to asymmetric suspension was evaluated on the basis of two reported studies and is presented here.

Both studies of the transition between the symmetrically and asymmetrically suspended regimes involve the use of coarse particles suspended in liquids. No correlations developed using smaller particles have been reported. Use of Spells' (1955) or Ismail's (1951) correlations to predict the behavior of double-shell tank slurries containing particles on the order of 10 μm involves extrapolation. However, these correlations provide the only basis for predicting the degree of suspension achieved during transport of double-shell tank slurries.

The transition between symmetrically suspended and asymmetrically suspended regimes was studied using low concentrations of 80- μm to 800- μm diameter particles by Spells (1955); these mixtures had Newtonian rheologies. Spells suggests that the velocity, V_{m1} , marking the transition between symmetric and asymmetric suspension may be determined using the relation:

$$V_{m1}^2 = 0.075 \left(\frac{\rho_m D V_{m1}}{\mu_m} \right)^{0.775} g d (s - 1) \quad (3.10)$$

where V_{m1} = transition velocity between symmetric and asymmetric suspension (L/T)

D = pipe diameter (L)

ρ_m = mixture density (M/L³)

μ_m = mixture viscosity (M/LT)

g = acceleration of gravity (L/T²)

d = average particle diameter (L)

s = density ratio (ρ_s/ρ_l).

This relation may be restated to allow direct evaluation of V_{m1} :

$$V_{m1}^{1.225} = 0.075 \left(\frac{\rho_m D}{\mu_m} \right)^{0.775} g d (s - 1) \quad (3.11)$$

or in terms of a Reynolds number as:

$$Re_{m1}^{1.225} = 0.075 \frac{D^2 g d (s - 1) \rho_m^2}{\mu_m^2} \quad (3.12)$$

where Re_{m1} = the Reynolds number for the transition from asymmetric to symmetric suspension ($\rho_m V_{m1} D / \mu_m$).

Govier and Aziz (1972) suggests an alternative method of predicting the transition velocity based on the concentration profile measured by Ismail (1951). Ismail studied the distribution of sand-water mixtures containing sand particles in the size range from 48 mesh (355 μm) to 1/4 in. Symmetric suspension is expected at Reynolds numbers greater than the transitional value predicted to be:

$$Re_{m1} = 294 \left(\frac{\rho_m D V_s}{\mu_m} \right)^{8/7} \quad (3.13)$$

where V_s = the settling velocity of the particles (L/T).

The settling velocity for dilute suspensions of particles with small Reynolds numbers may be predicted on the basis of Stokes' law:

$$V_s = \frac{\rho_1 (s - 1) g d^2}{18 \mu_m} \quad (3.14)$$

Substitution results in:

$$Re_{m1} = 294 \left(\frac{D d^2 \rho_l \rho_m g(s - 1)}{18 \mu_m^2} \right)^{8/7} \quad (3.15)$$

Equations (3.12) and (3.15) were used to predict the volumetric flow rate, Q, required to achieve symmetric suspension in the transport lines on the Hanford Site. The properties in Table 3.1 are those reported by Gray, Peterson, Scheele, and Tingey for a slurry made up of 10% solids and 90% supernatant from a core sample from tank 101-AZ. Viscosity based on three separate samples was reported. The lowest viscosity was selected for prediction of the degree of stratification because low viscosity leads to predictions of greater amounts of stratification. The same calculation was applied to determine the volumetric flow rate required to suspend particles with a specific gravity of 2.5 in water. Prediction of the degree of stratification achieved in water will result in an upper bound prediction of the velocity required to achieve suspension because the viscosity and specific gravity of water are lower than those found reported for double-shell tank slurries. Less stratification is expected in more viscous slurries at similar velocities.

Results of these calculations are shown in Figures 3.7a-d. The predictions based on Spells' correlation (1955) are expected to be more reliable than Ismail's when used to predict the behavior of particles with

TABLE 3.1. Core Sample Properties Taken from Tank 103-AN

<u>Property</u>	<u>Sample</u>	
	<u>101-AZ at 10% Solids</u>	<u>Water Slurry</u>
Mixture density, kg/l	1.34	1.0
Viscosity, cP	24.0	1.0
Specific gravity of solids	1.79	2.5
Supernatant density, ρ_l	1.24	1.0
Density ratio, ρ_s/ρ_l	1.44	2.5

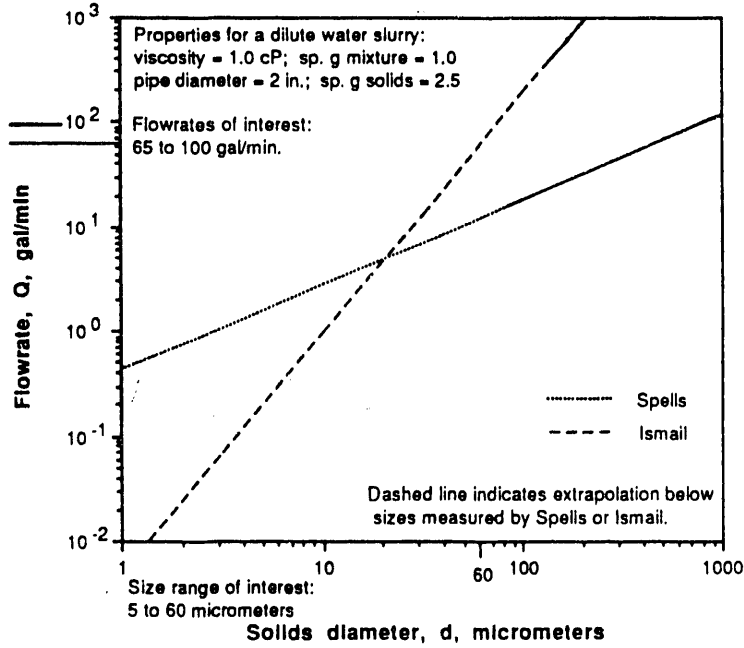


FIGURE 3.7a. Flow Rate Required to Achieve Symmetric Suspension in Water (Upper bound of flow rate required to suspend particles in 2-in. pipe.)

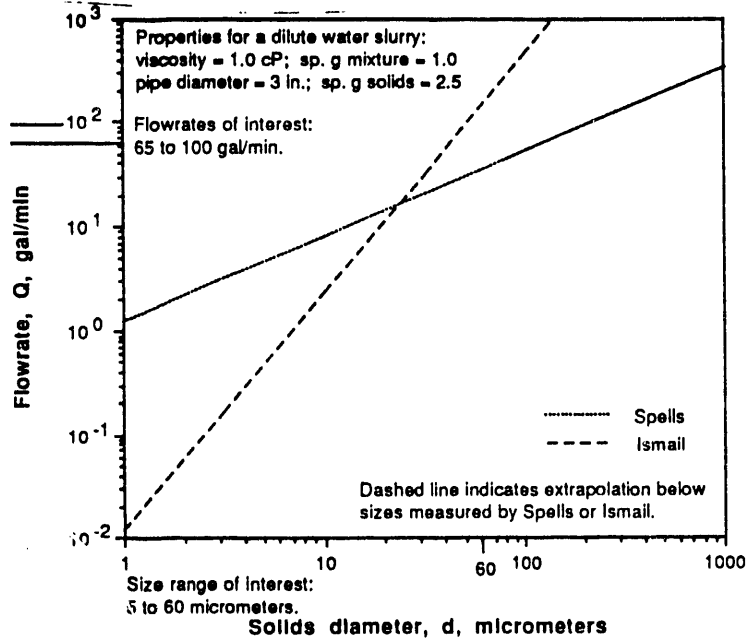


FIGURE 3.7b. Flow Rate Required to Achieve Symmetric Suspension in Water (Upper bound of flow rate required to suspend particles in 3-in. pipe.)

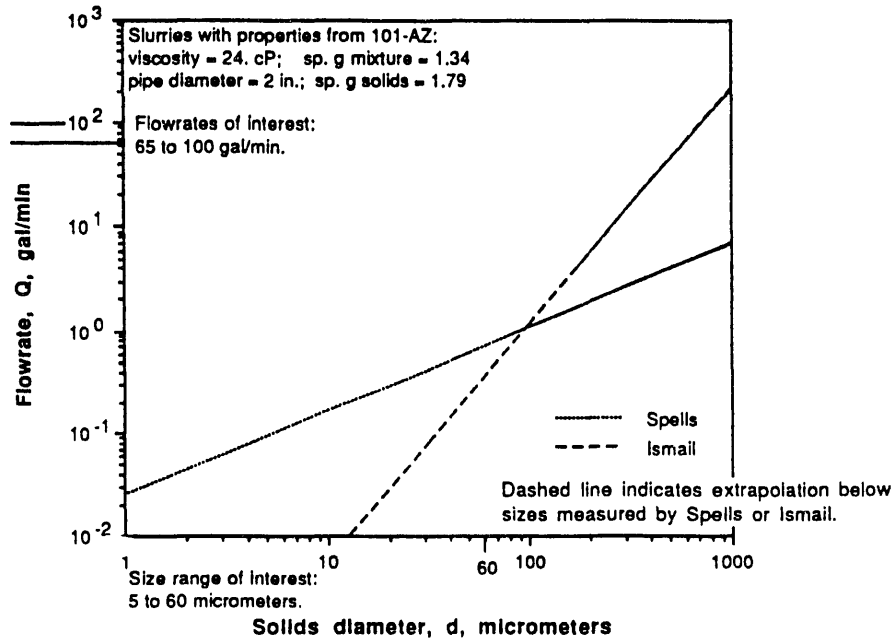


FIGURE 3.7c. Flow Rate Required to Achieve Symmetric Suspension of Particles in Tank 101-AZ Waste for 2-in. Diameter Pipe

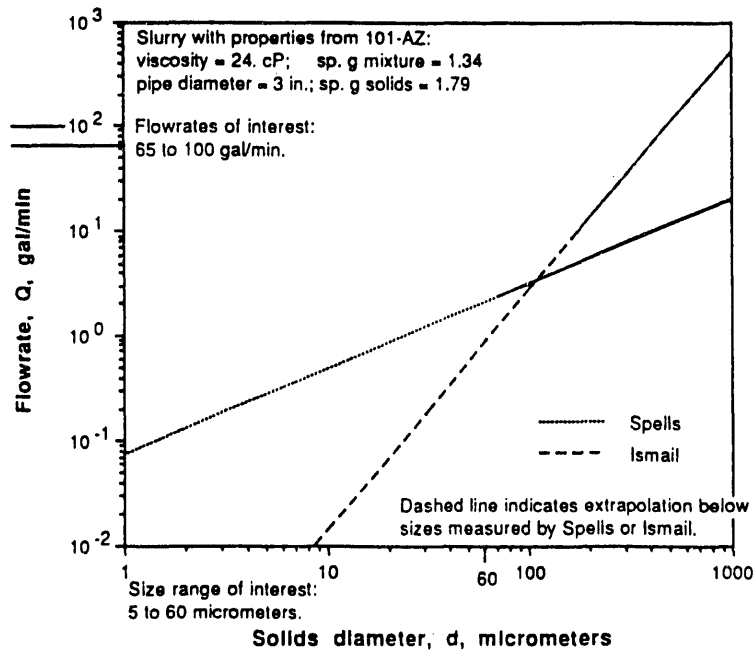


FIGURE 3.7d. Flow Rate Required to Achieve Symmetric Suspension of Particles in Tank 101-AZ Waste for 3-in. Diameter Pipe

diameters less than 80 μm because the data were gathered using particles with diameters between 80 and 800 μm . Ismail's data (1951) is expected to be less reliable than Spells' because this data was obtained using much coarser particles. Predictions based on Spells' correlations suggest that 100- μm particles will be symmetrically distributed in the viscous slurry from 101-AZ at volume flow rates as low as 1 gal/min through a 2-in. pipe; flow rates of 3.1 gal/min would be required to achieve symmetric suspension in a 3-in. pipe. Higher flow rates are required to achieve symmetric suspension in the less viscous water slurry. Here, flow rates of 17.9 gal/min are required in the 2-in. pipe and 52.1 gal/min in the 3-in. pipe. Symmetric suspension of smaller particles in either fluid would be achieved at lower flow rates.

Predictions based on Spells' correlation indicate that settling is not expected under normal operating conditions for slurry transport. Particle size analysis of a core sample from 101-AZ indicates that the volume average particle size is 5 μm . The largest reported particle diameters are from a core of 102-SY; this core has a volume average particle size of 50 to 60 μm . Typical flow rates in the transport lines are expected to fall between 65 and 100 gal/min. The calculations suggest that even the 60 μm particles will be suspended in the actual waste at the proposed flow rates. Use of Spells' correlation suggests that 60 μm particles would be suspended even in water. In contrast, the calculation based on Ismail's results indicates that some stratification may be possible if 60 μm particles are transported in water.

It should be noted that the correlation suggested by Spells is based on experimental data collected in fully turbulent pipe flow. In general, flow is expected to be fully turbulent during transfer. Application of Spells' correlation indicates that particles with diameters of 150 μm and specific gravity of 2.5 would be transported in the symmetrically suspended regime when water flows at 65 gal/min in a 3-in. pipe. The maximum size that could be transported would increase if the particles were less dense or if the fluid were more viscous. Because the maximum particle size in double-shell tank wastes is less than 60 μm , it is likely that particles will be transported in the symmetrically suspended regime.

The results of the analyses of the degree of stratification suggest that the slurries should flow in the symmetrically suspended regime. Some degree of stratification may be possible if 60 μm particles, such as those found in tank 102-SY, are transported in a slurry with a viscosity as low as that of water (1 cP). Better suspension can be achieved by maintaining high fluid viscosity. However, the higher slurry viscosity is likely to elevate the magnitude of the pressure drop across the transport line. A spread sheet indicating the Reynolds numbers and flow rates at which the predicted transition to complete suspension occurs is included in the Appendix.

Prediction based on the correlations cited above indicates that symmetric suspension should be achieved by double-shell tank slurries containing particles less than 60 μm in diameter at almost all proposed transport velocities. In contrast, slurries containing appreciable quantities of particles with diameters in excess of 100 μm may exhibit some degree of stratification.

Prediction of the solids distribution regime in double-shell tank slurries suggests that pseudohomogeneous analyses should produce reasonable predictions for the pressure losses in pipe flows provided that the solids suspended in the slurry do not exceed 60 μm in diameter. There does not currently appear to be a need to study the effect of stratification on the pressure drop characteristics because it appears that the solids phase will be completely suspended. However, it is recommended that the degree of stratification be monitored during the transport experiments to detect any deviations from Spells' predictions because the correlation has been applied to smaller particles than those used in its development and because the Ismail correlation sometimes predicts greater degrees of stratification.

The analysis of the degree of stratification performed here suggests that symmetric suspension cannot be guaranteed for low viscosity slurries containing particles larger than 60 μm . Extremely dense particles might also exhibit greater degrees of settling than those analyzed here. It is recommended that an analysis of this type be repeated if results of waste sample analyses indicate that the particles contained in the slurries are larger in diameter or have greater specific gravities than those examined here.

It should be emphasized that the slurry characteristics used here are those taken from analyses of core samples of untreated wastes. Some of the chemical processes, such as washing or treating with chemical flocculents, may affect the mean diameter or density of the solids contained in the slurry or they may affect the rheology of the supernatant. For example, washed solids were found by Gray, Peterson, Scheele, and Tingey to settle more rapidly than untreated solids from 101-AZ. Consequently, slurries containing washed solids may exhibit greater degrees of stratification than those containing untreated solids. However, because the size and density of washed solids reported by Gray, Peterson, Scheele, and Tingey are reported to be smaller than those of the unwashed solids reported by Peterson, Scheele, and Tingey, this suggests that the enhanced settling is caused by decreased viscosity. Because it is unlikely that the supernatant viscosity is less than that of water, the limiting water slurry case is expected to provide the maximum possible flow rate required for suspension. Thus, even slurries containing washed solids are expected to be symmetrically suspended.

To determine whether stratification is possible at any time during transport, the size, density, and settling velocity of particles after each type of treatment should be investigated. The data obtained may then be used to determine the degree of stratification that might be expected during transport. If settling is predicted during the transport of any of these slurries, experimental studies of the critical deposit velocity will be required to allow design of transport systems in which settling and plugging can be avoided. In addition, experiments in which the pressure drop characteristics of stratified waste slurries are determined will be required; these experiments would provide the pressure drop predictions required to avoid excess pressure losses in the lines.

3.1.5 Transport of Other Wastes

It is almost certain that double-shell tank slurries will be suspended during transport; however, there are plans to transport wastes containing much larger particles. These plans include Hanford Waste Vitrification Plant (HWVP) wastes containing frit. It is anticipated that the added frit will fall between No. 80 and No. 200 ASTM standard sieve sizes. Consequently, the

diameter of frit will be larger than 75 μm and smaller than 180 μm . It is likely that settling will be possible when frit is transported.

It is important to recognize that the friction factor data describing pressure drop during transport of symmetrically suspended wastes is not expected to be applicable to the prediction of pressure drop during transport of settled wastes. A separate study of the pressure drop characteristics of wastes transport in the sliding bed regime may be required to predict pressure drop characteristics of wastes containing large particles.

In addition, studies to predict the minimum transport velocity should be performed prior to transport of wastes containing large particles. Currently, published data exists describing the minimum transport velocity, V_{m2} . However, correlations based on the different data sets are not in agreement. It is recommended that the correlations and data on which they are based be compiled and reanalyzed under the following circumstances:

1. if the mean size of double-shell wastes to be transported across the site approaches 100 μm
2. if significant solids stratification is detected during flow of waste simulants to be used in this study
3. if there is a current need to predict settling of HWVP wastes.

Follow-up testing to verify proposed correlations should be conducted after compilation and analysis of the available data.

Analysis of the needs for transport of double-shell wastes indicates that this HWVP information will not be relevant to the transport of double-shell wastes because double-shell tank wastes contain particles less than 60 μm in diameter.

3.2 NEWTONIAN FLUID FLOW

Methods to predict pressure changes for flow of Newtonian fluids in pipelines and components are described in this section.

3.2.1 Energy Balance in Pipe Flows

Pressure changes in pipe flow may be predicted by applying an energy balance. In the most general form, a pipeline may include enlargements and/or

contractions that result in changes in cross-sectional area and components such as elbows and valves; in addition pipe elevation may vary. A typical section of a pipeline is shown in Figure 3.8. When no heat is added and no work is performed, the energy balance for an incompressible fluid between any two points requires that

$$0 = \dot{m} \left(\frac{P_2}{\rho} - \frac{P_1}{\rho} \right) + \dot{m}g(Z_2 - Z_1) + \int_{A_2} \frac{v_2^2}{2} \rho v_2 dA - \int_{A_1} \frac{v_1^2}{2} \rho v_1 dA + \frac{\dot{m} dP_{\text{loss}}}{\rho} \quad (3.16)$$

where

- \dot{m} = mass flow rate of fluid through the pipe (M/T)
- P = pressure (M/LT)
- ρ = fluid density (M/L³)
- g = acceleration of gravity (L/T²)
- Z = elevation of the pipe section (L)
- A = cross-sectional area (L²)
- v = mean fluid velocity at location in pipe cross section (L/T)

dP_{loss} = irreversible pressure loss that occurs as a result of friction (M/LT).

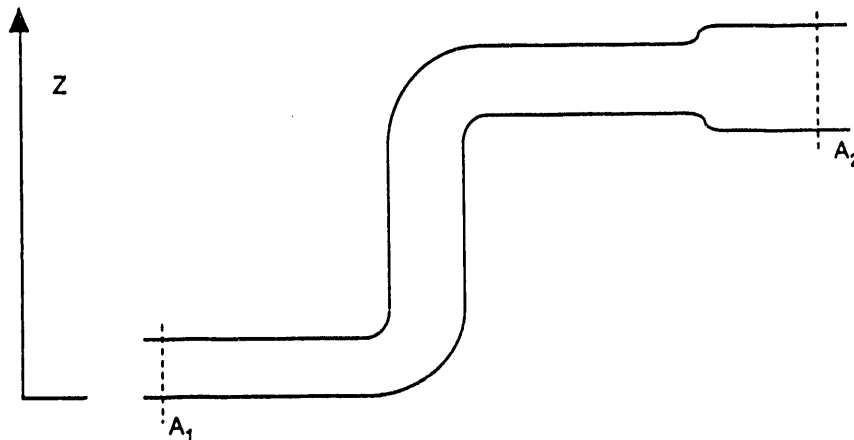


FIGURE 3.8. Typical Pipeline Section

This equation is often written in the form:

$$\frac{P_1}{\rho} + \alpha_1 \frac{\bar{V}_1^2}{2} + g Z_1 = \frac{P_2}{\rho} + \alpha_2 \frac{\bar{V}_2^2}{2} + g Z_2 + \frac{dP_{\text{loss}}}{\rho} \quad (3.17)$$

where the bulk mean velocity, \bar{V} , is related to the fluid volumetric flow rate, Q by:

$$Q = \bar{V} A \quad (3.18)$$

where A = pipe cross-sectional area (L²)

Q = volumetric flow rate in the pipe (L³/T)

\bar{V} = bulk velocity (L/T).

The quantity α , a kinetic energy flux coefficient, is defined as:

$$\alpha \frac{\bar{V}^2}{2} = \int_A \frac{v^2}{2} (v \, dA) \quad (3.19)$$

where the integration is performed over the pipe cross-sectional area.

The magnitude of the kinetic energy flux coefficient depends on the shape of the velocity profile. When the velocity profile is uniform, $\alpha = 1.0$; α attains its maximum value in laminar flow through a circular pipe where the velocity profile is parabolic and $\alpha = 2.0$. The shape of the mean velocity profile in the turbulent regime is affected by the Reynolds number. However, Fox and MacDonald (1973) suggest that a value of 1 may be used in turbulent flow because a relatively uniform velocity profile results in turbulent flow. The value of α may vary in non-Newtonian flows.

Thus, pressure changes in any pipe flow arise as a result of elevation changes, velocity changes, or as a result of frictional losses that are represented in the quantity dP_{loss} . All three types of energy changes must be accounted for when designing piping networks. Pressure changes accounted

for in the gravity and kinetic energy terms by elevation or velocity changes are reversible; that is, the pressure change can be reversed by returning the flow to its previous elevation or velocity. In addition, the pressure increment caused by elevation or velocity changes is unaffected by the details of the velocity profile, or by the rheological equation for the fluid. Pressure changes caused by reversible factors are identical in Newtonian and non-Newtonian flows, and may be determined on the basis of the fluid elevation and velocity alone.

Friction in pipe flow leads to irreversible pressure losses, that arise as a result of viscous dissipation of energy within the fluid. The magnitude of the viscous dissipation is strongly affected by details of the velocity field and by the rheological properties of the fluid. In principle, prediction of frictional pressure losses in pipe flows requires solution of the differential equations governing the fluid. In practice, this method is limited to prediction of pressure drops in fully developed laminar flow of Newtonian fluids in straight pipes. Accepted methods for predicting the pressure drop in turbulent Newtonian flows and in all slurry flows are based on experimentally verified empirical models or on experimentally determined correlations. The uncertainties involved in predicting pressure changes in pipe networks arise as a result of the inexact nature of the empirical models.

Current engineering practice divides frictional pressure losses into two categories: 1) pipe losses - frictional losses that occur in fully developed pipe flow, and 2) component losses - frictional losses that occur in the vicinity of a flow disturbance. Flow disturbances arise as a result of changes in the flow direction (e.g., in elbows), changes in flow velocity (e.g., flow in enlargements or contractions), or as a result of flow development in pipe entrance regions.

Both pipe and component losses in Newtonian fluids are of great industrial interest and have been studied extensively. Standard methods of predicting losses in fully developed pipe flows are discussed in the ASHRAE Handbook of Fundamentals (1989), Marks' Standard Handbook for Mechanical Engineers (Avallone and Baumeister 1978), and Crane Co. (1988). A brief summary

of the methods used to predict pipe and component losses in the flow of Newtonian fluids, as well as the differences between fully developed flow will be given here.

3.2.2 Prediction of Pressure Losses for Flow of Newtonian Fluid in a Circular Pipe

In pipelines, fluid enters the pipe with a velocity profile determined by conditions upstream of the inlet. The profile develops as the flow progresses downstream, until an asymptotic profile is reached. At this point the velocity profile is termed "fully developed". In the developing region, the pressure gradient in the pipe varies as a function of axial distance along the pipe until it reaches the asymptotic level equal to the gradient in fully developed flow. While the processes are similar for both profiles, the developing region for the pressure gradient is often shorter than that for the velocity profile. An example of a developing region is illustrated in Figure 3.9.

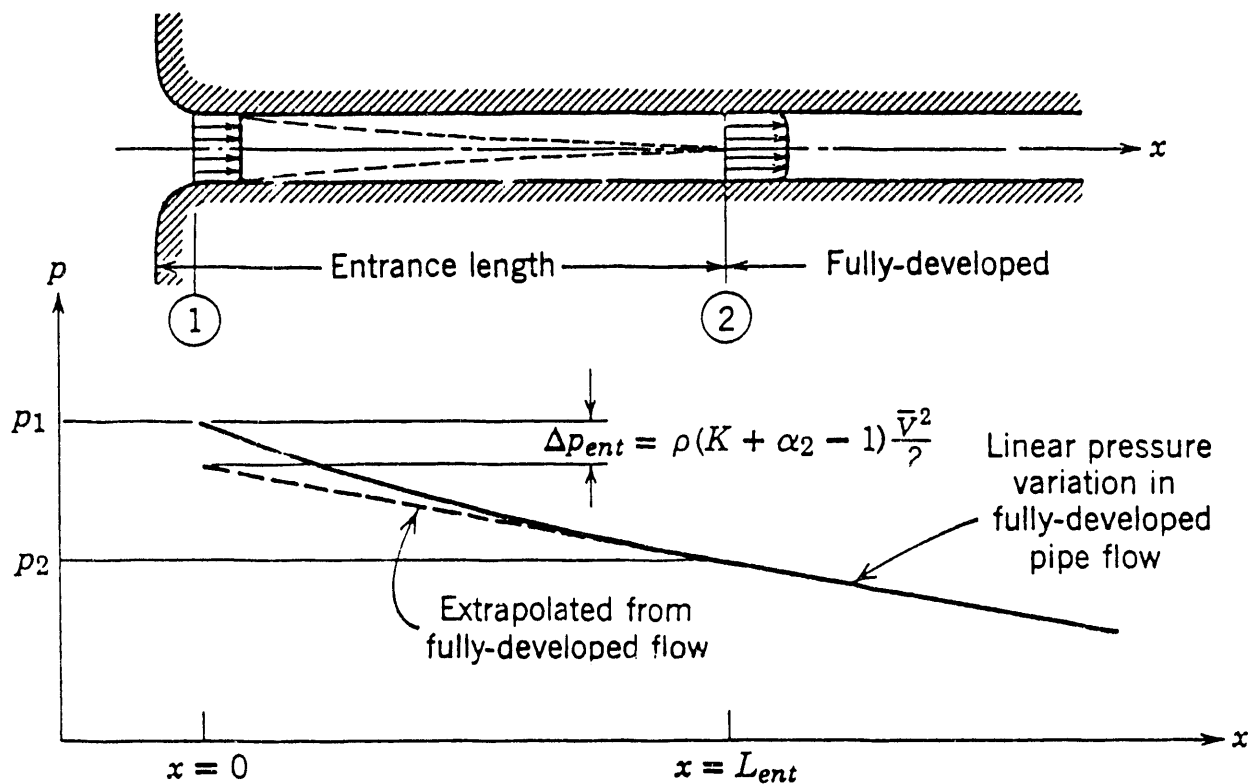


FIGURE 3.9. Pipe Flow Developing Region

The magnitude of the pressure gradient required to overcome friction in the fully developed region is affected by the nature of the flow. At low flow rates, flow is laminar; in Newtonian flows, an exact solution to the momentum equation governing the fluid velocity in laminar flow is known and may be used to predict the pressure drop. The pressure gradient required to overcome friction in fully developed laminar flow of a Newtonian fluid is:

$$\left(\frac{dP}{dx}\right)_{\text{loss}} = \frac{32 \mu \bar{V}}{D^2} \quad (3.20)$$

where $\left(\frac{dP}{dx}\right)_{\text{loss}}$ = irreversible pressure gradient (M/L²T²)

μ = viscosity (M/LT)

\bar{V} = bulk velocity of the fluid (L/T)

D = pipe diameter (L).

Thus the pressure loss when fluid flows through a pipe may be determined using the relation:

$$dP_{\text{loss}} = 32 \frac{L}{D} \left(\frac{\mu \bar{V}}{D}\right) \quad (3.21)$$

where L = pipe length (L)

D = pipe diameter (L)

μ = absolute viscosity of the fluid (M/LT)

\bar{V} = bulk velocity of the fluid (L/T).

This pressure loss is often expressed in dimensionless terms as a relation between the Darcy friction factor, f, and the flow Reynolds number, Re as:

$$f = \frac{64}{Re} \quad (3.22)$$

where the Darcy friction factor, f , and Reynolds number, Re , are defined respectively as:

$$f = \left(\frac{dP_{\text{loss}}}{\frac{1}{2} \rho V^2} \right) \left(\frac{D}{L} \right) \quad (3.23)$$

and

$$Re = \frac{\rho \bar{V} D}{\mu} \quad (3.24)$$

where ρ = fluid density (M/L³).

This solution for the friction factor in laminar flow is shown graphically in Figure 3.10, which is referred to as the Moody diagram.

The Reynolds number defined above is of fundamental importance in pipe flow, and may be used to predict the transition from laminar to turbulent flow in homogeneous Newtonian fluids. Laminar flow is characterized by steady nonfluctuating behavior and is observed to exist at pipe Reynolds numbers below 2300 (Fox and MacDonald 1978). However, the value of the Reynolds number at which transition occurs depends on a number of factors that cannot be controlled; these include pipe roughness, flow disturbances in the entrance region of the pipe, and noise (vibration) in the vicinity of the pipe. The Moody diagram shown in Figure 3.10 suggests that the critical region for transition to turbulence extends from Reynolds numbers of 2100 to 4000. Turbulent flow would be expected in most industrial settings at Reynolds numbers in the lower portion of this range.

Turbulent flow is characterized by unsteady random velocity and pressure fluctuations. While no exact solutions for the fluid velocity exist for turbulent flows, extensive measurements of the pressure drop that occurs during flow of Newtonian fluids through pipes have been performed. These measurements form the basis of the turbulent flow portion of the Moody diagram, Figure 3.10. The Moody diagram may be used to determine the friction factor in fully

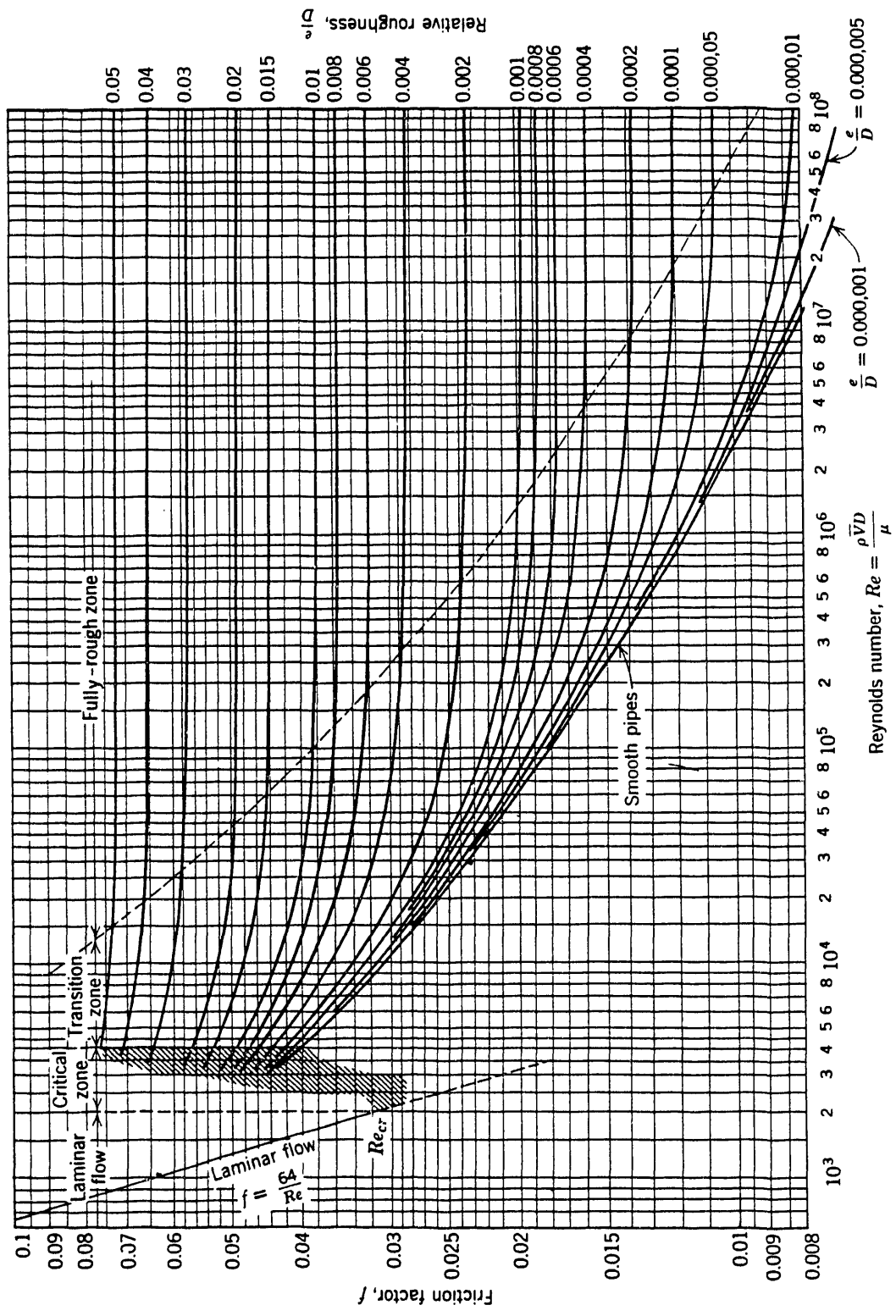


FIGURE 3.10. Moody Diagram

developed pipe flow as a function of the pipe Reynolds number and the pipe roughness factor, ϵ/D . Pipe roughness, ϵ , is a measure of the irregularity in the pipe surface, and is a characteristic of the pipe. Factors that affect pipe roughness include the pipe material and the methods used to manufacture the pipe and any post-manufacture changes. Pipe roughness may change over the lifetime of the pipe if erosive or abrasive materials are transported through the pipe.

The turbulent portion of the Moody diagram can also be described in equation form, and is referred to as Colebrook's natural roughness function. In the turbulent region, the friction factor may be obtained using the relation:

$$f^{-1/2} = 1.14 + 2 \log \left(\frac{D}{\epsilon} \right) - 2 \log \left[1 + \frac{9.3}{\text{Re} \left(\frac{\epsilon}{D} \right) \sqrt{f}} \right] \quad (3.25)$$

from ASHRAE Handbook of Fundamentals (1989).

As in laminar flow, the pressure drop in turbulent flow is related to the friction factor. The definition of the friction factor [Equation (3.23)] may be inverted to give:

$$dP_{\text{loss}} = f \left(\frac{L}{D} \right) \frac{\rho V^2}{2} \quad (3.26)$$

Pipe networks also contain significant regions in which flow is not fully developed. In the example in Figure 3.9, the region downstream of the inlet is referred as the developing region. Flow development in this region leads to an excess pressure drop; the excess pressure drop associated with flow development and turbulent friction at the pipe entrance is marked dP_{ent} in Figure 3.9.

It may be seen that some of the excess pressure drop occurs far downstream of the entry region. The extent of the developing region depends on the exact nature of the flow disturbance. When fluid enters through a rounded entrance,

as in Figure 3.9, and flows in the laminar regime, the developing lengths for both the velocity and pressure gradient depend on the Reynolds number. The developing length for the velocity profile is:

$$\frac{L}{D} = 0.06 \text{ Re} \quad (3.27)$$

The maximum developing length occurs at the transitional Reynolds number near 2000, and occurs at a ratio of $L/D = 120$. Thus, for a 3-in. pipe, the developing length would be 30 ft. The developing length for pressure in this situation is significantly shorter than that for the velocity profile (ASHRAE Fundamentals 1989).

3.2.3 Loss Coefficients

Standard engineering practice treats the excess losses associated with piping components and with flow development in the entrance regions of pipes as though all excess loss occurs in the component itself. Excess losses in individual components are expressed in terms of a dimensionless loss coefficient, or K factor. The loss coefficient, K, is defined:

$$K = \frac{dP_{\text{excess}}}{\frac{1}{2} \rho V^2} \quad (3.28)$$

where dP_{excess} = excess flow development and turbulent friction pressure drop.

The loss coefficients are unique for any individual component; even subtle differences in design may affect the magnitude of K. For example, the loss coefficient for a sharp-edged entrance in the turbulent regime is found to be $K = 0.5$, while that for a rounded entrance is only 0.05, or 1/10th that value. In general, loss coefficients may vary with Reynolds number; however, the dependence is often found to be weak at Reynolds numbers that are sufficiently high to ensure turbulent flow through the component. Crane Co. (1988) has found that loss coefficients vary with Reynolds number in a manner similar to the friction factor. Other studies of the loss coefficient

variation with Reynolds number include Jamison and Villemont (1971), Kittredge and Rowley (1957), Hooper (1981), Williamson and Rhone (1973), Ito and Imai (1973), Weissberg (1962), and Mills (1968). In general, the loss coefficient, K , is found to vary strongly with Reynolds number in the laminar region; variation with the Reynolds number is weak, or non-existent, at high Reynolds numbers.

Loss coefficients reported in design manuals assume that the variation of K with Reynolds number is negligible at high Reynolds numbers. Typical values reported in the literature are shown in Table 3.2. It is worth noting that loss coefficients in the turbulent region rarely exceed two. Exceptions include components such as globe valves, in which the fluid is forced to flow through extremely small gaps. This type of geometry leads to high fluid strain rates and results in significant amounts of viscous stress at the component surface.

Once the loss coefficients and the friction factors for fully developed flow through a pipe in a section are known, the total irreversible pressure drop may be obtained by summing all pipe and component losses:

$$dP_{\text{loss}} = \left(f \frac{L}{D} + \sum K \right) \frac{1}{2} \rho V^2 \quad (3.29)$$

Errors associated with the calculation of pressure losses in pipes commonly occur when two components are closely spaced along the pipe run. When one component is within the developing region downstream of another component, the loss coefficient for both components is affected. This may occur in an expansion loop, Figure 3.11, where 90° elbows are closely spaced. Typically in this configuration some elbows may fall within 10 pipe diameters of each other. The loss coefficient for this series of elbows is not equal to the sum of the loss coefficients for four isolated elbows. Instead, the expansion loop must be treated as an individual component with its own loss coefficient. Accurate prediction of pressure losses requires that all such configurations be identified prior to calculation.

TABLE 3.2. Some Fitting Loss Coefficients in Turbulent Flow

Fitting	Geometry	$K = \frac{dP_{\text{excess}}(a)}{\frac{1}{2} \rho V^2}$
Entrance	sharp	0.50
	well-rounded	0.05
Contraction	sharp ($D_2/D_1 = 0.5$)	0.38
90° elbow	miter	1.3
	short radius	0.30 to 0.90
	long radius	0.23 to 0.60
	miter with turning vanes	0.2
Globe valve	open	10
Angle valve	open	3.1 to 5
Gate valve	open	0.10 to 0.22
	75% open	1.10
	50% open	3.6
	25% open	28.8
Tee	Straight through	0.5
	Flow through	1.8

(a) ASHRAE (1989), Crane (1988), and Olson (1973)

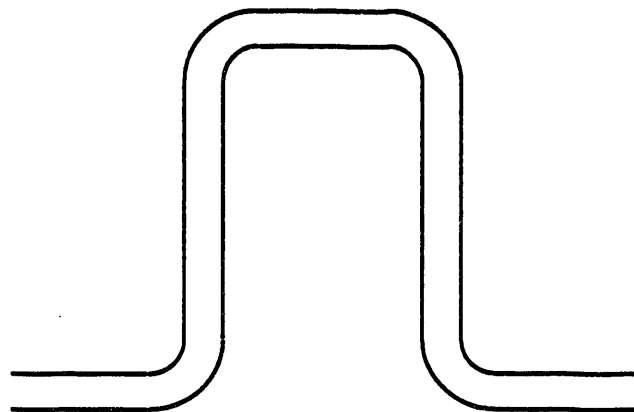


FIGURE 3.11. Typical Expansion Loop

3.3 NON-NEWTONIAN FLUID FLOW

Methods used to predict the frictional pressure losses in slurry flows will be discussed in this section. Special emphasis will be given to methods currently used to predict the pressure losses in pseudohomogeneous slurries especially those that are found to exhibit yield pseudoplastic behavior because double-shell tank slurries are thought to exhibit this type of behavior. The similarities and differences between the behavior of yield pseudoplastic and Newtonian fluids will be noted.

Pseudohomogeneous mixtures containing high concentrations of small particles often exhibit yield pseudoplastic behavior. This type of behavior has been observed in double-shell tank slurries and reported in September 1987 by Fow, Scott, Whyatt and Reucker. The importance of the non-Newtonian characteristics during the transport of the wastes through 2-in. and 3-in. pipes was evaluated for a number of actual waste samples and some simulated wastes. Analysis was limited to samples that have been reported to exhibit yield pseudoplastic behavior. These analyses include samples from tank 101-AZ reported by Peterson, Scheele, and Tingey in 1989 and Gray, Peterson, Scheele, and Tingey in 1990; tank 103-AN reported by Fow in 1987; and simulated NCAW wastes (Fow et al. 1986).

The flow of yield pseudoplastics share some features with the flow of Newtonian fluids. Of foremost importance is the existence of both laminar and turbulent regimes. Turbulence exists in fluid flows because the terms in the fluid momentum equation describing convective mass transport are nonlinear and lead to instability of the flow field. The instability of the convective terms is unaffected by fluid rheology; thus, flows exhibit transition at some critical velocity regardless of the form of the constitutive equation governing the fluid rheology.

The primary difference between the flow of Newtonian and non-Newtonian fluids, at least in terms of predicting pressure drop in pipe flow, arises in the manner in which energy may be dissipated by viscous actions in the different types of fluid. As a result of this difference, friction factors

in yield pseudoplastic fluids vary in a different manner than in Newtonian fluids.

At low Reynolds numbers, the flow of yield pseudoplastic fluids is expected to be laminar. Exact solution of the fluid momentum equation in this circumstance results in a relation between the friction factor (f), Reynolds number (Re), flow behavior index (n), and a new dimensionless parameter, the Hedstrom number (He), where the Hedstrom number, He , is defined as:

$$He = \frac{\rho D^2}{\tau_y} \left(\frac{\tau_y}{K} \right)^{2/n} \quad (3.30)$$

where ρ = fluid density (M/L^3)
 D = pipe diameter (L)
 τ_y = yield stress (M/LT^2)
 K = consistency index ($M/L T^{2-n}$)
 n = flow behavior index.

The Darcy friction factor, f , is related to the yield pseudoplastic Reynolds number, Re_p :

$$f = \frac{64}{\psi Re_p} \quad (3.31)$$

where

$$\psi = (1 + 3n)^n (1 - \xi_0)^{1+n} \left[\frac{(1 - \xi_0)^2}{1 + 3n} + \frac{2\xi_0(1 - \xi_0)}{1 + 2n} + \frac{\xi_0^2}{1 + n} \right]^n \quad (3.32)$$

n = flow behavior index
 ξ_0 = unsheared dimensionless pipe radius that is an implicit function of Reynolds number and Hedstrom number as defined in Equation (3.32).

The quantity ξ_0 is an implicit function of the Reynolds number and the Hedstrom number and obeys the relation:

$$\text{Re} = 2 \text{He} \left(\frac{n}{1 + 3n} \right)^2 \left(\frac{\psi}{\xi_0} \right)^{2-n/n} \quad (3.33)$$

The Reynolds number for a yield pseudoplastic, Re_p , is defined by Hanks and Govier and Aziz as:

$$\text{Re}_p = 8 \left(\frac{n}{1 + 3n} \right)^n \frac{\rho a^n v^{2-n}}{K} \quad (3.34)$$

where n = flow behavior index
 ρ = fluid density (M/L³)
 K = consistency index (M/L T²⁻ⁿ)
 v = fluid velocity (L/T)
 a = pipe radius (L).

which is reduced to the definition for Newtonian fluids when $n = 1$. The definition of the friction factor in a yield pseudoplastic fluid is identical to that in Newtonian flow, Equation (3.23).

The effort involved in evaluating the friction factor may be reduced significantly by providing the results of the friction factor calculations in the form of a diagram, similar to the Moody diagram used in Newtonian flows. A chart of friction factor as a function of the Hedstrom and Reynolds number at a flow behavior index of $n = 1$ (Bingham plastic chart) is shown in Figure 3.12. Predictions for laminar flow behavior correspond to the steeply sloping line to the left of the dashed line marked Re_c . Predictions for laminar flow of a Newtonian fluid are shown on this curve and correspond to a Hedstrom number of 0. A separate chart is required for each flow behavior index, n .

The Hedstrom numbers were calculated for each of these wastes. Results are presented in Table 3.3. The results of greatest interest are those for tank 101-AZ because these wastes have relatively low consistency indices (K),

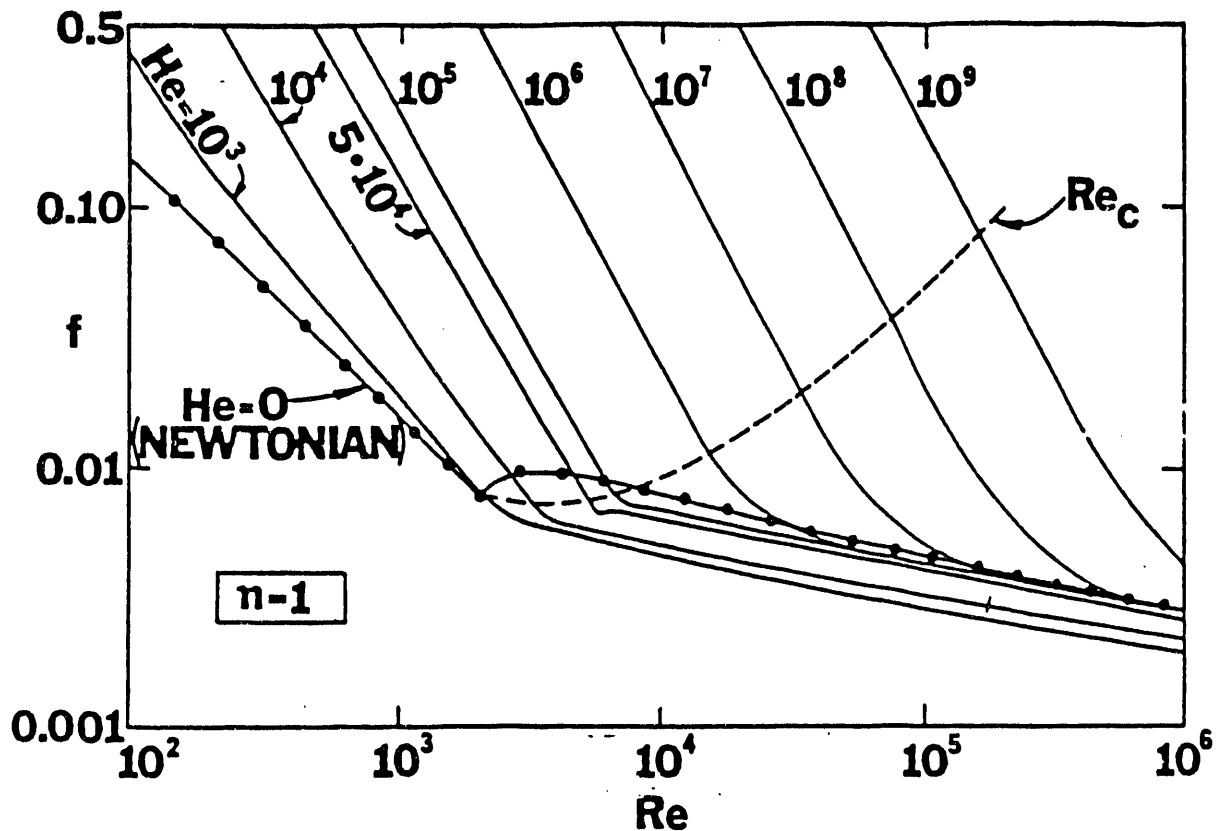


FIGURE 3.12. Friction Factor Versus Hedstrom Number and Reynolds Number

and are likely to be pumpable. (In contrast, the non-Newtonian wastes from tank 103-AN have much larger consistency indices that would result in high pressure drops.) The Hedstrom number that will be achieved if a slurry containing 30% solids concentration from 101-AZ is pumped through a 3-in. pipe is 2.3×10^4 . Flow at this Hedstrom number will exhibit pressure drop characteristics that differ from those observed in Newtonian flow. This may be seen by comparing the curve at $He = 0$ (Newtonian) to that at $He = 10^4$ on Figure 3.12.

Gray, Petersen, Scheele, and Tingey in 1990 report that slurry made up of 10% solids and 90% supernatant from 101-AZ did not exhibit a yield stress but was viscoelastic. It had a flow behavior index between $n = 0.59$ and 0.69 . Consequently, the behavior of this slurry would not be easily predicted on the basis of Newtonian analysis either. The Hedstrom number for this case is 0. In contrast, Petersen, Scheele, and Tingey in 1989 measured the rheology

TABLE 3.3. Hedstrom Number Range for DST Wastes and Simulants

Voluetric Flow Rate, Q , gal/min	Pipe Diameter, D , in.	Density at 20C, ρ , kg/m ³	Consistency Index, n K , Pa-s ^{n}	Flow Behavior Index, n	Yield Stress, T_s , Pa	Hedstrom Number, He	Reynolds Number, Re
101-AZ washed solids							
65	3	1004	0.0118	0.829	4.83E-1	9.36E+04	1.22E+04
100	3	1004	0.0118	0.829	4.83E-1	9.36E+04	2.02E+04
65	2	1004	0.0118	0.829	4.83E-1	4.16E+04	2.25E+04
100	2	1004	0.0118	0.829	4.83E-1	4.16E+04	3.72E+04
101-AZ 30% solids							
65	3	1350	0.0500	0.787	1.26	2.27E+04	4.63E+03
100	3	1350	0.0500	0.787	1.26	2.27E+04	7.81E+03
65	2	1350	0.0500	0.787	1.26	1.01E+04	9.00E+03
100	2	1350	0.0500	0.787	1.26	1.01E+04	1.52E+04
Ziflex cladding							
65	3	1200	0.1530	0.650	9.60	2.47E+05	2.43E+03
100	3	1200	0.1530	0.650	9.60	2.47E+05	4.35E+03
65	2	1200	0.1530	0.650	9.60	1.10E+05	5.59E+03
100	2	1200	0.1530	0.650	9.60	1.10E+05	9.99E+03
103-AN sample 18-1:1							
65	3	1800	0.0587	1.000	3.78	1.14E+04	2.10E+03
100	3	1800	0.0587	1.000	3.78	1.14E+04	3.23E+03
65	2	1800	0.0587	1.000	3.78	5.07E+03	3.15E+03
100	2	1800	0.0587	1.000	3.78	5.07E+03	4.85E+03
NCAW (simulated)							
65	3	1270	0.0042	1.000	1.49E-1	6.23E+04	2.07E+04
100	3	1270	0.0042	1.000	1.49E-1	6.23E+04	3.19E+04
65	2	1270	0.0042	1.000	1.49E-1	2.77E+04	3.11E+04
100	2	1270	0.0042	1.000	1.49E-1	2.77E+04	4.78E+04
NCAW (simulated)							
65	3	1360	0.0130	1.000	1.50E-1	7.01E+03	7.17E+03
100	3	1360	0.0130	1.000	1.50E-1	7.01E+03	1.10E+04
65	2	1360	0.0130	1.000	1.50E-1	3.12E+03	1.00E+04
100	2	1360	0.0130	1.000	1.50E-1	3.12E+03	1.65E+04
NCAW-TRU-PNL (simulated)							
65	3	1020	0.0017	1.000	1.45E-1	2.97E+05	4.11E+04
100	3	1020	0.0017	1.000	1.45E-1	2.97E+05	6.33E+04
65	2	1020	0.0017	1.000	1.45E-1	1.32E+05	6.17E+04
100	2	1020	0.0017	1.000	1.45E-1	1.32E+05	9.49E+04
NCAW-TRU-PNL (simulated)							
65	3	1020	0.0011	1.000	4.70E-2	2.30E+05	6.36E+04
100	3	1020	0.0011	1.000	4.70E-2	2.30E+05	9.78E+04
65	2	1020	0.0011	1.000	4.70E-2	1.02E+05	9.53E+04
100	2	1020	0.0011	1.000	4.70E-2	1.02E+05	1.47E+05

of a sample containing 9.4% weight washed solids from tank 101-AZ and report that the mixture exhibited yield pseudoplastic behavior. Physical properties of this slurry were evaluated on the basis of two samples. The Hedstrom numbers expected if these samples are pumped through a 2-in. or 3-in pipe are 4.2×10^4 and 9.4×10^4 , respectively.

In general, yield pseudoplastic behavior is observed for the more concentrated slurries. However, in 1989, Peterson, Scheele, and Tingey observed a variation of the apparent viscosity with shear rate for the supernatant. This curve is reproduced in Figure 3.13. The fact that the apparent viscosity approaches infinity as the shear rate falls to 0 suggests yield pseudoplastic behavior. No analysis of the possible magnitude of the yield stress is reported so the Hedstrom number achieved while pumping supernatant was not estimated. However, data in Figure 3.13 suggests that yield pseudoplastic behavior may occur even in the absence of solids.

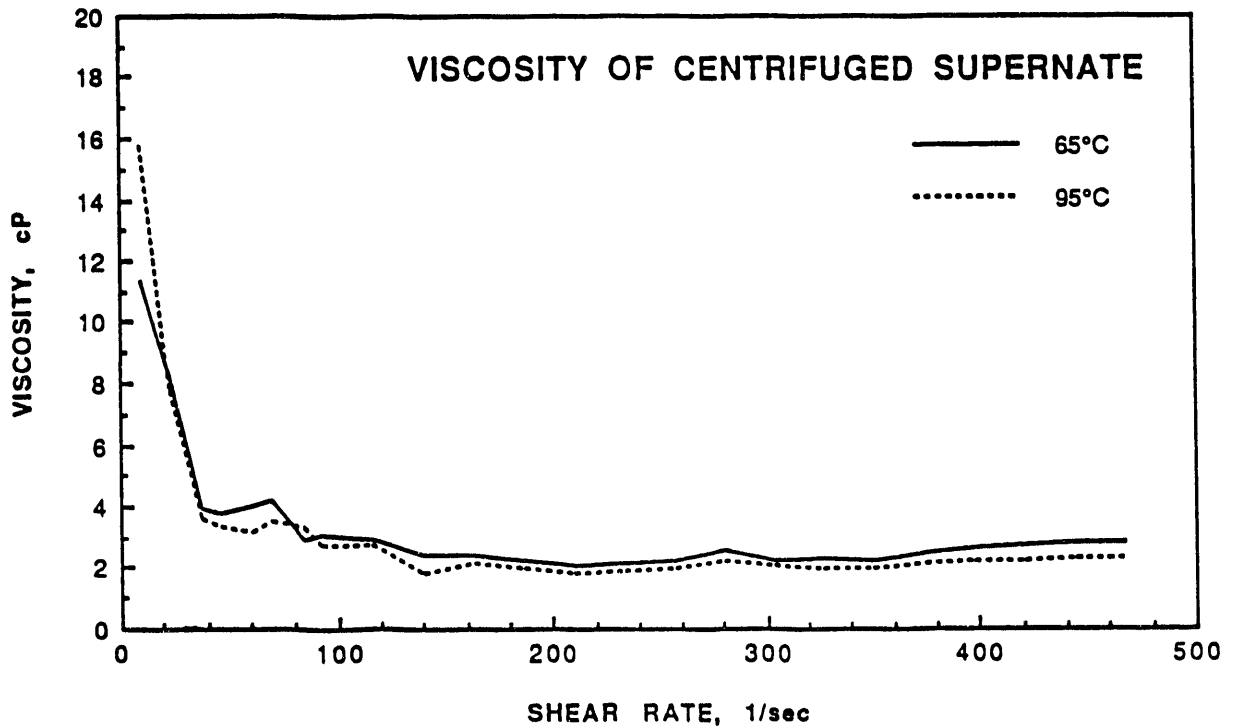


FIGURE 3.13. Viscosity of the Centrifuged Supernate from DST 101-AZ

Calculation of the Hedstrom numbers expected during transport suggests that the magnitude of the yield stresses measured for actual wastes are sufficiently large to require the use of pseudoplastic correlations to predict the critical Reynolds number and the friction factors that will occur during transport. Correlations for the friction factor and critical Reynolds number for yield pseudoplastics have been proposed, but not verified. Because proper design of transport lines can only be achieved by the use of an experimentally verified correlation, measurement of both the critical Reynolds number and the friction factor using yield pseudoplastic materials is required.

This section will describe methods that may be used to predict the pressure drop in the flow of pseudohomogenous slurries with constant properties that exhibit yield pseudoplastic behavior. Analysis of slurries that do not behave as constant density pseudo-homogeneous mixtures will not be attempted in this section. However, it should be noted that slurries in the asymmetrically suspended regime have been analyzed as variable density single-phase fluids by Shook and Daniel (1965). Analyses of this sort could reasonably be applied to the flow of asymmetrically suspended mixtures provided that the velocity slip between phases was negligible. These types of analysis should be performed if future waste characterization indicates that stratification is possible.

3.3.1 Transitional Reynolds Number for a Yield Pseudoplastic Fluid

At some magnitude of the Reynolds number, flow is expected to become turbulent. Dimensional considerations suggest that the critical Reynolds number should be a function of 1) the flow behavior index, n ; 2) the Hedstrom number, He ; and 3) the pipe roughness, ϵ . In homogeneous Newtonian flows, pipe roughness affects transition to turbulence; however, the dependence in industrial situations is such that transition occurs near Re of 2300 in most circumstances. Similar behavior is expected in the flow of yield pseudoplastics, and in most industrial settings, the critical Reynolds number might be expected to be a function of flow behavior index and Hedstrom number only. Hanks (1978) proposed a model for transition to turbulence, which suggests that the critical Reynolds number is a function of the Hedstrom

number, He and the flow behavior index, n . Hanks suggests that the critical Reynolds number, Re_c , obeys the relation:

$$Re_c = \frac{6464 n}{(1 + 3n)^n} (2 + n)^{\frac{2+n}{1+n}} \left[\frac{\left(\frac{1 - \xi_{oc}}{1 + 3n} \right)^2 + \frac{2 \xi_{oc} (1 - \xi_o)}{1 + 2n} + \frac{\xi_{oc}^2}{1 + n}}{(1 - \xi_{oc})^n} \right]^{2-n} \quad (3.35)$$

where the value of the unsheared plug radius, ξ_o is an implicit function of the Hedstrom number:

$$He = \frac{3232}{n} (2 + n)^{\frac{2+n}{1+n}} \left[\frac{\xi_{oc}}{(1 - \xi_{oc})^{1+n}} \right]^{\frac{2-n}{n}} \left(\frac{1}{1 - \xi_{oc}} \right)^n \quad (3.36)$$

The magnitude of ξ_o as a function of Hedstrom number may be determined iteratively.

A curve denoting the critical Reynolds number as a function of the Hedstrom number for fluid with flow behavior index $n = 1$ is shown as a dashed line marked as Re_c in Figure 3.12.

Hanks' model for the transitional Reynolds number is based on a plausible physical model. However, the accuracy of the model for transition to turbulence for flow at yield pseudoplastics has not been subject to extensive experimental verification(a). The transition model has been compared to transition data collected using Bingham plastics (Hanks and Pratt 1967). Agreement was good for flows with Hedstrom numbers less than 5×10^4 . The theory underpredicted the critical Reynolds number for transition to turbulence of Bingham plastics flowing with Hedstrom numbers greater than 5×10^4 . Thus, accurate prediction of transition to turbulence requires further experimental investigation before it may be applied to predict transition for yield pseudoplastics or the critical Reynolds number for flows in which the Hedstrom

(a) Personal communication, L. M. Liljegren to R. W. Hanks, July 23, 1990.

number exceeds 5×10^4 . Some double-shell wastes will flow with Hedstrom numbers greater than 10^5 . Thus, the transition model may underpredict the critical Reynolds number for these wastes. Because it is important to identify the flow regime before predicting the friction factor, using this model for transition may introduce significant error into the prediction of friction factors at Reynolds numbers near transition.

3.3.2 Friction Factor in the Turbulent Flow of a Yield Pseudoplastic Fluid

Prediction of the friction factor in the turbulent regime requires turbulence modeling. To date no exact solutions for the velocity field in turbulent flow exist; therefore, all turbulence modeling incorporates some degree of empiricism.

Dimensional consideration may be used to show that the friction factor, f , in turbulent flow is a function of 1) Reynolds number, Re ; 2) Hedstrom number, He ; 3) flow behavior index, n ; and 4) pipe relative roughness, ϵ/D . Experimentation could be performed at various values of these parameters, and curve fits to the data could be performed to obtain predictive correlations. However, the appropriate algebraic form of these correlations may not be determined based on dimensional considerations alone.

Hanks (1978) has proposed a model for the prediction of friction factors for turbulent flow of yield pseudoplastics through pipes; his model is an extension of the mixing length model used in single-phase flow and provides predictions for the friction factor as a function of the Reynolds number, Re , Hedstrom number, He , and flow behavior index, n . The pipe roughness, ϵ that is known to affect the friction factor, f , in Newtonian flows is not included as a parameter in Hanks' model.

For Newtonian flows, mixing length models are found to provide useful qualitative predictions of velocity profiles for flows through pipes and past flat walls. Quantitative prediction requires the specification of two fitting parameters that have been derived empirically for the flow of Newtonian fluids in pipes. Thus, mixing length models may be seen to require a significant degree of experimental validation even in Newtonian flows.

3.3.3 Applying Hanks' Model

Detailed derivation of Hanks' model appears in Hanks (1978) and Hanks' course notes(a). Discussion of Hanks' model will be limited to a description of the procedure required to produce predictions of the friction factor, f , and to comments on those portions of the model that rely on empirically determined coefficients to provide accurate quantitative predictions. This procedure is also outlined by Hanks (1978). The procedure is listed in Table 3.4 for the convenience of the reader.

At any Reynolds number greater than the critical Reynolds number, Re_c , for transition to turbulence, the friction factor predicted by Hanks may be calculated in the following stepwise fashion. This discussion assumes that the Reynolds number, Hedstrom number, and flow behavior index for a particular pipe flow are already specified. The procedure is iterative and requires the use of an intermediate dimensionless parameter, R .

The dimensionless parameter R is defined as:

$$R = \left(\frac{1 + 3n}{n} \right) \left[Re \left(\frac{f}{16} \right)^{\frac{2-n}{2}} \right]^{1/n} \quad (3.37)$$

Hanks' model is not an exact solution and must be validated before it may be deemed reliable. The pseudoplastic flow model is an extension of Prandtl's empirical turbulence model, which has been found to adequately represent behavior in Newtonian pipe flows. The magnitude of a number of constants that appear in the model were determined empirically on the basis of data collected using coal slurries (Hanks 1978); values of some constants are taken from experiments with Newtonian flows. The particle sizes used to validate this constant are not stated in this report.

Reasonable agreement was obtained when the model was used to predict pressure drop data in experiments on iron oxide slurries, (Hanks and Hanks 1986). In addition, Hanks states that experiments using proprietary fluids

(a) Course notes, Hydraulic Design for Flow of Complex Fluids, Richard W. Hanks Associates, Inc., Orem, Utah.

TABLE 3.4. Procedure for Applying Hanks' Model

The following stepwise procedure may be followed to obtain the friction factor. Iteration during steps 4 through 6 is required.

1. Determine the critical Reynolds number for transition to turbulence, Re_c using Equations (3.35) and (3.36).
2. Evaluate Equation (3.32) at Re_c to obtain the friction factor, f_c , that occurs at transition to turbulence.
3. Evaluate the following equation using Re_c and f_c to determine the magnitude of the parameter R at transition; this will be referred to as R_c .

$$R_c = \left(\frac{1 + 3n}{n} \right) \left[Re_c \left(\frac{f_c}{16} \right)^{\frac{2-n}{2}} \right]^{1/n} \quad (T.1)$$

4. Choose a value of R greater than R_c . R is an implicit function of the Reynolds number (a correct choice for R will reproduce the desired value of Re in step 7.)
5. Evaluate the dimensionless unsheared plug radius, ξ_0 , using the relation:

$$R^2 = \frac{2 He}{\xi_0^{2n/n}} \quad (T.2)$$

6. Evaluate the following integral to determine the Reynolds number corresponding to the estimated value of R .

$$Re = (1 - \xi_0)^{\frac{2-n}{n}} \left(\frac{n}{1+3n} \right)^n R^2 \left[\int_{\xi_0}^1 \xi^2 \eta(\xi, \xi_0, R) d\xi \right]^{2-n} \quad (T.3)$$

where ξ = dimensionless pipe radius
 η = dimensionless shear rate.

TABLE 3.4 contd

Evaluation of this integral requires quadrature to obtain the positive root of the following equation, which specifies the dimensionless strain rate, η , as a function of dimensionless pipe radius:

$$0 = (\xi_0 - \xi) + (1 - \xi_0)\eta^n + \frac{1}{8} R^2 (1 - \xi_0)^{2/n} \lambda^2 \eta^2 \quad (T.4)$$

where $\lambda = L/a = k(1 - \xi)\{1 - \exp[-\phi(1 - \xi)]\}$ (T.5)
 $L =$ mixing length (L)
 $a =$ pipe radius (L).

The constant k is an empirically determined constant referred to as Von Karman's constant; Hanks recommends the use of $k = 0.36$.

The quantity ϕ is a turbulence damping function proposed by Hanks and is equal to:

$$\phi = \frac{R - R_c}{\sqrt{8} B} \quad (T.6)$$

B is an adjustable parameter in Hanks' model. The value of B must be determined experimentally.

Hanks suggests that the value of B is a function of Hedstrom number and may be determined using:

$$B = \frac{22}{n} \left[1 + \frac{0.00352 \text{ He}}{(1 + 0.000504 \text{ He})^2} \right] \quad (T.7)$$

7. Compare the value of Re obtained in step 6 to the target value. The parameter R increases monotonically with Re . If Re determined after step 6 is smaller than the target value, a smaller value of R should be selected, otherwise larger value of R should be selected. Repeat steps 4 through 6 until the solution converges to the desired value of the Reynolds number.

8. Compute f using:

$$f = (16) \left\{ \left[R \left(\frac{n}{1 + 3n} \right) \right]^n Re^{-1} \right\}^{\frac{2}{2-n}} \quad (T.8)$$

indicate that his model produces reliable results for numerous types of fluids^(a); however the results of the studies using proprietary fluids have not been published. Hanks' model may be considered to be partially validated on the basis of the coal-water and iron oxide data, but further validation is required to determine if the constants found to predict coal slurries can be used to predict the behavior of double-shell tank slurries.

Briefly, the constants determined on the basis of data from Newtonian fluid or from coal slurries are:

1. Von Karman's constant, k , appears in Equation (T.5) (Table 3.4), and is used in the prediction of the mixing length. The magnitude recommended by Hanks is based on extensive measurements in Newtonian flows.
2. The quantity 6464, which appears in Equation (3.35) predicting the transitional Reynolds number, Re_c , is selected to allow the physical model proposed by Hanks^(b) to correctly predict the transition to turbulence in Newtonian flows.
3. The B factor proposed by Hanks is an empirically determined parameter. A value of 22 is shown to reproduce the turbulent smooth line of the Moody diagram for Newtonian fluids. The manner in which B is proposed to vary in Equation (T.7) (Table 3.4) is ad hoc; two additional empirical parameters are introduced in this equation.

It is not clear how pipe roughness might affect the magnitude of the fitting parameters; Hanks^(a) indicates that all data were collected using industrially rough pipes. He believes that pipe roughness does not affect the friction factor in the flow of slurries through pipes either because solid particles in the slurries collect in the surface irregularities resulting in smooth surfaces or because abrasive surfaces smooth the pipe^(b). This argument may be plausible, but the dependence of the friction factor on pipe roughness in Newtonian flow is sufficiently large to require that its effect be examined in the flow of yield pseudoplastics.

(a) Personal communication, L. M. Liljegren to R. W. Hanks, July 23, 1990.

(b) Course notes, Hydraulic Design for Flow of Complex Fluids, Richard W. Hanks Associates, Inc., Orem, Utah.

3.4 PLUGGING AND RESUSPENSION

The general problem of resuspension of settled solids and plugging of transport lines by slurries is affected by a large number of slurry properties including particle size, rheology of the slurry, and adhesive properties of the slurry. In a general case, solids are expected to settle and may form particle plugs whenever the mean fluid velocity is sufficiently low.

3.4.1 Plugging Scenarios

It has been shown that the solids contained in the transported slurry are sufficiently small to make settling unlikely at the design transport rates. Consequently, plugging is expected only under abnormal circumstances such as pump outages. Plugging may also occur if any valves are inadvertently allowed to close partially leading to pressure losses and restrictions in velocity.

During a pump outage, the fluid velocity could be expected to drop rapidly. Once the velocity falls below the critical settling velocity (V_{m2} in Figure 3.4) a bed begins to form. Because the fluid velocity would fall extremely rapidly, particles would not be expected to be transported far from their location at the time of the pump outage. Consequently, particles would be expected to settle uniformly along a horizontal section and form a partial plug. In a vertical section, particles would settle until they hit an upward turning elbow. Particles would then be expected to form a complete plug.

The plugging scenario would be qualitatively similar for settling of both "dilatant" or sand-like materials, and "cohesive" or clay-like materials. However, some differences would exist. Slurries containing "sand-like" particles generally exhibit dilatant rheology. The particles in these slurries will settle until the solid particles are in contact with each other and will form densely packed plugs. The particles in the densely packed plugs will be held together by Coulombic attractive forces between the quartz grains, which will be positively charged and the interstitial water, which will be negatively charged (Weyl and Ormsby 1960). The mechanical strength of these bonds may be sufficient to prevent the sand grains from completely draining from the vertical section into the horizontal section. In addition frictional

forces may prevent sliding of particles in the plug and a typical vertical plug made of a dilatant material would appear as in Figure 3.14. These types of materials are not expected to cling to the wall.

Pseudoplastic behavior is typical of cohesive materials that are able to immobilize water and cause it to form a mixed layer around each particle. These materials would form plugs that may be termed cohesive. Typical cohesive mixtures, such as those made of clay and water, may contain as much as 50% water and still remain rigid. The particles in these mixtures are surrounded by films of water that have been immobilized and rendered rigid. The thickness of the water films depends on the nature and size of the clay particles; in extreme cases such as when the clay is bentonite, as little as 1 gm of clay can produce a yield strength that is large enough to trap air bubbles (Weyl and Ormsby 1960).

Because of these properties, plugs that form in cohesive materials will not be highly packed but will be rigid and exhibit a shear strength. Cohesive plugs may become rigid in as little as 6 seconds or the transformation to a rigid plug may take several hours. The magnitude of the shear strength will be affected by the orientation of the clay particles relative to the applied

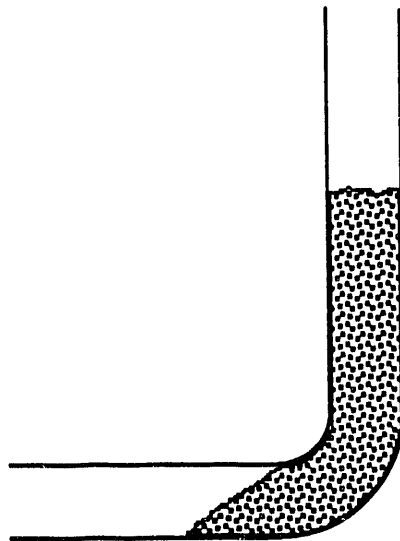


FIGURE 3.14. Example of Vertical Plug

stresses, the size of the particles, and the electrical properties of the continuous fluid. Any factors that affect the orientation of the particles can affect the shear strength of a cohesive material. Factors affecting shear strength include the effect of the flow field on a particle orientation prior to settling, vibrations present during settling, and stresses applied to the plug after settling.

Plugs formed of cohesive materials are expected to occupy larger volumes than those formed of an equal mass of dilatant materials. In addition, cohesive materials are expected to adhere to the pipe walls. Consequently, the strength of the bond to the wall may have to be overcome before unplugging is achieved. This implies that resuspension of cohesive plugs may be extremely difficult.

Resuspension of cohesive plugs may, however, be less difficult because of the thixotropy of these materials. Often, the rigidity of the water film may be overcome by vibration. The shear strength then drops dramatically as a result. In this case, the relatively loose packing of the material may allow significant permeability, which would allow resuspension of the particles in the plug.

The settling behavior of dilatant plugs allows the height of the settled plug to be estimated readily. The probable height of a vertical plug and depth of a settled bed can be estimated on the basis of the solids concentration and the expected void fraction at maximum packing. The settling behavior of cohesive solids renders prediction of the bed depth in the horizontal pipe and plug height in a vertical pipe more difficult to predict. Consequently, the settling volumes of various materials must be estimated on the basis of measured settling volumes.

Measurements of solids concentration in 101-AZ by Petersen, Scheele, and Tingey in 1989 indicate that the composite core sample contained 16% centrifuged solids by volume and 48% settled solids by volume. Washed slurry contained 58.5% settled solids by volume and 15% centrifuged solids by volume. The large differences between centrifuged solids volume and settled solids

volume is typical of materials that form cohesive plugs and that exhibit pseudoplastic behavior. The materials were allowed to settle and were found to exhibit a shear strength of 2100 to 2600 dynes/cm (210 to 260 Pa). Penetrometer tests indicated that the penetration resistance was negligible. (A penetration resistance of 0 psi was obtained.) This behavior indicates that the material is cohesive. In addition, both the washed solids and the supernatant from this waste appeared to exhibit yield pseudoplastic behavior, as is typical of fluids that form cohesive plugs. Consequently, wastes from 101-AZ are expected to form cohesive plugs with low solids fractions and to form long, loosely packed plugs.

3.4.2 Resuspension Scenarios

Resuspension may be accomplished by forcing fluid to flow past the settled solids at sufficiently high velocities to overcome the adhesive forces holding the particle to the bed and then lift the particle into the flow. The magnitude of the minimum resuspension velocity is governed by two forces. The first is the adhesive force holding the particle to the bed. The second is the gravitational force drawing the particle downward. For small particles, adhesive forces are dominant; while for larger particles, gravitational forces are dominant.

A typical variation of minimum resuspension velocity with particle size is shown in Figure 3.15. The minimum resuspension velocity occurs near 100 μm for solid particles in air (Fromentin 1989). Calculation of the exact shape of this curve for a particular settled layer of particles requires modeling of the Van der Waals and capillary forces holding particles together as well as the gravitational force drawing particles downward. Fromentin (1989) states that the influence of the adhesive forces is much greater than that of the gravitational forces for small particles. However, no suggestions for quantifying the magnitude of the adhesive forces in real particles are provided; in particular, no measurement technique is suggested. Methods of quantifying the degree of surface adhesion should be investigated.

The minimum resuspension velocity in water is not known. It is expected that qualitatively similar behavior will occur in liquids and that a minimum

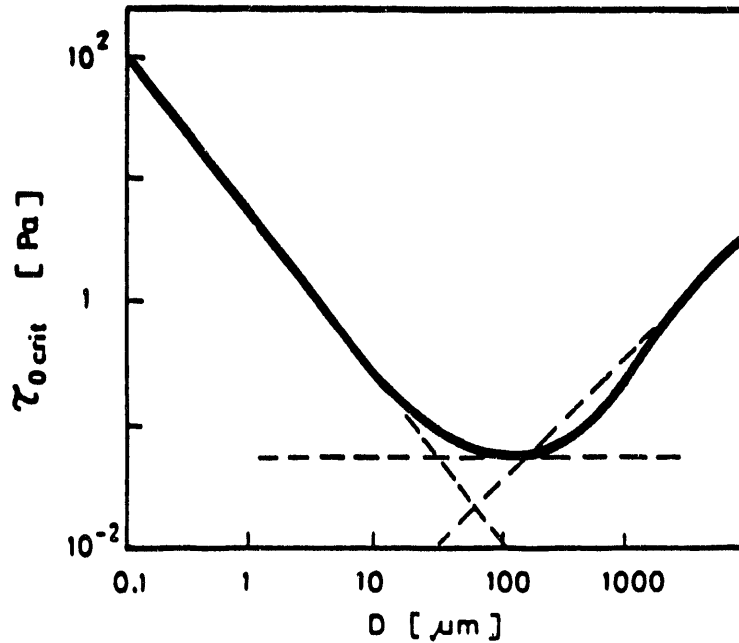


FIGURE 3.15. Wall Shear Stress τ_0 Required to Entrain a Particle of Diameter D into the Air

resuspension velocity will also occur. The exact particle size at which the minimum will occur will depend on the relative magnitude of adhesive forces and gravitational forces in the wastes.

Cohesive slurries generally contain small particles; thus, the important limiting feature governing resuspension is likely to be the adhesive force between particles. In dilatant slurries that exhibit low shear strengths, but often contain larger particles, the important feature limiting resuspension is likely to be the force required to lift solids into the fluid against gravity. Because the magnitude of the adhesive force cannot be quantified, testing will be performed using materials with different shear strengths. In general, materials with high shear strength will be assumed to have large adhesive forces.

In normal operation the mixture velocity is expected to be sufficient to maintain solids suspension. Settling is expected to occur during the operation of the slurry transport lines wherever and whenever the mean fluid velocity is allowed to fall below some critical value. In the discussion of flow

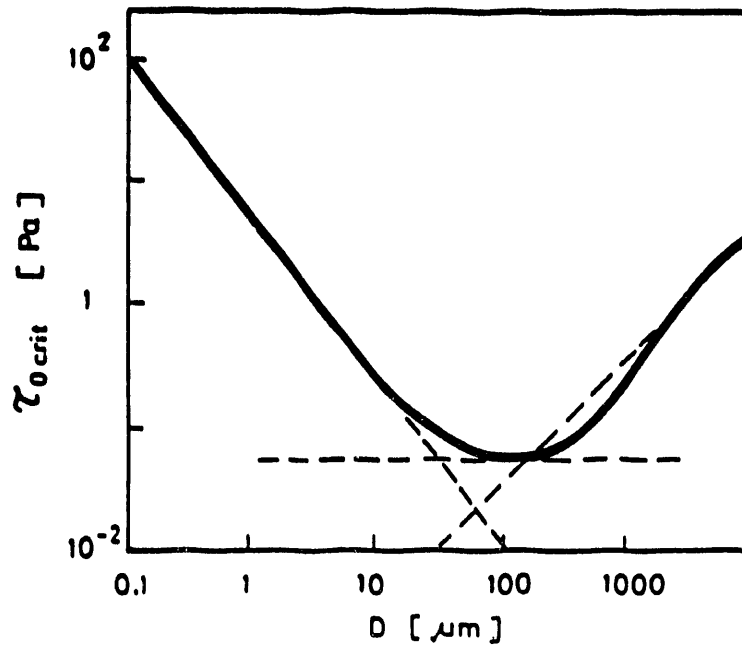


FIGURE 3.15. Wall Shear Stress τ_0 Required to Entrain a Particle of Diameter D into the Air

resuspension velocity will also occur. The exact particle size at which the minimum will occur will depend on the relative magnitude of adhesive forces and gravitational forces in the wastes.

Cohesive slurries generally contain small particles; thus, the important limiting feature governing resuspension is likely to be the adhesive force between particles. In dilatant slurries that exhibit low shear strengths, but often contain larger particles, the important feature limiting resuspension is likely to be the force required to lift solids into the fluid against gravity. Because the magnitude of the adhesive force cannot be quantified, testing will be performed using materials with different shear strengths. In general, materials with high shear strength will be assumed to have large adhesive forces.

In normal operation the mixture velocity is expected to be sufficient to maintain solids suspension. Settling is expected to occur during the operation of the slurry transport lines wherever and whenever the mean fluid velocity is allowed to fall below some critical value. In the discussion of flow

3.4.3 Resuspension of Vertical Plugs

Resuspension in a vertical section of pipe is similar in the sense that some maximum pressure gradient is required to lift the particles. However, extremely large pressure gradients may be required to obtain the velocities required to suspend the particles in a long vertical plug.

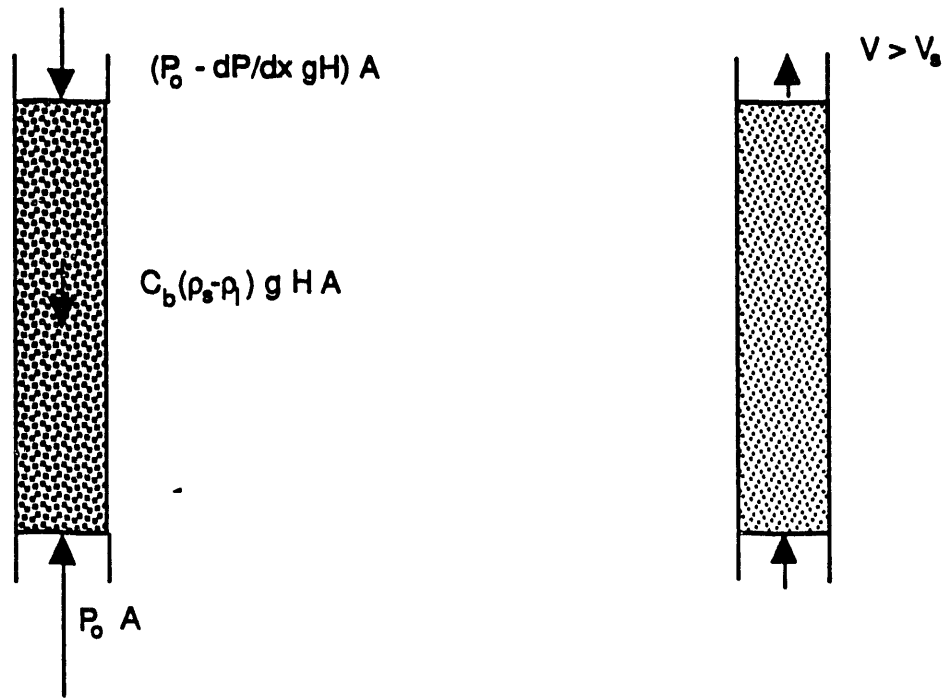
Because the mode of resuspension for vertical or horizontal plugs differ in some ways, the factors affecting resuspension of each type of plug will be discussed separately in the new two sections.

Because of the nature of solids settling, vertical plugs are likely to fill the entire cross-sectional area of the pipe. Consequently, fluid may flow through the plug or pressure may be exerted across the plug surface area (see Figure 3.16, a and b). A force balance indicates that a vertical plug may be resuspended by applying an excess pressure that is sufficient to overcome the sum of hydrostatic head of the column of solids and pressure required to overcome the cohesive stress exerted by the plug at the walls. Applying this pressure would allow the entire plug to be lifted intact. Thus, a vertical plug may always be resuspended by applying an excess pressure differential that is sufficient to exceed the sum:

$$P_1 - P_2 = C_b(s - 1)\rho_l g H + 4\tau_s H/D \quad (3.38)$$

where H = height of the plug (L)
 C_b = solids volume fraction
 s = density ratio, ρ_s/ρ_l
 ρ_l = liquid density (M/L³)
 g = acceleration of gravity (L/T²)
 P = pressure (M/LT²)
 τ_s = shear strength of plug (M/LT²)
 D = pipe diameter (L).

This formulation neglects the head changes caused by the elevation of the liquid because the pressure difference between the top and bottom of the column will vary hydrostatically even when the pump applies no head.



- a) The entire plug will be lifted when the pressure drop exceeds the static head, or when $\frac{dP}{dx} > C_b(\rho_s - \rho_l)g + 4 \tau_s/D$
- b) Particles in the top layer may be lifted if the mean fluid, V , exceeds the particle settling velocity, V_s , or when $V > V_s$.

FIGURE 3.16. Vertical Plug Resuspension Mechanisms

When the vertical plug is extremely long, the pressure required to lift the weight of the plug may be high. For example, an excess pressure of approximately 10 kPa is required when water is used to resuspend a 1-m (3-ft) plug of packed solids with a solids fraction of 1 and a specific gravity of 2, even when the wall shear stress is 0. (In reality, solids packing fractions of 1 are not attainable, but very small void fractions are possible with dilatant materials that contain numerous fines.) In contrast, only 0.6 kPa are required to transport 50 gal/min of water through 3 ft of 3-in. diameter pipe.

Brandt and Johnson (1963) indicate that a packed bed will fluidize when the normal stress inside the bed falls to 0. When fluid flows up through a

plug, the normal stress will fall to 0 when the pressure drop through the bed balances the hydrostatic head of the packed column. Under this circumstance, the normal stress exerted at the wall and the frictional stress exerted at the wall are expected to be 0. Consequently, fluidization is possible when the pressure drop exactly balances the hydrostatic head for the particles.

When the shear strength exerted at the wall is large, the force required to overcome the adherence to the wall may be even greater. An order of magnitude estimate of the relative magnitudes of the ratio of pressure required to overcome the static head to the pressure required to overcome the cohesive strength of the sludge was based on the measured shear strength of sludge from 103-SY reported by Fow et al. (1986). The largest shear strength measured for a sample was 1643 Pa. Assuming that a plug had a specific gravity of 2 and a shear strength of 1643 Pa, the ratio of the pressures required to overcome the hydrostatic head to that required to overcome the adhesive force is 0.08. Thus, the pressure required to overcome the adherence to the wall may be an order of magnitude greater than that required to overcome gravity. This suggests that for highly cohesive materials, overcoming the adhesion to the wall may be most important. Materials with low degrees of cohesion may resuspend when the hydrostatic pressure is overcome.

The previous discussion provides an upper limit for the pressure required to resuspend a plug. It may, in principle, be possible for the plug to be destroyed at smaller values of the pressure gradient. When a plug is very permeable, fluid may filter through the plug. Particles in the top layer of the plug may be suspended if the fluid velocity exceeds the particle settling velocity and if the fluid velocity is sufficient to tear away a particle.

Ergun's correlation(a) (Perry and Chilton 1973) may be used to predict the pressure drop, dP , that occurs when fluid filters through a porous media.

$$dP = \left[\frac{150 C_b \mu}{d} + 1.75 \rho v \right] \left[\frac{C_b}{(1 - C_b)^3} \right] \left[\frac{V H}{d g_c} \right] \quad (3.39)$$

(a) Equation (3.39) requires the use of English system units as follows: μ , lb_m/ft-hr; d , ft; Q , ft³/hr; L , ft; ρ , lb_m/ft³; and $g_c = 4.17 \times 10^8$ ft-lb_m/lb_f-hr².

where V = bulk mean velocity of fluid in a clear pipe = Q/A (L/T)
 d = particle diameter (L)
 C_b = solids packing fraction
 g_c = gravitational acceleration constant (ML/T² F)
 H = height of plug (L)
 ρ = fluid density (M/L³)
 μ = viscosity (M/LT).

In general, the pressure drop across the plug is expected to be great when the solids packing fraction is high.

Erosion of the upper layer of particles may occur when the pressure drop associated with fluid flowing through the plug at the particle settling velocity is less than the pressure required to lift the entire plug as a solid block. That is, erosion might possibly occur when:

$$\left[\frac{150 C_b \mu}{d} + 1.75 \rho V_s \right] \left[\frac{C_b}{(1 - C_b)^3} \right] \left[\frac{V_s H}{d g_c} \right] \leq C_b (\rho_s - \rho_l) g H + \frac{4 \tau_s}{D} \quad (3.40)$$

where V_s = particle settling velocity (L/T)
 ρ_l = liquid density (M/L³)
 ρ_s = solids density (M/L³).

Otherwise, the entire plug will be lifted as a solid mass when the pressure drop across the plug is equal to the sum gravitational head and the force of adhesion of the plug to the wall.

Because there are two possible modes of resuspension, the method of resuspension depends on which mode occurs at the lower pressure drop. In general, dilatant beds of small particles form plugs with extremely small void fractions (Weyl and Ormsby 1960). In this case, the pressure drop through the packed bed is expected to be very large. As a result, the fluid flow rate at low pressure gradients will never be sufficient to lift the top layer of particles, and resuspension will not occur unless the pressure gradient is sufficient to lift the entire plug en masse.

In contrast, materials that form cohesive plugs generally have relatively high void fractions (Weyl and Ormsby 1960), consequently a cohesive plug may be very permeable, provided that the material is not in its gelled state. It is possible that the vibrations that occur during the resuspension attempts may sometimes be sufficient to desolidify the plug and allow resuspension at relatively low fluid velocities provided that the permeability of the plug is high. If not, the plug will not resuspend until the pressure is sufficient to raise it en masse.

The relation in Equation (3.39) suggests that the frictional pressure drop in a porous plug increases monotonically with the solids packing fraction. Thus, the solids volume fraction of the plug is an important factor to determine the permeability of the plug. The particles in dilatant slurries, such as those that contain sand, contact each other when settled. When particles of different sizes are present, it is possible for the fines to fill the voids between large particles and increase solids packing significantly. As a result, porosity may be very small. Vibration of the plug often leads to increased packing by allowing the small particles to trickle down and fill the voids more efficiently; this packing makes the plug less permeable. As a result of low permeability, extremely high pressures are often required to resuspend vertical plugs in dilatant materials.

In contrast, the particles in cohesive materials, such as wet settled clays, are not in contact with each other (Weyl and Ormsby 1960). Thus, the solids volume fraction in clay may be very low. However, the low solids volume fractions in clays does not lead directly to increased permeability because the clays may "gel" when allowed to rest. Permeability is expected to decrease significantly when the material gels; however, the gelled state often may be eliminated by vibrating the clay mixture. The clay then enters the "sol" state. In this case, the permeability of the clay increases dramatically, and may be predicted using Equation (3.39). Because of the low solids loading, clay in its sol state is expected to be very permeable and may be easily resuspended.

It is difficult to apply Ergun's correlation to estimate the pressure drop across a settled plug because the solids packing fraction of the fluid

is not known. In addition, it is not clear that Ergun's correlation applies to cohesive plugs. However, for the case where the mean fluid velocity is 2×10^{-4} m/s (7.21×10^{-4} ft/s) (which is sufficient to lift a $10 \mu\text{m}$ particle with specific gravity of 2), the supernatant viscosity is 2 cP (4.82 lbm/ft-hr), the fluid density is 10^3 kg/m^3 (62.3 lbm/ft^3), the solids specific gravity is 2 and the solids packing is 0.5, the pressure drop per unit height of the plug would be 364 Pa/m. This is significantly smaller than the pressure drop of 5 kPa that could be required to overcome the gravitational head for a 1-m plug. However, the analysis assumes that the major force holding the particle down is gravitational. It is possible that much larger forces are required to break away individual particles. The analysis does suggest that fluid might flow through a loosely packed plug and pick up particles at a pressure gradient that is less than that required to lift the plug en masse. Significantly higher pressure drops would be predicted when the solids packing is high, as might occur for dilatant solids. However, the solids packing used for the calculation appears reasonable for some settled solids in double-shell tank wastes. Low solids packing fractions for settled solids have been reported in 1989 by Petersen, Scheele, and Tingey, who found that settled solids from 101-AZ occupied 48% of a composite core sample while the centrifuged solids occupied only 16%. This suggests that solids packing may be lower than $1/3$, and that the assumption of $C_b = 0.5$ would give an upper bound of the pressure drop across the plug. Thus, the possibility that solids will be eroded from the top of the plug cannot be entirely discounted. This mechanism may, however, not be possible if the pressure drop through the loosely packed cohesive plug is much larger than that predicted on the basis of Ergun's correlation, which seems probable.

The above discussion suggests that movement of dilatant plugs would require that the fluid pressure drop exerted across the plug be equal to the hydrostatic head plus the wall shear stress of the slurry. In this case, the plug would be expected to yield when the pressure gradient dP/dx :

$$\frac{dP}{dx} = C_b(\rho_s - \rho_l)g + \frac{4\tau_s}{D} \quad (3.41)$$

where $C_b = 1$ solids volume fraction.

In which case, the plug would be lifted by bulk resuspension and resuspension would occur at a constant value of the parameter:

$$N_b = \frac{dP/H}{C_b(\rho_s - \rho_l)g + 4\tau_s/D} \quad (3.42)$$

where dP = pressure exerted across the plug (M/TL)

H = height of the plug (L).

The parameter N_b will be called the bulk resuspension parameter. In the limiting case where the shear strength is high, this would vary as

$$N_b \approx N_y = \frac{D}{4} \frac{dP/H}{\tau_s} \quad (3.43)$$

The parameter N_y will be called the yield resuspension parameter to indicate that resuspension occurs when the bonds at the wall yield. When shear strength is negligible, this would vary as

$$N_b \approx N_g = \frac{dP/H}{C_b(\rho_s - \rho_l)g} \quad (3.44)$$

The parameter N_g will be called the gravitational resuspension parameter to indicate that resuspension occurs when the body force is overcome.

The same mechanisms could govern the unplugging of cohesive plugs. However, it is possible that cohesive plugs would be lifted by erosion and in this case would be destroyed at some smaller value of the pressure gradient. If this mechanism is possible, then plugs would be expected to be eroded when the fluid velocity was large enough to lift the particles in the top layer of the plug. In which case plugs would be eroded when the dynamic pressure exerted by the fluid was large enough to overcome the force of gravity acting

on the particle. This would occur when the fluid velocity exceeds the particle settling velocity slightly or when

$$N_s = \frac{V}{V_s} \geq 1 \quad (3.45)$$

where V = fluid velocity (L/T)

V_s = particle settling velocity emerging from the bed (L/T).

N_s will be referred to as the settling parameter because it describes erosion that occurs when the fluid velocity exceeds the settling velocity. The minimum pressure drop across the plug could be obtained by evaluating Ergun's correlation at the particle settling velocity, V_s .

3.4.4 Resuspension of Horizontal Partial Plugs

Partial horizontal plugs may be resuspended by exerting a pressure gradient sufficient to allow the fluid velocity to exceed the critical value for transition from stationary bed to sliding bed flow. Literature providing predictive correlations for this value are sparse; in general, data exists for predicting the critical fluid velocity required to maintain particle suspension rather than the pressure drop that would allow resuspension to be achieved. A number of these methods are discussed by Govier and Aziz (1972) and by Thomas (1979). In the absence of adhesive forces in the plug, the resuspension velocity might be expected to be equal to the critical deposit velocity. If significant adhesive forces are present, the resuspension velocity will exceed the critical deposit velocity.

Some qualitative theories of resuspension may be taken from reports of resuspension in tanks using jets. In 1987 Fow, Scott, Whyatt and Reucker reported that in regions where jet velocity was low, erosion was found to be the dominant resuspension mechanism. Consequently, it might be expected that the minimum requirement for resuspension in pipes would occur when the erosive forces were sufficient to tear away particles and then lift them into the flow.

In a horizontal pipe, fluid flows along the settled bed and there is no mean vertical motion to lift particles against gravity. However, turbulent eddies can occasionally provide sufficient vertical velocity to lift particles. In addition, the turbulent flow causes a shear stress to be exerted on the bed that might be sufficient to tear away particles of the settled material.

In a cohesive plug, erosive forces would be required to break particles away from the settled layer. Assuming that the shear exerted by the fluid was a turbulent wall stress, the shear stress applied by the fluid at the bed surface, τ_w would be equal to:

$$\tau_w = \rho (u^*)^2 \quad (3.46)$$

where τ_w = shear stress exerted at the duct wall (M/LT²)

ρ = fluid density (M/L³)

u^* = friction velocity (L/T).

This velocity is a characteristic velocity for the turbulent eddies in the region of the bed surface (see Figure 3.17a).



a) The upper layer of particles in a cohesive plug will yield when $\tau_w > \tau_s$

b) Particles in the upper layer of a dilatant plug may be lifted by eddies with characteristic velocities, u^* , that exceed the particle settling velocity, V_s , or when $u^* > V_s$

FIGURE 3.17. Mechanisms for the Erosion of Partial Plugs in Horizontal Pipes

In turbulent pipe flows, the friction velocity, u^* , is related to the pressure drop through the relation:

$$f = \frac{dP (D_H/L)}{\frac{1}{2} \rho V^2} = 8 \left(\frac{u^*}{V} \right)^2 \quad (3.47)$$

where f = Darcy friction factor
 D_H = hydraulic diameter (L).

The magnitude of the adhesive forces holding particles to the bed is difficult to quantify. It will be assumed here that the adhesive force holding particles to the bed is proportional to the bed shear strength. In fully developed turbulent flow the plug might be expected to erode when the ratio of the stress exerted at the wall to the shear strength of the settled bed is equal to some constant value. That is, erosion would occur at some magnitude of the parameter N_e :

$$N_e = \frac{\tau_w}{\tau_s} = \frac{\rho (u^*)^2}{\tau_s} \quad (3.48)$$

where τ_s = shear strength of the plug (M/LT²).

Using Equation (3.47), this may be written as:

$$N_e = \frac{f \rho V^2}{8 \tau_s} \quad (3.49)$$

N_e will be referred to as the erosion parameter to denote that the plug is being destroyed by erosive action. In contrast, dilatant plugs would be eroded when the fluid velocity was sufficiently large to lift particles into the flow (see Figure 3.17b). Particles would be expected to be lifted into the flow when the dynamic forces exerted by the turbulent eddies are sufficient to overcome the gravitational force. In this case particles would be lifted

when the ratio of the friction velocity to the settling velocity exceeds one. The parameter describing this balance is defined as

$$\sqrt{N_{te}} = \frac{u^*}{V_s} \quad (3.50)$$

N_{te} will be referred to as the turbulent eddy erosion parameter because it describes an erosive mechanism dominated by lifting of particles by turbulent eddies. Thus, unplugging would then occur at a constant value of the parameter:

$$N_{te} = \frac{f V^2}{8 V_s^2} \quad (3.51)$$

In reality, there are three requirements for turbulent support of particles in pipe flows. These are discussed by Eyster, Lombardo, and Barnhart (1982). The first is that the ratio of the fluctuating velocity to the settling velocity, v'/V_s , must be sufficiently large. The second is that the ratio of the length of the energetic eddies to the particle diameter must be large. Finally, the force exerted by the fluid on the particle must exceed the submerged weight of the particle. This requires that the quantity $v'L/V_s d$ exceed some constant K_3 .

Typical suspension requirements are shown in Figure 3.18. Here suspension will occur only in the region

$$\frac{v'}{V_s} > K_1 \quad (3.52)$$

$$\frac{L}{D} > K_2 \quad (3.53)$$

$$\frac{v'}{V_s} \frac{L}{d} > K_3 \quad (3.54)$$

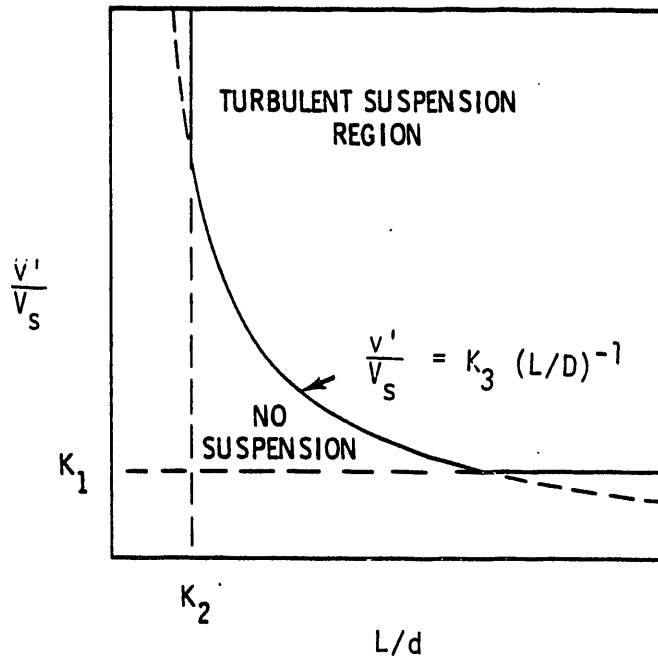


FIGURE 3.18. Necessary Conditions for Turbulent Suspension (Eyler, Lombardo, and Barnhart 1982)

where v' = characteristic velocity fluctuation that is on the order of the friction velocity u^* near the bed wall (L/T)

V_s = settling velocity of particle (L/T)

d = particle diameter (L)

K_1 = constant of unknown value, expected to be order one

K_2 = constant of unknown value, expected to be order one

K_3 = constant of unknown value, expected to be order one

L = characteristic length scale of the turbulent eddies.

In pipe flows, the length scale of the turbulent eddies is on the order of the pipe radius. Consequently, if the double-shell tank slurries contain particles with diameters no larger than $100 \mu\text{m}$, the ratio L/d is expected to be on the order of 250 in a 2-in. pipe. Consequently, the critical condition for resuspension of small particles will be that the ratio of the fluctuating velocity to the settling velocity is sufficiently large.

A method for predicting the pressure drop required to achieve a given flow velocity in a stationary bed flow with saltation in the upper layer is

suggested by Shook and Daniel (1965). In saltating of flow, particles in contact with the lower pipe wall are motionless but particles in the upper layer of the solid bed are occasionally lifted and redeposited. Shook and Daniel's analysis applied to a closed square horizontal duct, but the analysis shares similarities to pipe flow. Shook and Daniel suggests that the pressure gradient is composed of two terms. The first is the shear stress on the duct wall; the second is the shear stress exerted at the bed surface. Shook and Daniel (1965) suggests that the shear stress, τ_w , on the upper wall may be obtained using

$$\tau_w \sim \frac{f \rho v_{mu}^2}{8} \quad (3.55)$$

where f = Darcy friction factor for single-phase fluids
 ρ = fluid density (M/L³)
 v_{mu} = velocity in the unplugged portion of the pipe Q/A_u (L/T)
 A_u = unplugged pipe area.

Shook and Daniel (1965) explains the differences between concentration profiles predicted using a turbulent transport theory to describe particle motions and concentration profiles that have been measured by postulating the existence of a normal dispersive "Bagnold" force at the bed surface. They suggest that the shear stress at the bed surface is equal to

$$\tau = P_b \tan \alpha \quad (3.56)$$

where $\tan \alpha$ = a coefficient of dynamic friction that is a function of a dimensionless group G such that:

$$\begin{aligned} \tan \alpha &= 0.32 \text{ for } G^2 > 3700 \\ \tan \alpha &= 0.75 \text{ for } G^2 < 28 \\ \tan \alpha &= \phi(G^2) \text{ for } 28 < G^2 < 3700 \end{aligned}$$

σ = average distance between particle surfaces (L)
 P_b = Bagnold force at bed surface (M/LT).

$$G^2 = \rho_s P_b b d \sigma / \mu^2 \quad (3.57)$$

where ρ_s = solids density (M/L³)
 d = particle diameter (L)
 μ = viscosity (M/LT).

The total Bagnold force acting on the bed varies as:

$$P_{Bb} = (\rho_s - \rho)g C_b \quad (3.58)$$

Thus, the shear stress exerted on the bed is postulated to be:

$$\tau_b = (\rho_s - \rho)g \tan \alpha C_b h_u \quad (3.59)$$

where $h_u = a - h_b$ (L) = height of unplugged portion of duct
 a = square duct height (L)
 h_b = bed depth (L).

They suggest shear stress on the bed is

$$\tau_b = (\rho_s - \rho_l)g \tan \alpha C_b h_u \quad (3.60)$$

where ρ_s = solids density (M/L³)
 ρ_l = liquid density (M/L³)
 g = acceleration of gravity (L/T²)
 $\tan \alpha$ = coefficient of dynamic friction for the bed
 C_b = solids volume fraction

The total pressure gradient, dP/dx , may then be determined using

$$\frac{dP}{dx} = \frac{\tau_w + \tau_b}{h_u} \quad (3.61)$$

where τ_w = shear stress exerted at the duct wall (M/LT²)
 τ_b = shear stress exerted at the bed (M/LT²).

This model could be used to predict the pressure drop required to produce a fluid velocity that will allow the plug to be overcome by evaluating

Equations (3.55), (3.60), and (3.61) at the velocity required to overcome the plug. Thus, the actual pressure drop required would depend on the height of the settled bed as well as the properties of the bed. In contrast, the velocity required would be a function of properties of the plug only.

3.4.5 Summary of Resuspension Mechanisms

The mechanism for resuspension is expected to differ depending on whether the particles in the plug are cohesive or dilatant and whether the plug is vertical or horizontal. In each case the forces exerted on the particles by the fluid must be sufficiently large to overcome some resistive force.

- Vertical dilatant plug: resuspension is expected to occur when the total pressure exerted by the fluid is sufficient to lift the plug en masse. This requires a pressure equal to the sum of the gravitational head and the pressure required to overcome the adherence of the plug to the wall.
- Vertical cohesive plug: resuspension is expected to occur when the mean fluid dynamic forces are sufficient to lift individual particles by pushing or by channeling.
- Horizontal dilatant plug: resuspension is expected to occur when the turbulent dynamic pressure associated with the eddies near the wall are sufficient to lift particles.
- Horizontal cohesive plug: resuspension is expected to occur when the turbulent stress is sufficient to break particles away from the plug. Because the force of adhesion is difficult to quantify, this is expected to occur when the turbulent shear stress is equal to the shear strength of the plug.

3.5 REVIEW OF TESTING TO DATE

In 1988 Peterson and Powell reported results for transport and resuspension experiments. A review of their work follows.

3.5.1 Transport Experiment Review

The friction factors and loss coefficients in Newtonian and non-Newtonian flows were studied by Peterson and Powell. The objectives of the experiments were to:

- verify/modify Hanks' computer model to correctly predict the required velocity and associated pressure drop for homogeneous slurry transport based on measured rheological properties

- develop a predictive correlation between pressure drop and flow rate for the flow of slurries through actual transfer line jumpers and valves
- determine minimum and maximum acceptable operating flow rates for transporting waste simulants in a pipeline.

A test facility that included pipe diameters of 2-in. and 3-in. was used to obtain friction factor data. Newtonian tests were performed using three fluids that allowed tests to be run at Reynolds numbers between 1200 and 10^5 .

Non-Newtonian experiments were performed with two fluids. If target properties had been attained, the fluid Reynolds numbers for the non-Newtonian tests would have fallen between 1.3×10^3 and 2.5×10^4 . Hedstrom numbers achieved using the first fluid would have been 1.1×10^5 and 2.5×10^5 . The Hedstrom numbers using the second fluid would have been 1.2×10^5 and 2.7×10^5 . Because measured fluid properties varied, it is difficult to quantify the exact range of Reynolds and Hedstrom numbers obtained during the experiments.

The wide scatter in the data reported by Peterson and Powell resulted primarily from the use of absolute pressure transducers to measure the pressure drop across the pipe components. The resolution achieved with some of these transducers was not sufficient to produce reliable data. Typical values of the absolute pressure readings measured at the upstream and downstream locations used to determine the friction factor in fully developed flow are provided in Tables 3.5 and 3.6. Data in Table 3.5 show the most challenging case in terms of obtaining good accuracy in the pressure drop measurement in Newtonian flow as a percentage of full-scale. Data in Table 3.6 show one of the less challenging cases.

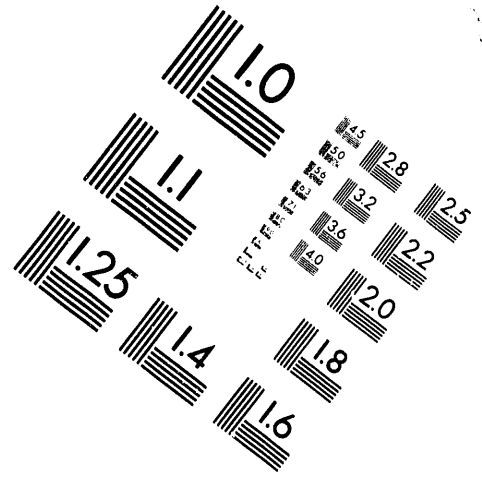
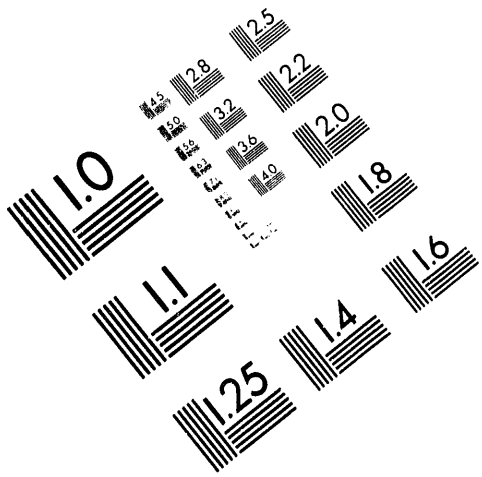
The use of absolute pressure transducers required the selection of transducers capable of measuring the maximum expected absolute pressure that might be achieved at a particular location in the pipe. Pressure transducers selected had full-scale readings of 10 psig and accuracies equal to 0.3% (0.03 psig). The accuracy achieved for the actual pressure drop measurement



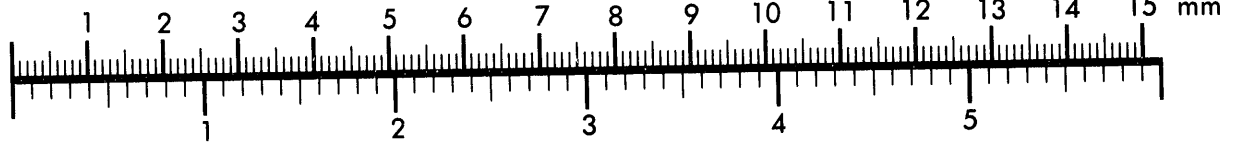
AIM

Association for Information and Image Management

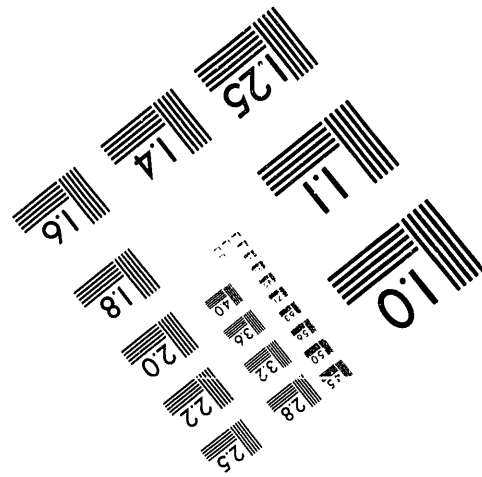
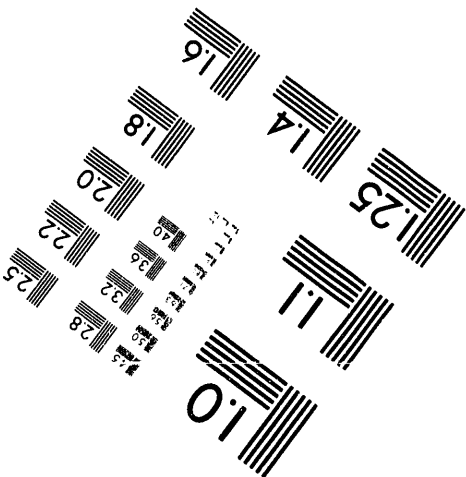
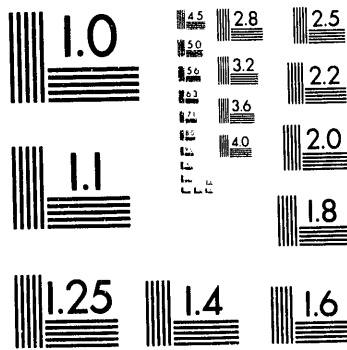
1100 Wayne Avenue, Suite 1100
Silver Spring, Maryland 20910
301/587-8202



Centimeter



Inches



MANUFACTURED TO AIM STANDARDS
BY APPLIED IMAGE, INC.

2 of 2

TABLE 3.5. Accuracy of the Pressure Transducers Used to Measure the Friction Factor in Fully Developed Flow of Water in 3-in. Pipe at 20 gal/min (Most difficult case for achieving good resolution.)

<u>Location</u>	<u>Pressure Measured, psi</u>	<u>Absolute Accuracy, psi</u>		<u>Accuracy as a Fraction of the Reported Measurement dP/P, %</u>	
		<u>Achieved</u>	<u>Manufacturer's Specifications</u>	<u>Achieved</u>	<u>Manufacturer's Specifications</u>
P1	0.70	±0.43	±0.03	±61.4%	±4.3%
P2	0.73	±0.43	±0.03	±58.9%	±4.1%
P1-P2	-0.03	±0.61	±0.042	±2030%	±235%

TABLE 3.6. Accuracy of the Pressure Transducers Used to Measure the Friction Factor for 80% Glycerol Flowing through a 3-in. Pipe at 89.3 gal/min (Less difficult Newtonian case)

<u>Location</u>	<u>Pressure Measured, psi</u>	<u>Absolute Accuracy, psi</u>		<u>Accuracy as a Fraction of the Reported Measurement dP/P, %</u>	
		<u>Achieved</u>	<u>Manufacturer's Specifications</u>	<u>Achieved</u>	<u>Manufacturer's Specifications</u>
P1	5.72	±0.43	±0.03	±7.51%	±5.2%
P2	5.17	±0.43	±0.03	±8.32%	±5.8%
P1-P2	0.55	±0.61	±0.042	±111%	±7.6%

expected using these transducers would be 0.042 psig.(a) The frictional pressure drop in the case of water flowing at 20 gal/min through a 32-ft long, 3-in. diameter pipe is expected to be approximately 0.018 psig. Consequently, the accuracy expected for the quantity of interest was ±235%. This was the level of accuracy that would have been obtained if the accuracy given in the manufacturer's specifications had been achieved. It is clear that the experiment, as designed, could not have produced reliable measurements of the

(a) The resolution for a differential pressure measurement is equal to the square root of the sum of the squares of resolution of the individual measurements when the errors in two measurements are uncorrelated.

friction factor for this case. Peterson and Powell reported that the accuracy achieved using the transducers was degraded during testing. Each pressure measurement had an accuracy of ± 0.43 psig.

The reported values for the accuracy achieved using the pressure transducers in the experiment are shown in Tables 3.5 and 3.6. The accuracy actually achieved during testing was degraded by a number of factors. Peterson and Powell report that the following factors affected the accuracy of the pressure measurements.

- Entrained air bubbles in the test section affected the pressure measurements when bubbles accumulated in the region of the pressure transducers.
- Pressure pulses induced by the Moyno pump reduced resolution of the pressure measurement.
- The pressure transducer calibration curve was suspected to have shifted during testing.

These sources of error could be eliminated by altering the test section. Trapped air could be eliminated by adding a bleed valve to the test section. Pressure pulses could be reduced by using a centrifugal pump. Finally, calibration drift could be easily detected by checking that a zero reading is obtained when no flow is present and installing a bank of manometers and comparing differential pressure readings taken using the transducers to those taken using the manometers. Significant discrepancies would indicate calibration shift.

Additional difficulties arose during the non-Newtonian experiments. The simulant properties obtained at bench-scale were not replicated at lab-scale. Consequently, the target simulant properties were not attained. Tests were conducted using simulants with nearly identical yield strengths that resulted in replication of data. Based on the experience of Peterson and Powell, it is recommended that the material properties be measured prior to the onset of testing and if required that the lab-scale recipe be modified prior to testing.

In the final analysis, the results of Peterson's and Powell's experiments were not sufficiently accurate to allow prediction of the pressure losses in the Hanford transport lines. The experiment must be improved in two major

areas. The test loop must be modified to provide more accurate pressure drop measurements and more attention must be paid to simulant preparation to ensure that target properties are met.

3.5.2 Resuspension and Plugging Experiment Review

The pressure gradient required to achieve resuspension was examined by Peterson and Powell. The objectives of the experiments were to:

- develop a basis for determining the velocity and pressure drop required to resuspend settled solids
- relate the settled solids flow behavior to the velocity required to resuspend the solids and the associated pressure drop
- evaluate the susceptibility to plugging for various pipe components and configurations.

The requirements for resuspension were studied by first allowing solids to settle into a bed, then allowing water to flow at a predetermined volumetric flow rate through the test section. The maximum pressure applied to the entire flow loop and the time required to achieve resuspension were monitored during a resuspension test. The time rate of change of the maximum pressure was reported.

The test plan called for the use of two dilatant simulants with different shear strengths. It was expected that a fluid with a higher shear strength simulant would be more difficult to resuspend than one with a lower shear strength. However, the shear strengths of the dilatant fluids measured after testing were not found to match those measured prior in the laboratory. This discrepancy resulted in uncertain values of the shear strength during testing; thus, interpretation of the data was difficult.

Fluids that exhibit pseudoplastic behavior are generally observed to be cohesive. Thus, because double-shell tank slurries have been observed to exhibit pseudoplastic behavior, they are expected to form cohesive rather than dilatant plugs. The test performed could be improved by studying the resuspension of cohesive materials (which are more indicative of actual wastes), rather than dilatant materials (which are easier to resuspend). Two

materials with differing shear strengths could then be manufactured; this would lead to greater reproducibility of the shear strength because shear strength is a property of a cohesive material.

The results of the resuspension study should be presented for individual pipeline components. The total pressure drop across the experimental flow loop is of little interest to designers because this value factors in the pressure drop across straight pipe, elbows, connectors, and other features arranged in an uncontrolled fashion. This information is difficult to interpret because the requirements for unplugging a horizontal pipe may differ drastically from the requirements for unplugging some other component, such as a vertical pipe or an elbow. More useful information may be obtained by examining the unplugging requirements for individual components and reporting the pressure gradient and flow rate required to unplug the component.

The instrumentation to monitor pressure drops across each component was available in the test performed by Peterson and Powell. Stripchart recordings of each pressure transducer reading were provided in the Appendix of their draft report. However, only the overall pressure drop was analyzed and reported. In principle, the data obtained by Peterson and Powell could be reanalyzed. However, because the same transducers used in the transport experiment were used in the resuspension experiment, it is unlikely that the data obtained will be of sufficient accuracy to provide useful information. In addition, because the shear strength of the plug is unknown, interpretation of the data would not be possible.

In summary, the tests reported by Peterson and Powell did not result in information that could be used to predict the pressure gradient needed to unplug the transport lines because: the experiments did not achieve the appropriate simulant properties, the mode of data presentation was too general, and accuracy of the data was likely to have been inadequate.

4.0 NEWTONIAN AND NON-NEWTONIAN TRANSPORT EXPERIMENTS

In this section the details of the Newtonian and non-Newtonian transport experiments are described including: experiment objectives, equipment, simulants, test approach and data analysis, anticipated results, and experiment limitations.

4.1 OBJECTIVES

Proper design of waste slurry transport lines requires accurate prediction of the pressure losses during operation. This information can be used to determine the pumping capacities needed and to ensure that excess pressure losses do not occur in the lines. Currently accepted engineering design methods allow the pressure losses in fully developed pipes to be predicted with confidence when the fluid flowing through the transport lines is Newtonian. Difficulties in predicting pressure losses in Newtonian flows arise only when unique flow components that have not been well characterized are added to the lines. In general, pressure drops in Newtonian flows can be predicted with confidence.

Prediction of the pressure drop in non-Newtonian flows is more challenging. A correlation for friction factors in non-Newtonian flows has been suggested (Hanks 1978). However, this correlation has been verified using Bingham plastic (Hanks and Pratt 1967) and power law fluids (Hanks and Ricks 1975) but has not been verified for yield pseudoplastic fluids. Consequently, it is not clear that Hanks' correlation may be used to predict pressure drops in yield pseudoplastic fluids. In addition, Hanks' correlation does not predict the effect of non-Newtonian behavior on the loss coefficients that occur in components such as elbows, valves, and connectors nor does it predict the effect of pipe relative roughness ϵ/D . Testing is required both to verify Hanks' correlation and to quantify the component loss coefficients. If verified, Hanks' correlation may be used to predict the pressure losses during slurry transport.

It is currently thought to be important that the slurries flow in the turbulent regime to ensure that particles remain suspended. A theory for the transition to turbulence for a non-Newtonian slurry has been proposed by Hanks

(1978) but has not been verified for yield pseudoplastic fluids. The theory suggests that the critical Reynolds number increases with Hedstrom number. Thus, the critical Reynolds number would be larger for yield pseudoplastic than for Newtonian fluids; this suggests that if turbulence is important to maintain suspension, then greater stratification may occur in non-Newtonian slurries than in Newtonian slurries at equal Reynolds numbers. Because the theory has not been verified for use with yield pseudoplastic slurries, the Reynolds number at which non-Newtonian pipe flows become turbulent cannot be predicted. Because transition to turbulence is somewhat random in Newtonian flows, randomness in the transition to turbulence is also expected in non-Newtonian flows. However, some information bracketing the Reynolds number at which the flow becomes turbulent is required to allow specification of the minimum flow rates that will allow turbulence to be maintained. In addition, tests are required to determine the transition to turbulence for two reasons. First, operating in the turbulent range is expected to decrease the degree of stratification. It would be useful to know when transition to turbulence occurs to allow conservative design of the slurry transport pipeline. Second, even in the case of slurries that are transported homogeneously in the laminar range, knowledge of the critical Reynolds number for transition is necessary for prediction of the pressure drop characteristics.

Although turbulence is not a necessary condition for particle suspension (Thomas 1979), it appears to enhance the ability of the fluid to suspend particles. Consequently, the critical Reynolds number for transition to turbulence should be determined. Operating above this Reynolds number may be important if slurries containing larger particles are ever transported across the Hanford Site.

4.1.1 Newtonian Flow Experiments

Experiments will be conducted using Newtonian and non-Newtonian fluids in a pipe network. The primary objectives of the Newtonian experiments are to:

1. Determine the magnitude of component loss coefficients in Newtonian flow for components such as elbows and connectors. Components that are unique

to the Hanford cross site transfer lines will be included in this study. These components include

- one Pittsburgh brass 3-in. diameter three-way ball valve
- one 3-in. diameter expandable jumper cable
- one PUREX connector
- one 3-in. diameter expansion loop
- one elbow.

2. Measure baseline friction factors in Newtonian fluids at a number of Reynolds numbers. These measurements will allow the roughness of the corroded pipes used in the test facility to be determined.

The first objective will provide baseline values of the loss coefficients for system components; these values will later be compared to the values obtained in the non-Newtonian experiments. The second objective will allow the pipe roughness to be stated; this information is important if the effect of pipe roughness on the friction factor in non-Newtonian flows is to be determined.

The Newtonian experiments will be considered complete when:

1. the results for the friction factors in fully developed flow are shown to be well represented by the Colebrook equation (or Moody diagram)
2. component loss coefficients for the non-unique components are reported and shown to be similar in magnitude to those reported for similar components in the literature (see Table 3.2)
3. component loss coefficients for the unique components are reported.

In addition, the Newtonian experiments will be used to verify test system performance. Verification of the system performance is essential to achieve all other objectives. Non-Newtonian experiments will not be undertaken with an unverified system.

4.1.2 Non-Newtonian Flow Experiments

The primary objectives of the non-Newtonian experiments are to:

1. measure the pipe friction factor for fully developed flow of a non-Newtonian fluid through a circular pipe. (Measurements will be performed at a number of bulk flow Reynolds numbers using two different pseudoplastic fluids, two pipe diameters, and two pipe roughness factors.)

2. measure the component loss coefficients for a number of components
3. bracket the critical Reynolds number for transition to turbulence.

The information obtained in this experiment will allow designers to predict pressure drops in the transport of either Newtonian or non-Newtonian wastes through pipelines and to ensure that flow in the transport lines is turbulent.

The non-Newtonian experiments will be considered complete when:

1. friction factors in fully developed flow at the test Hedstrom numbers, Reynolds numbers, and roughness factors are reported
2. the reliability of Hanks' correlation for predicting the friction factors in both smooth and rough pipes is assessed and reported (the correlations will be more limited in scope than Hanks' theory)
3. if Hanks' correlation is found to be unreliable, correlations based on the friction factor data will be generated and reported
4. component loss coefficients for all components in the system are calculated and reported.

Item 4 will include comparison of the loss coefficients to the values for the identical components measured in Newtonian flows.

4.2 EQUIPMENT AND SIMULANT DESCRIPTION

The experimental test facility must provide conditions that allow the friction factors in fully developed flow and the component loss coefficients associated with components to be measured accurately. On a practical basis, three requirements are necessary: 1) selection of pressure transducers with sufficient accuracy to measure the design pressure drops, 2) calibration of the pressure transducers and flowmeters, and 3) verification that fully developed flow has been attained in the regions in which friction factors are measured, and that the pressure transducer used to measure the pressure downstream of a flow component is situated so that the entire excess pressure gradient associated with the component is measured. Failure to properly locate pressure transducers would lead to excessively high measurements for the friction factors in fully developed flow and to excessively low measurements of the loss coefficients for the components.

4.2.1 Equipment Description

The test section must include components that are typical of those in the transport lines. These components include elbows, ball valves, purex connectors, and expansion loops. In addition, the pipes used should replicate the roughness characteristics of pipes on the Hanford Site. A commercial steel pipe with a diameter of 2 in. has a relative roughness of 0.0009. In Newtonian flows, the Darcy friction factor for this pipe with a diameter of 2 in. at a Reynolds number of 10^5 is approximately $f = 0.022$. An attempt was made to measure the roughness of a corroded pipe using a Surfindicator^(a) instrument. However, the extent and thickness of the scale was such that the measurement could not be made. The roughness height was measured visually to be between 1/32 in. and 1/16 in. A roughness of 3/64 in. in a 2-in. pipe results in a relative roughness of 0.024; this would result in a friction factor of approximately 0.052. Thus, pipe roughness may increase the friction factor by as much as 140%. Thus, the effect of roughness may be significant and must be examined in the non-Newtonian case. The roughness of pipes in the full-scale transfer lines is not well known, and may vary. Consequently, tests must be performed using both the greatest probable roughness and the least probable roughness in the transport lines.

In addition, the rheological properties and densities of the simulants used in this study must span the range that may reasonably be expected of double-shell tank slurry wastes. This simulant range will allow the results of this experiment to be applied to predict pressure drops in the Hanford cross site transfer lines. Double-shell tank slurries have been shown to exhibit yield pseudoplastic behavior and are believed to contain sufficiently small particles to flow in a pseudohomogeneous fashion. Simulants that replicate these characteristics must be developed and used during testing.

The test equipment used in this experiment will be similar to that used in the study performed by Peterson and Powell in 1988. Changes will be incorporated to increase the accuracy of the results. These changes apply primarily to the length of the straight horizontal pipe; the distance

(a) Brush Electronics Company, Division of Clevite Corporation, Cleveland, Ohio.

separating the flow components; the type, number, and placement of the pressure transducers; and the type of pump used.

The test facility requires a pipe flow loop consisting of the following components:

- one 60-ft, straight horizontal pipe
- one centrifugal pump capable of providing flow rates from 20 gal/min to 100 gal/min
- one hold tank of sufficient volume to contain the required amount of simulant
- special fittings and components including one elbow, one PUREX connector, two ball valves and one expansion loop
- two differential pressure transducers for each set of pressure measurement to be performed (18 differential pressure transducers)
- one flowmeter to measure the volume flow rate of fluid in the test loop.

Tests will be performed using four different 60-ft straight horizontal pipes; these will be composed of 1) a 2-in. carbon steel pipe, 2) a 3-in. carbon steel pipe, 3) a 2-in. roughened pipe, and 4) a 3-in. roughened pipe. These pipes will represent two smooth and two rough conditions. In the current plan the flow loop will contain only one 60-ft straight horizontal pipe for each test. This pipe will be changed as required for the different tests. If possible, the flow loop will be configured to allow simultaneous installation of at least two and possibly all four pipes. This would significantly reduce the time required to perform tests but would also require a much larger test area and holding tank.

The fluid properties to be measured are:

- density, ρ , and viscosity, μ , as a function of temperature for the Newtonian fluids
- density, ρ ; yield stress, τ_y ; consistency index, K; and flow behavior index, n, for the non-Newtonian fluids.

The effect of temperature variation on these properties will be measured.

Fluid density will be monitored during testing to verify that this property is not changing due to evaporation. Other rheological properties will be measured before and after each transport experiment. In addition, the fluid temperature will be monitored continuously and will be recorded each time pressure data are collected.

Seven key changes to the existing facility are recommended to ensure the success of these experiments. The justification for these changes is provided below.

1. The length of the straight horizontal pipe section will be increased from 32 ft to 60 ft.

At least one straight horizontal section of sufficient length to allow measurement of the pressure drop in fully developed flow is required. Calculations of the developing length based on information in single-phase flow indicate that 30 ft of pipe are required to ensure fully developed flow in a 3-in. pipe at a Reynolds number of 2000. Once flow has developed, the remaining portion of the test section must be sufficiently long to allow the pressure drop achieved to be measurable. The minimum pressure drop will occur in the test with the lowest viscosity fluid flowing at the minimum flow rate. Calculation of the pressure drop indicates that 25 ft are required after fully developed flow is reached to measure the friction factor, f , within 10% for the most challenging case proposed.

Because the maximum developing length and minimum pressure gradient do not occur in the same test case, it is possible to reduce the total pipe length required for accurate measurement of the pressure drop. In Newtonian flow using the pipe diameters and fluids proposed, the required length is 36 ft.

The relationship between the Reynolds number and the developing length in a non-Newtonian flow is not known. If it is assumed that transition occurs near a Reynolds number of 8000, as indicated from Hanks' curves, the developing length in the Newtonian cases could be as much as 120 ft in a 3-ft pipe at transition. This estimate is based on the assumption that:

$$L/D = 0.06 \text{ Re}_p \quad (4.1)$$

where L = pipe length (L)
 D = pipe diameter (L)
 Re_p = pseudoplastic Reynolds number

which is similar to the relation describing the developing length in Newtonian flow.

This 120 ft length may be significantly greater than the actual developing length for a number of reasons. The difference in developing length in the two flow regimes is primarily caused by the differences between the shape of the fully developed velocity profile in laminar and turbulent flow. The Newtonian flow relationship assumes that boundary layers form when fluid enters the pipe. Fully developed flow is reached when the boundary layers thickness grows to a thickness of one radius and reaches the pipe center. When a fluid has a yield stress, an unsheared core forms in the pipe center. The size of this unsheared core increases with increasing Hedstrom number. If an analysis of boundary layer growth equivalent to that used in Newtonian fluids is performed, the fully developed state would occur when the boundary layers reach the unsheared core. This condition would occur at a shorter distance than required for the boundary layers to grow to a full radius.

Because of the uncertainty in the developing length in non-Newtonian flow, it is recommended that the pipe length used be 50% larger than actually required for the Newtonian tests. Thus, a length of 54 ft is recommended. The pressure will be monitored at an intermediate point to detect whether or not the pressure gradient is fully developed.

2. Increasing the distance between pipe components.

It is important that each component be outside the developing region of any other component and that the downstream pressure measurement be taken at a point where the flow is fully developed. Consequently, at least 10 pipe diameters should be allowed upstream of each component and at least 40 pipe diameters should be allowed downstream. For a 3-in. diameter pipe, 10 ft of straight pipe will be required downstream of each component. It is assumed in making this recommendation that interest in the component loss coefficients is limited to turbulent flow regimes; in the turbulent regime, flow is expected to develop fully in 40 pipe diameters. Accurate measurement of the loss coefficients in the laminar region would require as much as 120 pipe diameters of straight pipe downstream of each component. Allowing 30 ft of pipe between each component is not thought to be practical; therefore, loss coefficients will only be measured in the turbulent flow regime.

3. Replacing the absolute pressure transducers used to measure the pressure drop with differential pressure transducers.

Poor resolution in the determination of the differential pressure resulted in significant scatter in the data reported by Peterson and Powell. Use of differential pressure transducers rather than absolute pressure transducers provides increased accuracy in the measurement of the pressure losses. The accuracy of measurements using absolute pressure transducers is significantly degraded by the need to subtract two measurements; subtraction of two measurements containing random amounts of error generally increases the error in the derived quantity by at least

a factor equal to the square root of 2. In the case of the pressure measurements performed here, an even greater amount of error is likely to be introduced by the use of two absolute pressure transducers because of the need to obtain transducers with higher full-scale readings. The effect of using absolute pressure transducers was discussed in Section 3.5.

Preliminary calculations have been performed to allow selection of the appropriate pressure transducers. The minimum pressure drop across the 30 ft of pipe, expected to be approximately 120 Pa, occurs for the case where water flows through a 30-ft long, 3-in. diameter pipe at 20 gal/min. A resolution of 10 Pa would allow the pressure drop to be measured to within 10%. This percentage is considered the maximum acceptable uncertainty in the differential pressure measurement. The pressure drops expected in all other Newtonian test cases are shown in Table 4.1.

Low range wet/wet differential pressure transducers that allow full-scale measurements from 0.5 to 2.5 psid (3.45 kPa to 17.2 kPa) with a resolution of 0.25% of full-scale are available from SENSOTEC(a). These transducers would provide a resolution of 0.00125 psid (8.9 Pa) when set to a full-scale reading of 0.5 psid. The accuracy of all proposed friction factor measurements can be kept within 10% using this instrument. (See the Appendix for uncertainty analysis.)

Because the accuracy of commercial transducers is generally limited to some fraction of full-scale, selection of pressure transducers with lower full-scale readings could result in better accuracy; their availability will be investigated. Differential pressure transducers with full-scale pressure readings of as little as 0.2 psid are available from Honeywell(b). However, engineers who have used these instruments report that these transducers exhibit almost daily calibration drift. Suspected shifts in the transducer calibration was one of the reported reasons for poor accuracy in Peterson and Powell. Use of slightly less sensitive transducers with stable calibration curves is considered preferable here.

4. Increasing the number of pressure taps at which pressure will be measured.

Because the friction factors of interest are those in fully developed flow, fully developed flow must be experimentally verified. If flow is not fully developed, the friction factors measured in the lab will exceed those observed in the field. In contrast, if measurements of the component loss coefficients are taken without allowing the flow to become fully developed, the measured loss coefficients will underpredict the pressure losses in the field. In either case, it is important to verify

(a) Registered trademark of SENSOTEC Incorporated, Columbus, Ohio.

(b) Honeywell, Incorporated, Fort Washington, Pennsylvania.

TABLE 4.1. Uncertainty for Newtonian Pipe Flow Experiments

Fluid	Flow Rate, Q , gal/min	Pipe Diameter, D , in.	Density, ρ , kg/m ³	Viscosity, μ , Pa s	olds Number	Friction Factor	Distance Between Taps, L , ft	Expected Differential Pressure dp , psi	Expected Accuracy of Transducer Measurement, dP_{err}	Accuracy as % of Differential Pressure dP_{err}/dP
Water	20	3	1000	0.001	2.11E+04	0.026	30	1.73E-02	1.25E-03	7.21
	30	3	1000	0.001	3.16E+04	0.023	30	3.45E-02	1.25E-03	3.62
	40	3	1000	0.001	4.22E+04	0.022	30	5.07E-02	1.25E-03	2.13
	50	3	1000	0.001	5.27E+04	0.021	30	6.75E-02	1.25E-03	1.43
	60	3	1000	0.001	6.33E+04	0.020	30	1.29E-01	1.25E-03	1.04
	70	3	1000	0.001	7.38E+04	0.019	30	1.55E-01	1.25E-03	0.81
	80	3	1000	0.001	8.44E+04	0.019	30	2.03E-01	1.25E-03	0.62
	90	3	1000	0.001	9.49E+04	0.018	30	2.43E-01	1.25E-03	0.51
	100	3	1000	0.001	1.05E+05	0.018	30	3.00E-01	1.25E-03	0.42
	Water	20	2	1000	0.001	3.16E+04	0.026	30	1.32E-01	1.25E-03
30		2	1000	0.001	4.75E+04	0.023	30	2.62E-01	1.25E-03	0.48
40		2	1000	0.001	6.33E+04	0.022	30	4.45E-01	1.25E-03	0.26
50		2	1000	0.001	7.91E+04	0.021	15	3.32E-01	1.25E-03	0.38
60		2	1000	0.001	9.49E+04	0.020	15	4.58E-01	1.25E-03	0.27
70		2	1000	0.001	1.11E+05	0.019	15	5.89E-01	1.25E-03	0.21
80		2	1000	0.001	1.27E+05	0.019	9	4.62E-01	1.25E-03	0.27
90		2	1000	0.001	1.42E+05	0.018	6	3.69E-01	1.25E-03	0.34
100		2	1000	0.001	1.58E+05	0.018	6	4.58E-01	1.25E-03	0.27

TABLE 4.1. contd

Fluid	Flow Rate, Q, gal/min	Pipe Diameter, D, in.	Density, ρ , kg/m ³	Viscosity, μ , Pa s	Reynolds Number	Friction Factor	Distance Between Taps, L, ft	Expected Differential Pressure dP, psi	Expected Accuracy of Transducer Measurement, dPerr	Accuracy as % of Differential Pressure dPerr/dP
70% glycerol	20	3	1181	0.0195	1.28E+03	0.050	30	3.94E-02	1.25E-03	3.17
	30	3	1181	0.0195	1.92E+03	0.033	30	5.91E-02	1.25E-03	2.11
	40	3	1181	0.0195	2.56E+03	0.025	30	7.88E-02	1.25E-03	1.59
	50	3	1181	0.0195	3.19E+03	0.044	30	2.16E-01	1.25E-03	0.58
	60	3	1181	0.0195	3.83E+03	0.039	30	2.76E-01	1.25E-03	0.45
	70	3	1181	0.0195	4.47E+03	0.038	30	3.66E-01	1.25E-03	0.34
	80	3	1181	0.0195	5.11E+03	0.036	30	4.53E-01	1.25E-03	0.28
	90	3	1181	0.0195	5.75E+03	0.035	15	2.79E-01	1.25E-03	0.45
	100	3	1181	0.0195	6.39E+03	0.034	15	3.35E-01	1.25E-03	0.37
	70% glycerol	20	2	1181	0.0195	1.92E+03	0.033	30	2.00E-01	1.25E-03
30		2	1181	0.0195	2.88E+03	0.044	15	2.96E-01	1.25E-03	0.42
40		2	1181	0.0195	3.83E+03	0.037	15	4.42E-01	1.25E-03	0.28
50		2	1181	0.0195	4.79E+03	0.037	9	4.15E-01	1.25E-03	0.30
60		2	1181	0.0195	5.75E+03	0.035	6	3.77E-01	1.25E-03	0.33
70		2	1181	0.0195	6.71E+03	0.032	6	4.69E-01	1.25E-03	0.27
80		2	1181	0.0195	7.67E+03	0.031	3	2.97E-01	1.25E-03	0.42
90		2	1181	0.0195	8.63E+03	0.030	3	3.63E-01	1.25E-03	0.34
100		2	1181	0.0195	9.58E+03	0.030	3	4.48E-01	1.25E-03	0.28

that the flow is fully developed. Verification will be particularly important during the non-Newtonian tests because no reliable predictions of the developing length for non-Newtonian flows exist.

The pressure taps will be installed on a straight pipe (as shown in Figure 4.1) and on all components. In each case taps 1 and 3 will be used to determine the actual pressure loss in the component. Taps 2 and 3 will be used to verify that the flow is fully developed. It is important to note that the accuracy in the determination of the mean pressure gradient between points 2 and 3 will be less than that reported for the measurement using taps 1 and 3. Statistical methods will be used to compare the two pressure gradient measurements to determine if there is a significant difference in the two pressure gradients. If there is significant difference, the flow will not be considered fully developed, and this will be noted in the report. However, it is currently thought that the length provided is sufficient to ensure flow development. Multiple taps will be installed in the test pipe to allow the distance between the taps to vary from experiment to experiment. Multiple taps are required to allow the use of identical transducers in all tests.

5. Replacing the Moyno pump used with a centrifugal pump.

Peterson and Powell reported excessive pressure fluctuations in the lines when a Moyno pump was used, that degraded the resolution of pressure measurements. In addition, the pulsations induced by the progressive cavity pump may be expected to facilitate resuspension in the second portion of the experiment. The pulsations may have produced unrealistically optimistic prediction for the pressure drop required to resuspended slurries in the Hanford transport lines. Consequently, it is recommended that a centrifugal pump that does not induce abnormal pressure pulses be used in this experiment. An additional advantage of the centrifugal pump is that it will allow any pressure surges that occur in the test section to be similar to those in actual transport lines where a centrifugal pump is used.

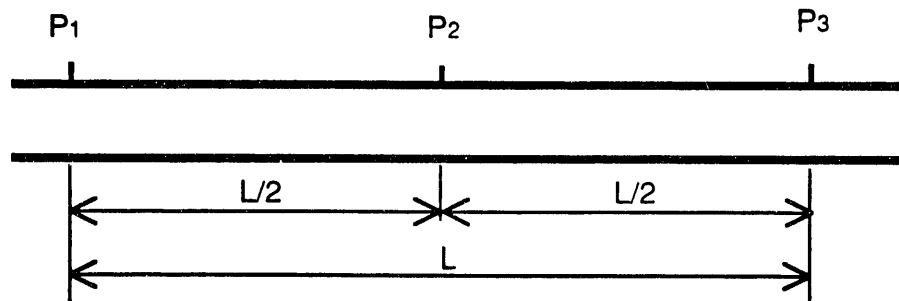


FIGURE 4.1. Example of Pressure Tap Installation

6. Bleed valves will be added to the high point of the test section to allow air introduced into the system to be released.

Peterson and Powell noted that air trapped in the test section significantly deteriorated the accuracy of pressure measurements in the first experimental study of friction factors in non-Newtonian flows.

7. A bank of manometer tubes will be added to the system to verify that no calibration drift has occurred.

The measurements obtained with the manometers will be used to check the pressure transducer measurements on a daily basis. This check will detect any calibration drift before the accuracy of the measurements has been degraded.

4.2.2 Fluids Used in Testing

Newtonian tests will be performed using two liquids: water and a 70% solution of glycerol in water. The proposed fluids have been selected to provide a wide range of Reynolds numbers during testing. The Reynolds numbers achieved with these liquids in the 2-in. and 3-in. pipes at the maximum and minimum flow rates delivered by the pump are shown in Table 4.2. Laminar and turbulent tests will be performed with glycerol; only turbulent tests will be performed with water because of the low viscosity of this fluid.

Measurements of the viscosities of wastes indicates that the viscosities of the Newtonian wastes are as low as 1 cP for diluted waste from 103-SY and as high as 85 cP for an undiluted sample from 103-SY measured by Fow, Scheele, McCarthy, Thornton, Heath, and Scott in 1986. If these wastes are pumped

TABLE 4.2. Range of Reynolds Numbers Achieved Using Proposed Newtonian Fluids

<u>Fluid</u>	<u>Kinematic Viscosity at 20°C, m²/s</u>	<u>Flow Rate, gal/min</u>	<u>Reynolds Number</u>
70% glycerol	16.5 x 10 ⁻⁶	20	1300
70% glycerol	16.5 x 10 ⁻⁶	100	9.6 x 10 ³
water	1 x 10 ⁻⁶	20	2.1 x 10 ⁴
water	1 x 10 ⁻⁶	100	1.6 x 10 ⁵

through either 2-in. or 3-in. pipes at flow rates between 65 and 100 gpm, the flow Reynolds numbers will fall between $Re = 800$ for the more viscous slurries in the larger pipes and $Re = 1.6 \times 10^5$ when the less viscous slurries are pumped at high flow rates through the smaller pipes. Data is required in the entire Reynolds number range of interest.

The proposed Newtonian tests will allow data to be collected in the Reynolds number range between $1300 \leq Re \leq 1.6 \times 10^5$ with no significant gaps. Thus, data will be collected in the entire turbulent range and some data will be collected in the laminar range of interest. This wide Reynolds number range will be spanned using only two fluids by varying the flow rate between 20 gpm and 100 gpm. Spanning the Reynolds number range of interest and maintaining volumetric flow rates near the flow rates used in actual transport would require the use of numerous fluids.

The Hedstrom numbers and Reynolds numbers for the two non-Newtonian fluids based on target properties recommended (but not achieved) by Peterson and Powell, are shown in Table 4.3. Use of these simulants will allow measurements at four Hedstrom numbers and two consistency indices. The four Hedstrom numbers will be 1.1×10^5 , 2.5×10^5 , 1.2×10^5 , and 2.7×10^5 . Reynolds numbers will range from 1.3×10^3 to 2.5×10^4 during testing. Thus, the Reynolds number range achieved using the Newtonian simulants will completely span the Reynolds numbers achieved using the non-Newtonian simulants.

Although the minimum transport velocity, V_{m2} , is important in proper design of transport lines, this test is not designed to determine the actual magnitude of this quantity for arbitrary slurries. Rather, it is designed to allow measurement of the friction factor for actual wastes. Selection of particles with settling characteristics that match those in real wastes is critical for obtaining accurate data because the friction factor curves are expected to be strongly affected by the flow regime.

Currently, all wastes are expected to be transported in suspended regimes. The flow regime that is achieved during testing will be monitored to verify that particles are fully suspended. It is anticipated that the friction factor

TABLE 4.3. The Hedstrom Numbers and Reynolds Numbers for the Two Recommended Non-Newtonian Test Fluids

Fluid	Flow Rate, Q, gal/min	Pipe Diameter, D, in.	Density, ρ , kg/m ³	Consistency Index, Pa s ⁿ	Flow Behavior Index, n	Yield Stress, Pa	Hedstrom Number, He	Reynolds Number, Re
Transport simulant 1	10	3	1200	0.07	0.60	2.00E+00	2.48E+05	4.81E+02
	20	3	1200	0.07	0.60	2.00E+00	2.48E+05	1.27E+03
	30	3	1200	0.07	0.60	2.00E+00	2.48E+05	2.24E+03
	40	3	1200	0.07	0.60	2.00E+00	2.48E+05	3.35E+03
	50	3	1200	0.07	0.60	2.00E+00	2.48E+05	4.57E+03
	60	3	1200	0.07	0.60	2.00E+00	2.48E+05	5.91E+03
	70	3	1200	0.07	0.60	2.00E+00	2.48E+05	7.33E+03
	80	3	1200	0.07	0.60	2.00E+00	2.48E+05	8.83E+03
	90	3	1200	0.07	0.60	2.00E+00	2.48E+05	1.04E+04
	100	3	1200	0.07	0.60	2.00E+00	2.48E+05	1.21E+04
Transport simulant 1	10	2	1200	0.07	0.60	2.00E+00	1.10E+05	1.17E+03
	20	2	1200	0.07	0.60	2.00E+00	1.10E+05	3.10E+03
	30	2	1200	0.07	0.60	2.00E+00	1.10E+05	5.46E+03
	40	2	1200	0.07	0.60	2.00E+00	1.10E+05	8.17E+03
	50	2	1200	0.07	0.60	2.00E+00	1.10E+05	1.12E+04
	60	2	1200	0.07	0.60	2.00E+00	1.10E+05	1.44E+04
	70	2	1200	0.07	0.60	2.00E+00	1.10E+05	1.79E+04
	80	2	1200	0.07	0.60	2.00E+00	1.10E+05	2.16E+04
	90	2	1200	0.07	0.60	2.00E+00	1.10E+05	2.54E+04
	100	2	1200	0.07	0.60	2.00E+00	1.10E+05	2.95E+04
Transport simulant 2	10	3	1600	0.035	0.90	1.00E+01	2.66E+05	6.15E+02
	20	3	1600	0.035	0.90	1.00E+01	2.66E+05	1.32E+03
	30	3	1600	0.035	0.90	1.00E+01	2.66E+05	2.06E+03
	40	3	1600	0.035	0.90	1.00E+01	2.66E+05	2.82E+03
	50	3	1600	0.035	0.90	1.00E+01	2.66E+05	3.61E+03
	60	3	1600	0.035	0.90	1.00E+01	2.66E+05	4.41E+03
	70	3	1600	0.035	0.90	1.00E+01	2.66E+05	5.23E+03
	80	3	1600	0.035	0.90	1.00E+01	2.66E+05	6.05E+03
	90	3	1600	0.035	0.90	1.00E+01	2.66E+05	6.89E+03
	100	3	1600	0.035	0.90	1.00E+01	2.66E+05	7.74E+03
Transport simulant 2	10	2	1600	0.035	0.90	1.00E+01	1.18E+05	1.04E+03
	20	2	1600	0.035	0.90	1.00E+01	1.18E+05	2.23E+03
	30	2	1600	0.035	0.90	1.00E+01	1.18E+05	3.49E+03
	40	2	1600	0.035	0.90	1.00E+01	1.18E+05	4.78E+03
	50	2	1600	0.035	0.90	1.00E+01	1.18E+05	6.11E+03
	60	2	1600	0.035	0.90	1.00E+01	1.18E+05	7.47E+03
	70	2	1600	0.035	0.90	1.00E+01	1.18E+05	8.85E+03
	80	2	1600	0.035	0.90	1.00E+01	1.18E+05	1.03E+04
	90	2	1600	0.035	0.90	1.00E+01	1.18E+05	1.17E+04
	100	2	1600	0.035	0.90	1.00E+01	1.18E+05	1.31E+04

correlations based on the data collected in the symmetrically suspended regime will apply to any yield pseudoplastic slurry flowing in the symmetrically suspended regime.

The volume mean diameter of particles contained in the two simulants will be approximately 50 μm to 60 μm . This range is comparable in size to the largest particles that occur in actual wastes. The volume mean diameter of solids in tank 102-SY is reported by Petersen to be 50 μm to 60 μm . This diameter represents the upper bound of reported particle sizes. It is anticipated that these particles will be completely suspended during transport. However, if settling is observed, this will indicate that there is a potential for settling in the transport lines. If settling is observed, testing to determine the minimum transport velocity, V_{m2} , would be recommended.

4.3 TEST APPROACH

Measurements will be performed to determine the friction factors and loss coefficients in Newtonian and non-Newtonian pipe flows. The independent parameters in the Newtonian tests are the Reynolds number, Re , and the pipe relative roughness, ϵ/D . The Reynolds number will be controlled by using the fluids described in Section 4.2 and by controlling the flow rate. The pipe roughness is a characteristic of the pipe and will be identical for all cases measured in an individual pipe. However, while pipe roughness is an independent parameter, it will be determined by finding the value of ϵ that produces the best fit to the Colebrook equation [Equation (3.25)].

The independent parameters in the non-Newtonian tests are Reynolds number, Hedstrom number, pipe roughness coefficients, and flow behavior indices. These will be controlled by

1. using fluids with properties specified in Section 4.2
2. controlling the volume flow rate of fluid
3. using the 2-in. and 3-in. diameter pipes of known roughness. Testing is planned using a commercial steel pipe with roughness near 0.0030 in. and a corroded steam pipe. The roughness of the steam pipe has been estimated to be between 1/32 in. and 1/16 in.

The friction factor and component loss coefficients are the dependent dimensionless parameters in both the Newtonian and non-Newtonian experiments. These loss coefficients are calculated from the measured pressure drops, which are the dependent dimensional parameters.

The measurements will be performed in a full-scale test facility. Most of the pipes in the transfer lines are standard 3-in. lines; some appear to be corroded. Pipe diameters in the test flow loop will be 2-in. and 3-in., and will include both smooth and rough pipes.

Testing will proceed in the following order.

1. Test to determine the friction factors and component loss coefficients using the Newtonian fluids.
2. Compare the magnitude of the friction factors and component loss coefficients to the values in the Moody diagram and values of component loss coefficients appearing in the literature as each test is performed. If the comparisons show unreasonable values for the friction factors, component loss coefficients, or values of the roughness coefficients halt Newtonian tests and determine sources of error; return to 1.
3. Determine the relative roughness for the corroded and smooth test loop pipe.
4. Develop the first non-Newtonian simulant at bench-scale. Verify that the simulant properties at lab-scale match the target properties before proceeding with testing. Communicate to Westinghouse Hanford discrepancies between the target simulant properties and those obtained as soon as detected. (This step may be conducted concurrently with steps 1 through 3.)
5. Test to determine the friction factor and component loss coefficients using the first simulant.
6. A sample of slurry will be removed from the tank during each test. Its specific gravity will be measured using a hydrometer, and a rheogram will be taken. The specific gravity, yield stress, consistency index, and flow behavior index will be recorded for each test. The values measured will be compared to the target range. If the properties have fallen outside the target range, Westinghouse Hanford will be informed. Attempts will be made to modify the simulant to achieve the simulant properties.

7. Calculate the magnitude of the friction factor and component loss coefficients as each test is performed. Evaluate the percent of full-scale accuracy of the friction factor measurements to determine whether sufficient accuracy is being obtained.
8. Evaluate each test to determine if the flow is fully developed in the horizontal pipe and at the downstream pressure transducer used to measure the component loss coefficient. If the flow is not fully developed, halt testing and inform Westinghouse Hanford of the difficulty. Evaluate the effects of insufficient flow development on the data and discuss possible solutions to the problem with Westinghouse Hanford.
9. Repeat steps 4 through 7 for the second simulant.
10. If possible, the degree of suspension will be monitored through a transparent window during each test. The exact method of monitoring has not yet been selected. Three possible methods have been identified. The first is the use of isokinetic sampling, which would require drawing samples of fluid from the test section. The second is measuring the attenuation of a light beam across different portions of the pipe. The third is qualitative visual observation of bed formation. The first two methods could allow detection of asymmetry; the third could only be useful for detecting a settled bed of solids, which is not expected to occur.

It is expected that symmetric suspension will be achieved during testing. A quantitative method for monitoring the degree of suspension will be investigated. This method will require the presence of at least one transparent window. Because settling during testing would imply that settling would be possible in the transport lines, the detection of settling would be information of critical importance to designers. If a settled bed is detected, Westinghouse Hanford will be informed and testing will be halted and redesign of the experiment to ensure that the critical settling velocity can be detected will be recommended. Testing will be continued at the direction of Westinghouse Hanford.

4.4 DATA ANALYSIS APPROACH

The friction factor in fully developed flow, the component loss coefficients, and Reynolds number will be obtained for each data point obtained in the Newtonian experiments. This may be done by applying Equations (3.23), (3.24), and (3.28). The friction factors and Reynolds numbers will then be used to determine the value of ϵ/D , relative roughness, that best represents

the relationship for the pipe tested. The best value of ϵ/D will be considered to be the value that minimizes the least square of differences between the Colebrook equation and the data collected. Both the value of ϵ/D and the magnitude of the scatter around the Colebrook equation will be reported.

The friction factors and Reynolds numbers will be obtained for each data point obtained in the non-Newtonian experiments. This may be done by applying the definition for both quantities, Equations (3.23) and (3.34). Data will be obtained at four Hedstrom numbers. The relative roughness determined for the single-phase experiments will be used in these experiments.

4.5 PROJECTED RESULTS(a)

The results of the transport experiments will be presented graphically showing the friction factor versus Reynolds number points superimposed on the appropriate predictive chart. For Newtonian fluids, this will be the Moody diagram; for non-Newtonian fluids, this will be the chart showing Hanks' prediction.

A graph showing expected results for the Newtonian experiment is shown in Figure 4.2. The discrete points represent the anticipated data; all results for the single-phase experiments will be presented on one graph because the Moody diagram is expected to represent all data. Different symbols will be used to represent the data in different pipes to indicate any differences that may be caused by pipe roughness. It is expected that all data collected in the "smooth" pipes will collapse on one of the ϵ/D curves on the chart. The data from the two corroded pipes will fall on ϵ/D curves that correspond to significantly higher values of roughness. No deviations of more than 10% from the Moody diagram predictions for a particular value of ϵ/D are expected for the Newtonian cases because of instrumentation accuracy.

The non-Newtonian data will be presented on two separate graphs. This is because figures with $n = 1$ and $n = 0.7$ were available. Each will represent

-
- (a) The anticipated results are included for purely illustrative purposes to show the type of presentation that will appear in the final report. None of the data presented in this section were collected in the laboratory.

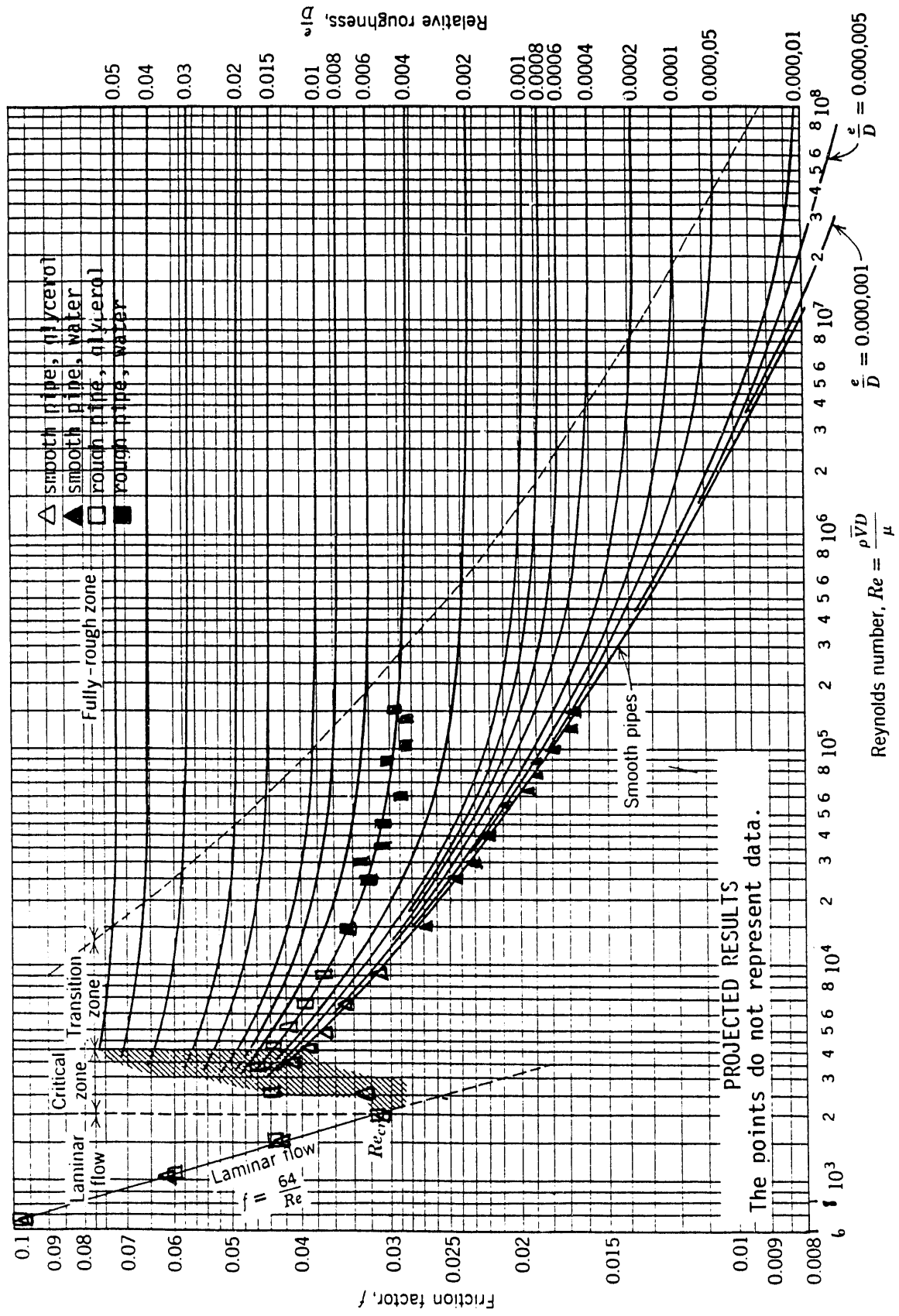


FIGURE 4.2. Predicted Newtonian Experimental Results

one flow behavior index appropriate for our fluids ($n = 0.6$ and $n = 0.9$) because Hanks' theory suggests that predictions for friction factor as a function of Reynolds and Hedstrom numbers depends on the behavior index. Different symbols will be used to represent the data collected in the different pipes because these are expected to have different roughnesses. The form of presentation is shown in Figures 4.3 and 4.4. (Anticipated data is shown superimposed on Hanks' predictive curves for $n = 0.7$ and $n = 1.0$ because curves for $n = 0.6$ and $n = 0.9$, our test cases were not available. Newtonian data is also included on Figure 4.4. In the final report, the data will be compared to Hanks' predictive curves that match the correct measured consistency index, n , for each fluid)

The effect of roughness will be evaluated statistically. Hanks suggests that roughness will not affect the friction factor in the non-Newtonian flows. If so, the data collected at different roughnesses will collapse on one curve. If the data collected at different roughnesses do not collapse on one curve, roughness will have been shown to have an effect. It is not clear whether the effect of roughness will be detectable; the predicted results shown here are an example of typical behavior if roughness does have an effect.

An attempt will be made to bracket the transition to turbulence that occurs in non-Newtonian flows. Turbulence will be detected by examining the data for "breaks" in the correlations predicting the friction factor. It is expected that the friction factor in turbulent flow will exceed the value that would be predicted by extrapolating the laminar results. The Reynolds number at which the flow becomes turbulent will only be detected if it falls in the range of planned experiments.

4.6 LIMITATIONS

It is expected that the results of the experiments performed here will allow prediction of the frictional pressure drop in non-Newtonian flows. However, there are a number of possible limitations to the applicability of correlations developed here. These limitations are described here:

1. The predictions may only be applied to predict pressure drops in slurries that are fully suspended.

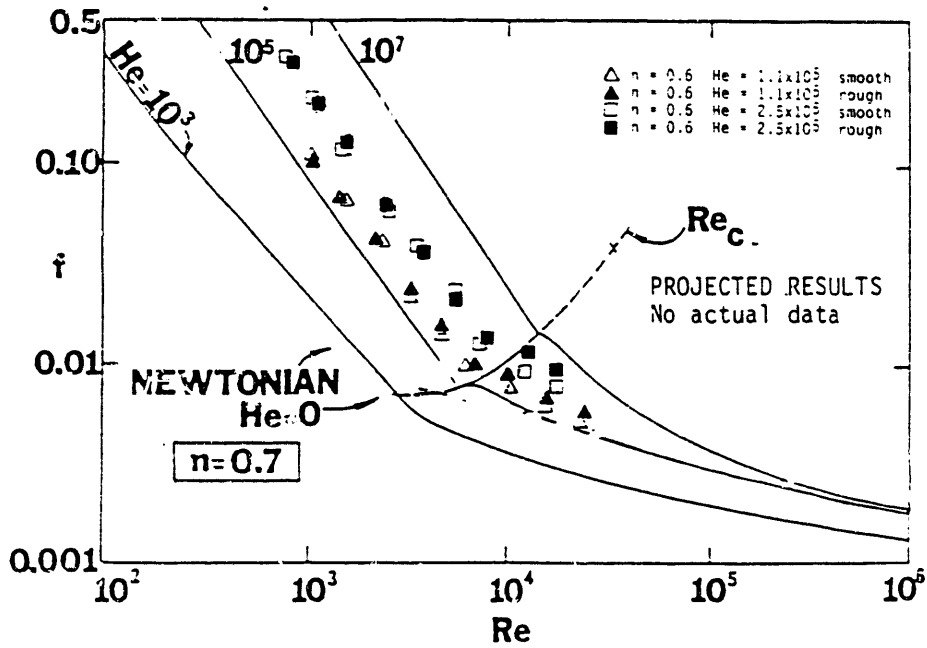


FIGURE 4.3. Predicted Non-Newtonian Experiment Results for $n_{\text{experimental}} = 0.6$ (a)

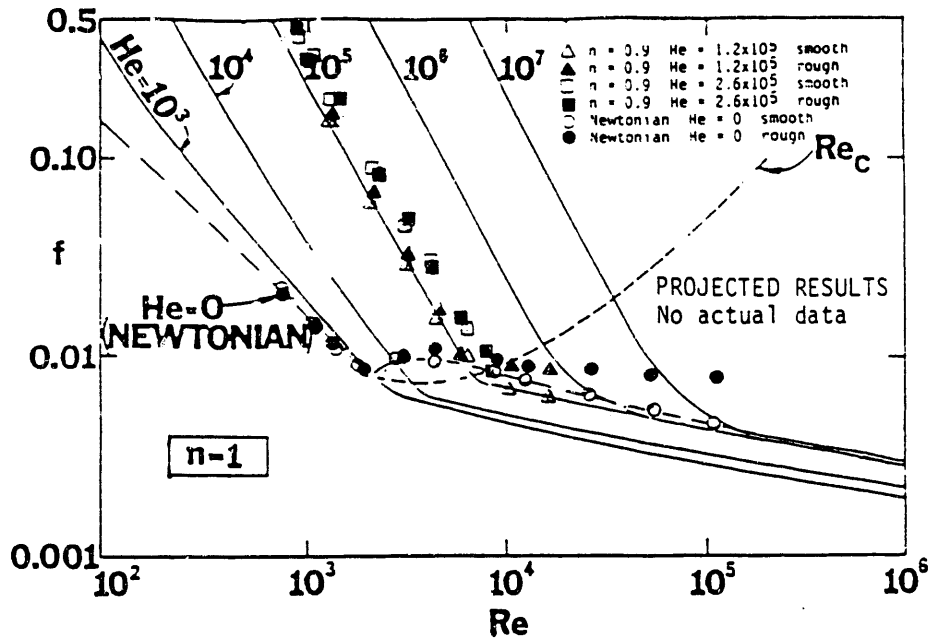


FIGURE 4.4. Predicted Non-Newtonian Experiment Results for $n_{\text{experimental}} = 0.9$ (a)

(a) Projected results. These graphs do not contain actual experimental data.

The size of particles in the double-shell tank slurries are believed to be small; consequently, particles are expected to be fully suspended during transport. It is unlikely that the correlations produced in this study will apply to flows containing large particles that stratify into a bed.

2. If Hanks' model is not validated, the correlation based on the data will be useful for predicting pressure drops for flows with dimensionless numbers in the following ranges:

when $n \approx 0.6$

$$1.1 \times 10^5 < He < 2.5 \times 10^5$$

$$4.8 \times 10^2 < Re < 3.0 \times 10^4$$

and when $n \approx 0.9$

$$1.2 \times 10^5 < He < 2.6 \times 10^5$$

$$6.2 \times 10^2 < Re < 1.3 \times 10^4$$

Newtonian data will be used to extend the correlation to

$$n = 1.0$$

$$He = 0$$

and $1.3 \times 10^3 < Re < 1.6 \times 10^5$

This correlation range of applicability should be sufficient for predicting the pressure drop in a fully suspended flow of a double-shell tank slurry. However, extrapolation outside of the limits tested would require extreme caution.

3. Component loss coefficients reported will apply only to the components and their configurations included in the test plan.

Slight variations in the geometry of components such as expansion loops can affect the loss coefficients.

4. Component loss coefficients in the laminar flow region may not be determined with sufficient accuracy caused by insufficient flow length downstream of the component.

Uncertainty intervals for the loss coefficients will be estimated and reported. Because current plans call for transporting the fluids in the turbulent regime, the lack of resolution for the component loss coefficients in laminar flow is not expected to be of great importance.

The maximum and standard deviation of the difference between the measured friction factors and the friction factors predicted on the basis of Hanks' correlation will be reported. The differences are expected to be relatively small for the smooth pipe data, but may be large for the rough pipe data.

Correlations for the friction factor as a function of the Reynolds number and Hedstrom number will be produced for each pipe. These correlations will be presented on separate graphs without Hanks' predictions superimposed.

5.0 RESUSPENSION AND PLUGGING EXPERIMENTS

In this section details of the resuspension and plugging experiments are provided including experiment objectives, equipment, simulants, test approach and data analysis approach, anticipated results, and experiment limitations.

5.1 OBJECTIVES

Resuspension and plugging experiments will be performed to determine the excess hydraulic pressure required to unplug horizontal and vertical pipes. The vertical case is expected to be more critical. The objectives of these experiments are to:

1. determine the excess pressure, velocity, and time required to resuspend particles that have settled out of a fluid to form a partial plug of granular noncohesive particles in a horizontal pipe
2. determine the excess pressure, velocity, and time required to resuspend particles that have settled out of a fluid to form a complete plug of granular noncohesive particles in a vertical pipe
3. determine the excess pressure, velocity, and time required to resuspend particles that have settled out of a fluid to form a partial plug of cohesive particles in a horizontal pipe
4. determine the excess pressure, velocity, and time required to resuspend particles that have settled out of a fluid to form a complete plug of cohesive particles in a vertical pipe.

5.2 EQUIPMENT AND SIMULANT DESCRIPTION

The equipment in this test must allow the determination of the minimum pressure drop and velocity required to resuspend a plug. In addition, the data produced must be amenable to analysis to allow the information gathered to be used to make recommendations about procedures for unplugging the Hanford cross site transfer lines. Thus, the plug properties and dimensions must be well characterized and the fluid velocity and the pressure drop across the plugs must be accurately measured.

The major components of the system will include the following items:

- One centrifugal pump, which may or may not be the same pump used in the transport experiments.

There are two major requirements in selecting the pump. The first requirement is that the pump must not induce excess pressure fluctuations that might affect the unplugging mechanism. A centrifugal pump will be selected to match the type of pressure fluctuations that would be induced by the centrifugal pump used during actual transport of wastes. The second requirement is that the pump must simultaneously provide the pressure and flow rate required to unplug the line. When the line is plugged, the head loss across the system is expected to vary with flow rate; however, at a given head loss, a lower flow rate will be achieved in the plugged system than in the unplugged system. Typical system curves are shown qualitatively in Figure 5.1. The flow rate and head loss applied to the system to achieve unplugging is marked. In order for this point to be determined, the pump used must allow both flow rate and head loss corresponding to this point to be achieved simultaneously. Pump curve 1 illustrates the choice of a pump that could not provide adequate pressure and flow to unplug the system. Pump curve 2 illustrates a pump that could unplug the system because the flow rate and head loss point lies within the envelope of the pump curve.

The pump used in testing will be selected by estimating the system curve for each type of plug. The system curve will be estimated by determining the pressure versus flow rate curve for a blocked pipe using the friction factor information determined during the transport experiment. Ergun's equation will be used to estimate the pressure/flow curve for vertical plugs. The pump will then be sized conservatively to ensure sufficient capacity.

- Two differential pressure transducers with different full-scale pressure readings.

Because the minimum pressure drop required to resuspend the particles cannot be predicted with any degree of precision, equipment must be available to allow accurate measurement of the pressure drop across the plug over a wide range of pressure drops. Pressure transducers that allow measurement of a differential pressure drop of 0.5 psi will be available from the resuspension portion of the test plan. Measurements by Petersen and Powell in 1988 indicate that the total system pressure during resuspension did not exceed the steady-state pressure by more than a factor of seven. Consequently, it is expected that the differential pressure across 1 m of a partial plug will not exceed 2 psi (14 kPa) during resuspension. A number of differential pressure transducers will be required to determine the pressure drop across a vertical plug. A maximum differential pressure reading of 2 psi (14 kPa) will be required to measure the pressure drop if resuspension is governed by the force required to overcome gravity. A larger differential pressure reading will be required if the adhesive forces holding the plug to the wall are larger than the static head. The approximate differential pressure reading required cannot be determined until the cohesive strength of the simulant is chosen. The most likely value of shear strength of settled

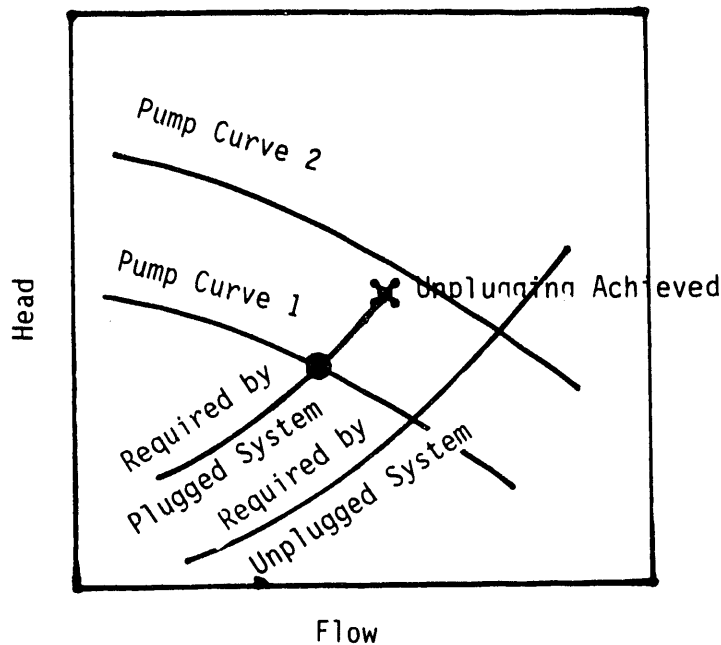


FIGURE 5.1. Pump Selection Example

solids must be investigated before an appropriate value for testing is selected. An additional transducer capable of measuring a differential pressure drop of 2 psi will be obtained to measure the pressure drop across the plug when higher pressure drops are needed to achieve resuspension. Use of two pressure transducers will allow an accuracy of 1.25% to be achieved in the pressure drop measurement provided that the pressure required to unplug falls between 0.1 psi and 2 psi. Other factors affecting the actual accuracy achieved will be discussed shortly.

- A removable horizontal and a removable vertical test section. These sections must be transparent to allow qualitative descriptions of the unplugging process to be obtained.
- Four plug simulant materials

The simulants include two cohesive materials with either a low or a high shear strength and two dilatant materials with different particle diameters. The shear strengths and particle diameters will be selected to allow testing to span the range of material properties that will be transported in the transport lines. Currently, the plans call for volume average particle diameters of 8 μm and 60 μm for the dilatant materials. The smaller size was based on the diameter distributions measured by

Scheele and McCarthy in 1986 for wastes of zirflex decladding material. The larger size was selected based on solids measured by Scheele and Peterson in 1989 from tank 102-SY. The cohesive materials will have shear strengths of 1500 Pa and 4000 Pa; shear strengths of 1500 Pa and 3900 Pa have been measured for slurries from tanks 101-AZ and 102-SY by Scheele and Peterson, respectively. Thus all four simulants are expected to exhibit resuspension behaviors similar to those in the transport lines.

- A flowmeter capable of measuring the fluid flow rate to 2% of the measured value
- A shear vane to measure the shear strength of the cohesive plugs

Determination of the plug shear strength prior to testing is critical to the success of this experiment. If the shear strength is not known with sufficient precision, it will not be possible to interpret the pressure and flow information.

The factor that imposes the greatest limitation on the accuracy with which the minimum pressure drop and velocity required for resuspension may be measured is the measurement procedure. The procedure that will be followed will call for setting either the velocity or the pressure at a predetermined level and observing if the plug is resuspended. If resuspension does not occur, resuspension will be attempted using a higher velocity. Currently, the fluid velocity, or pressure, will be incremented by approximately 4% at each attempt and the velocity at which resuspension is achieved will be reported. This will be a velocity sufficient to achieve resuspension, but may not be the minimum because the minimum resuspension velocity may fall between the previous velocity tested, which is too low to achieve resuspension, and the velocity at which resuspension was achieved. The reported value may exceed the minimum velocity by more than 4% but will not be less than the velocity required. Because the accuracy of the flowmeter is better than the resolution of the procedure, further improvements in the accuracy of the flow measurement are not required. A similar argument may be made for the accuracy of the pressure measurement.

The most critical aspect of the test equipment is the plug properties. Failure to quantify the physical properties (i.e., shear strength, particle size, solids packing fraction) and plug dimensions will result in data that, while accurate, cannot be interpreted. That is, it will be known that the

pressure applied was sufficient to unplug the test section, but because the characteristics of the plug are not known, it will be impossible to state whether plugs in the cross site transport lines would require larger or smaller pressure drops and flow rates to unplug.

5.3 TEST APPROACH

Two types of resuspension experiments are proposed. In the first series of experiments, the requirements for resuspension of vertical and horizontal plugs will be investigated separately using standard plugs. In the second series of experiments, resuspension will be attempted using a naturally settled plug in the pipe loop. It is expected that correlations based on the results of the first experiment can be used to predict the resuspension requirements in the second. Thus, the second test will be used both to provide additional data and to determine whether the information gathered on individual vertical and horizontal plugs can be used to predict the resuspension requirements for pipelines that contain both vertical and horizontal sections.

5.3.1 Resuspension of Standard Plugs

Tests will be performed in a pipe test facility using a 3-in. diameter flow loop containing two transparent removable test sections. A plug of known cohesive strength, particle size, solids packing, and plug dimensions will be allowed to form in one of the removable test sections and the section will be reinserted. The minimum velocity and pressure drop required to resuspend the plug will be measured and reported. Thus, plug shear strength, particle size, solids fraction, and plug dimensions will be the independent parameters, while minimum velocity and pressure drop across the plug will be the dependent parameters.

The manufacture and installation of the vertical plug may require the use of some sort of support screen in the lower portion of the transparent section. This support screen is not expected to affect the resuspension process significantly.

The test steps in the procedure for testing will be similar in both the vertical and horizontal configurations. These steps are described below.

1. Settled particles will be inserted into the transparent removable plug section. In the case of cohesive materials, the plug will be allowed to cure until sufficient cohesive strength has been developed. The cohesive strength of the material will be tested before the plug section is inserted into the test section. Two cohesive plugs will be made for each experiment. One will be used to determine the plug physical properties; the other will be used for actual testing.
2. The plug will be inserted into the test section. The test section will be filled with water on both sides of the plug. This will require bleeding of the test section to allow the removal of air.
3. For horizontal plugs, the fluid flow rate will be set to a predetermined low value. Water will be used during this test to avoid the possibility that the plug could grow at the low flow rates. If the fluid velocity is sufficient to resuspend particles, the pressure is expected to drop as the bed is eroded; if no erosion occurs, the pressure drop is expected to remain constant when water is used for resuspending the plug. The pressure drop across the plug will be measured to determine if any particle resuspension is taking place; erosion will not be considered to be occurring if the pressure drop varies by less than 5% over 10 min.

For vertical plugs, the pressure will be set to a predetermined value, initially there will be no flow. The pressure drop across the plug and flow rate will be monitored for 5 min. If the pressure is sufficient to cause the plug to yield, fluid will begin to flow and eventually the pressure drop across the taps will diminish. If no changes in the pressure drop and no flow rate is detected in 5 min, the pressure will be incremented by 10% of the current value.

4. The bed will be observed visually during the resuspension test. This will provide a second means of determining whether the plug is eroding and will allow qualitative description of the resuspension mode to be obtained.
5. If no erosion occurs at the flow rate being tested, the test will be repeated at increasing fluid flow rates. Because the shear stress at the wall, and the pressure drop across the plug are functions of velocity squared, the velocity will be incremented by a factor of 1.05, which will cause the wall stress and pressure drop to increase by a factor of approximately 1.10. That is, the wall stress and pressure drop will increase by approximately 10% at each increment. This may vary considerably because of difficulties in predicting flow rate ahead of time. The pressure and velocity during testing is expected to vary as shown in Figure 5.2, which would correspond to a test in which unplugging was not achieved at the first two velocities but was achieved at the third.

6. Tests will be repeated until erosion occurs or until the capacity of the pump is exceeded. If the pumping capacity is exceeded, tests will be redesigned using a shorter plug; this will allow similar flow rates to be achieved at lower total system pressure drops.

The hold points in this test are:

1. Unplugging tests will not be conducted unless proper plug properties are achieved. If target properties are not achieved, tests will be delayed to allow further simulant development efforts. If target properties cannot ultimately be achieved, Westinghouse Hanford will be informed. The decision to proceed using alternate properties will be made by Pacific Northwest Laboratory and Westinghouse Hanford.

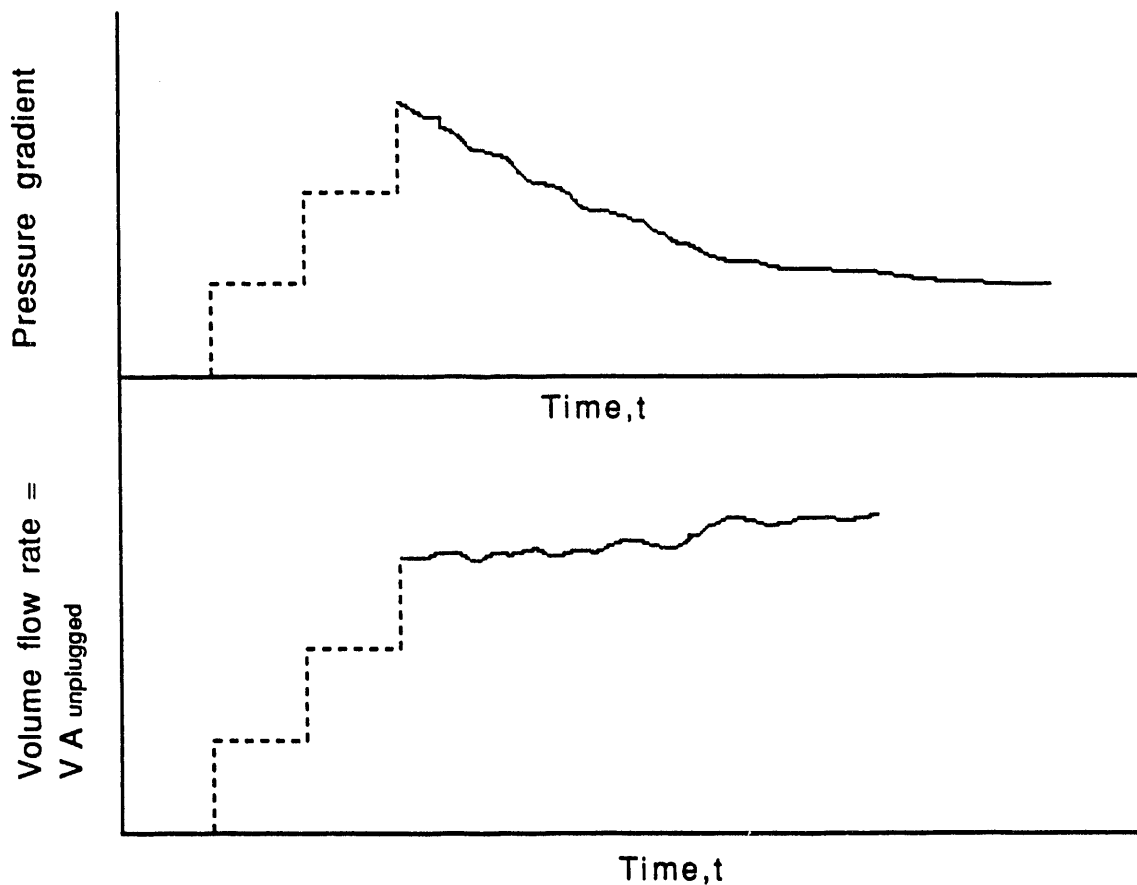


FIGURE 5.2. Anticipated Resuspension Scenario for Plug Resuspension

The use of the removable plug section will allow repeated tests to be performed to determine if results are reproducible. The proposed test cases are given in Table 5.1. The maximum vertical section in the existing transport lines appears to be 2 ft. The maximum possible vertical plug height depends on the settling characteristics of the slurry. Gray, Peterson, Scheele, and Tingey in 1990 report that the volume % of settled solids measured for a 10% solids concentration slurry from tank 101-AZ is 50%. This concentration suggests a maximum plug height of 1 ft or 31 cm. Shorter plugs will form if the material settles more compactly. Because the height and solids packing of the plug is expected to affect the pressure required for resuspension, tests are recommended using two plug heights, 31 cm and 10 cm. Each test will be repeated twice to determine if the results are reproducible.

TABLE 5.1. Proposed Resuspension Test Cases

<u>Test</u>	<u>Simulant</u>	<u>Shear Strength τ_s, Pa</u>	<u>Particle Diameter, μm</u>	<u>Plug Height in Vertical^(a), cm</u>	<u>Plug Length in Horizontal^(b), m</u>
1	Cohesive	1500		30	1
2	Cohesive	4000		30	1
3	Dilatant		8	30	1
4	Dilatant		60	30	1
5	Cohesive	1500		10	0.5
6	Cohesive	4000		10	0.5
7	Dilatant		8	10	0.5
8	Dilatant		60	10	0.5

(a) Entire cross-sectional area will be plugged in vertical plugs.

(b) One-half of the cross-sectional area will be plugged in horizontal plugs.

The proposed procedure has a number of advantages, including the following:

1. The small removable plug section reduces the risk of plugging the entire test section. System plugging would require shutdown of the entire experiment. Because the plug is removable, a wider range of cohesive and dilatant plugs can be evaluated.
2. Measuring the pressure drop across a plug section allows better interpretation of the resuspension data. The unplugging requirements for horizontal and vertical plugs can be evaluated separately in this configuration. This may be important if one type of plug is significantly more difficult to evaluate than another.
3. The removable plug section allows greater control of plug properties. The properties will be determined before filling the entire test section with settled material. In addition, if a number of removable sections are made, a number of plugs may be made simultaneously, and another useful plug will be available as soon as each unplugging test is completed. This will eliminate the need to wait as long as 48 hours between each test.
4. If a specimen is too difficult to unplug, the removal section can be removed instead of routing out the pipe line.

5.3.2 Resuspension of Naturally Settled Plugs

A second set of experiments will be performed to determine whether prediction of resuspension requirements based on data collected using standard plugs are accurate when used to predict resuspension of naturally settled plugs in existing lines. In this experiment a transparent test section containing both vertical and horizontal components will be filled with slurry. The pump will be turned off and slurry will be allowed to settle naturally.

A stepwise description of the test procedure follows:

1. The pump will be used to fill the test section with slurry. The flow rate during this time will be 65 gal/min in order to model the flow rate and fluid stresses during actual transport.
2. The pump will be turned off. A 1-l sample of slurry will be removed from the makeup tank. Both the sample and the slurry in the test loop will be allowed to settle for a predetermined time.
3. The shear strength and volume of settled solids of the 1-l sample will be measured. The height of the settled bed will be measured.

4. The pump will be set to a predetermined pressure or flow rate and resuspension will be attempted. The pressure drop across the plug and total flow rate will be monitored to determine whether resuspension is occurring. If no changes in pressure drop or flow rate occur during 5 min, the pressure drop will be increased 10% until resuspension is achieved. Resuspension will be monitored visually during this time. If possible, resuspension will be recorded on video tape.
5. The volume of settled solids in the 1-l flask will be compared to the volume determined on the basis of the bed height. If they agree within 10%, it will be assumed that the properties of the two samples are identical. If they do not agree, testing will be halted and Westinghouse Hanford will be informed. In this case it will be recommended that a method of measuring the shear strength of the solids in situ be designed. Testing will recommence after a successful method is developed.
6. Data collected in step 4 will be analyzed after each test and the results will be compared to those predicted on the basis of the standard plug experiments.
7. Video tapes of resuspension will be examined to allow identification of the resuspension mechanisms. Any qualitative mechanisms identified will be reported.

5.4 DATA ANALYSIS APPROACH

The pressure drop data obtained will be analyzed according to the general theories discussed in Section 3.4. Because the resuspension requirements are expected to differ depending on pipe orientation and on the properties of the solids, the analysis methods for each test will differ slightly.

In a vertical pipe, the velocity and pressure will be monitored. The velocity required for resuspension will be compared to the settling velocity of the particles in the plug for both cohesive and dilatant materials. The ratio of the bulk velocity required for resuspension to the particle settling velocity, V/V_s , will be reported. The pressure drop required to achieve this velocity will be compared to the value predicted using Ergun's correlation [Equation (3.39)]. If resuspension is by bulk displacement, the recorded velocity will be very near 0 and Ergun's correlation will not be useful in predicting the pressure drop required to resuspend.

The pressure drop required to resuspend will also be compared to the gravitational head of the settled column to determine if resuspension occurred by bulk lifting of the settled solids. If resuspension occurs by this mechanism, the resuspension requirement is expected to be some constant value of the ratio

$$N_b = \frac{dP/H}{C_b(\rho_s - \rho_l)g + 4 \tau_s D} \quad (5.1)$$

where dP = differential pressure applied to plug

H = height of plug

C_b = solids packing fraction

ρ_s = solids density (M/L³)

ρ_l = liquid density (M/L³)

g = acceleration due to gravity

τ_s = shear strength of plug

D = pipe diameter.

In a horizontal pipe, the minimum friction velocity required for resuspension will be compared to the particle settling velocity for both cohesive and dilatant material. That is, the minimum value of the turbulent eddy erosion parameter, $N_{te} = fV^2/V_s^2$, will be examined to determine if resuspension occurs at some constant value of this parameter. The pressure gradient required to achieve resuspension at the minimum velocity will be compared to the value predicted using Shook and Daniel's (1965) model for the pressure drop in the stationary bed mode.

Finally, the shear stress exerted at the wall will be compared to the shear strength of the cohesive solids in a horizontal bed. Thus, results from the four horizontal cohesive plug experiments will be compared on the basis of the erosion parameter, $N_e = f\rho V^2/8\tau_s$. If suspension occurs as a result of yielding of the cohesive material, resuspension will occur at similar values of this parameter in all four tests.

5.5 PROJECTED RESULTS(a)

The theory describing resuspension mechanisms is not as well developed as that predicting the friction factor in transport. As a result, only qualitative predictions may be made about the outcome of these tests. These are:

1. In vertical plugs of dilatant material, resuspension is expected to occur at some constant value of the bulk resuspension parameter

$$N_b = \frac{dP/H}{C_b(\rho_s - \rho_l)g + 4 \tau_s/D} \quad (5.2)$$

However, it may also occur at some constant value of the settling parameter

$$N_s = \frac{V}{V_s} \quad (5.3)$$

provided that the pressure drop required to achieved the resuspension velocity, V , is smaller than the hydrostatic head of the plug.

2. In vertical plugs of a cohesive material, resuspension may possibly occur at some constant value of the settling parameter

$$N_s = \frac{V}{V_s} \quad (5.4)$$

However, it may also occur at some constant value of the gravitational resuspension parameter $dP/C_b(s - 1)gH$, or at some constant value of the yield resuspension parameter

$$N_g = \frac{dP/H}{4 \tau_s/D} \quad (5.5)$$

-
- (a) This planning document is organized as a final report. The results presented are projected results and are shown to illustrate the presentation method in the final report. These results are not based on actual testing.

3. In a horizontal plug of a dilatant material, resuspension is expected to occur at some constant value of the turbulent eddy erosion parameter

$$N_{te} = \frac{f V^2}{8 V_s} \quad (5.6)$$

4. In a horizontal plug of a cohesive material, resuspension is expected to occur at some constant value of the erosion parameter

$$N_e = \frac{f \rho V^2}{8 \tau_s} \quad (5.7)$$

However, it may also occur at some constant value of the turbulent eddy erosion parameter

$$N_{te} = \frac{f V^2}{8 V_s} \quad (5.6)$$

The values of each of the relevant ratios will be calculated and presented in four tables, as shown in Tables 5.2 through 5.5.

5.6 LIMITATIONS

The resuspension experiment has been designed to provide both qualitative and quantitative information describing resuspension. The results are expected to allow the maximum pressure drop and flow rate required to resuspend settled plugs to be determined. However, there will be some limitations to the applicability of the results.

1. Data will be collected in 3-in. diameter pipes, and must be extrapolated cautiously to pipes of other sizes. This is not expected to be a severe limitation to the applicability of the data provided that the correct resuspension mechanisms are identified.
2. There is some risk associated with the resuspension experiments. The qualitative mechanisms governing resuspension are not known. The approach taken in this experiment was to examine a number of resuspension mechanisms and to design testing to allow the correct mechanism to be

TABLE 5.2. Cohesive Vertical Plugs

<u>Case</u>	<u>Plug Height, cm</u>	<u>Yield Strength, Pa</u>	<u>Particle Diameter</u>	<u>$N_s = V/V_s$</u>	<u>$N_g = dP/[C_b(\rho_s - \rho_l)gH]$</u>
1	20	1500	(a)	x	x
2	20	4000		x	x
3	10	1500		x	x
4	10	4000		x	x

TABLE 5.3. Dilatant Vertical Plugs

<u>Case</u>	<u>Plug Height, cm</u>	<u>Particle Diameter, μm</u>	<u>$N_s = V/V_s$</u>	<u>$N_g = dP/[C_b(\rho_s - \rho_l)gH]$</u>
1	20	8	x	x
2	20	60	x	x
3	10	8	x	x
4	10	60	x	x

TABLE 5.4. Cohesive Horizontal Plugs

<u>Case</u>	<u>Plug Length, m</u>	<u>Yield Strength, Pa</u>	<u>Particle Diameter</u>	<u>$N_{te} = fV^2/8 V_s$</u>	<u>$N_e = f\rho V^2/8 \tau_s$</u>
1	1.0	4000	(a)	x	x
2	1.0	4000		x	x
3	0.5	1500		x	x
4	0.5	1500		x	x

TABLE 5.5. Dilatant Horizontal Plugs

<u>Case</u>	<u>Plug Length, m</u>	<u>Plug Diameter, cm</u>	<u>$N_{te} = fV^2/8 V_s^2$</u>
1	1.0	8	x
2	1.0	60	x
3	0.5	8	x
4	0.5	60	x

(a) not yet determined.

identified. If one of the proposed mechanisms is correct, quantitative data will be obtained. If none of the proposed mechanisms are correct, visual monitoring of resuspension is expected to provide information on the correct qualitative resuspension mechanism. In this second case, the qualitative information will provide a basis for future experiments, which would be designed to provide more quantitative information.

3. It is possible that the results produced in the experiment using "standard" plugs will differ from the results produced in the natural settling experiment. In this case, the reasons for the discrepancy will be investigated.

6.0 PLUGGING AND LEAK DETECTION

Methods to detect incipient pipeline plugs and leaks are required by operating personnel to monitor routine waste transfer operations. The information provides real time assessment of operating conditions and allows changes in operation to be made to prevent plugs from developing. In the following sections several methods to detect plugs and leaks are presented and their applicability to waste transfer monitoring is assessed. Also innovative methods for plug removal in addition to line pressurization (presented in Section 5.0) are discussed.

6.1 OBJECTIVES

The objectives of this subtask are to

- identify and prioritize real time instrumentation systems' ability to monitor pipe flow to detect incipient flow blockages and leaks
- recommend each system for potential use or for laboratory evaluation based on the development level of the technology
- recommend alternative methods to line pressurization discussed in Section 5.0 for plug removal.

The scope is limited to analyzing existing and/or proposed technologies and does not involve developing new methods. However, the scope evaluation is not limited to only the methods presented in this strategy plan. Additional methods may be identified during the analysis.

6.2 LEAK AND PLUG DETECTION

Instrumentation to permit immediate detection and location of pipeline leaks and incipient plugs is required to permit successful slurry transfer operations. Several instrumentation methods to monitor and locate leaks have been described; however, no methods to locate incipient plugs have been found. In this analysis noninvasive methods are given preference to invasive methods. Several methods discussed by Liou (1990) are presented.

6.2.1 Evaluation of Methods to Detect Leaks

Mass balance over a time interval is a transient computational method to detect leaks that assumes the mass storage in the pipe stays constant. The flow rates at the inlet and the outlet of the pipe are compared. A leak is suspected when the difference of the in-flow and out-flow volumes exceeds a tolerance.

Flow simulation is a transient computational method to detect leaks driven by real time pressure and flow data. The numerical model assumes the pipeline to be intact. When a leak develops, the calculated and the measured pressure and flow at pipe ends soon diverge, thus indicating a leak. This method can potentially detect a leak while the line fill is changing. Several such leak detection systems have been implemented on major oil and petroleum products pipelines.

One method of locating leaks is to use the fact that the flow rate and the hydraulic gradient are greater upstream of a leak than downstream of a leak. The pressure may be measured at regular intervals along the straight pipe; hydraulic gradient lines may be drawn between each pair of measurements. When a leak occurs, a slope discontinuity in the hydraulic gradient line can be detected graphically, as shown in Figure 6.1. The leak cannot be located at the moment it occurs; it can only be located after the leak has established and the flow has settled into a new steady-state. The location of partial plugs may also be detected using this method. In the case of a partial plug, the hydraulic gradient lines are of identical slope before and after the plug; however, because there is excess pressure loss associated with the plug, the two lines will not meet. Plugs may be detected by extrapolating between measurements and examining for pressure discontinuities. This method is illustrated conceptually in Figure 6.2.

Time of arrival is another method of locating the leak based on the time of arrival of information at the pipe ends or metering stations neighboring the leak. Because the pressure sensors are polled at discrete intervals, the arrival times can be over- or under-estimated by one scan period. This method can be fooled by noise and transients in the system.

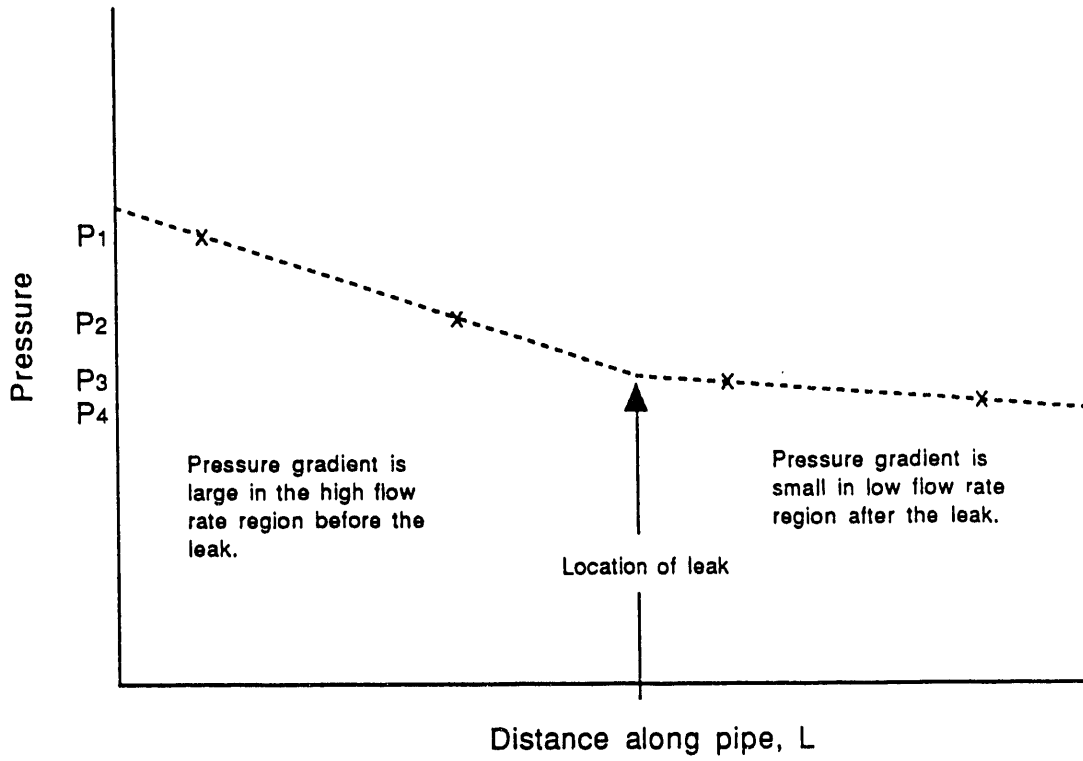


FIGURE 6.1. Method to Locate Leak

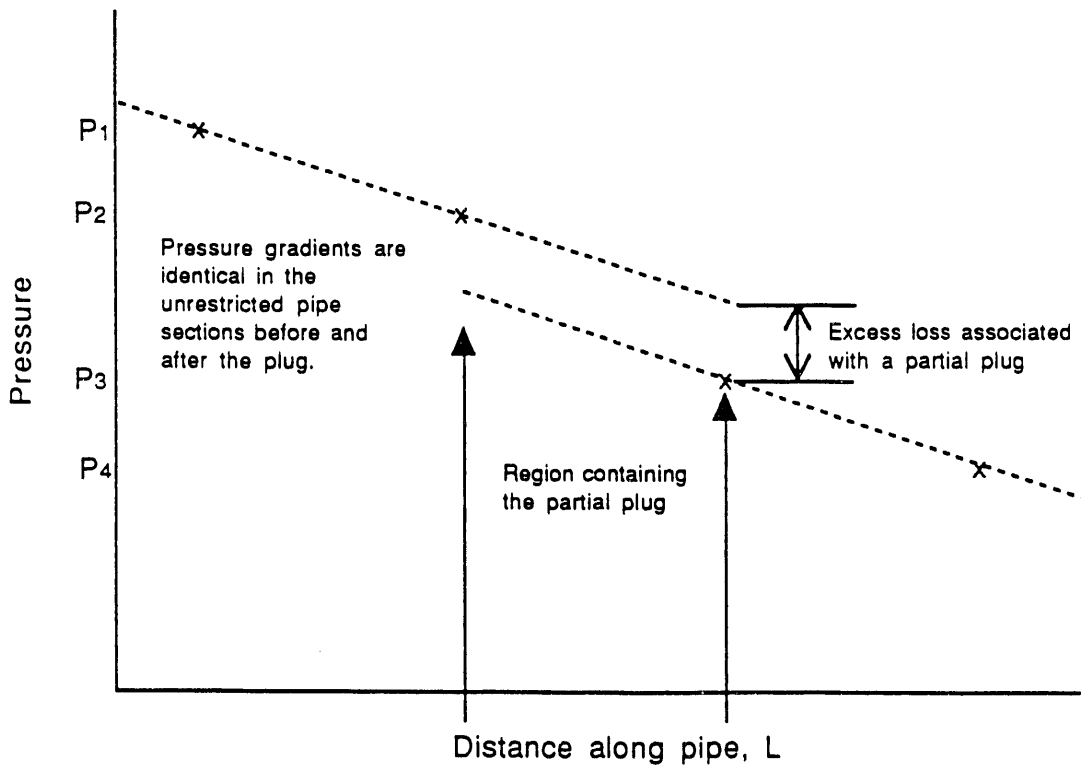


FIGURE 6.2. Method to Locate Plug

Liou (1990) developed a microcomputer based system to monitor pipeline integrity. The system uses a transient flow numerical model, driven by measured head and flow rate at the pipe inlet and outlet. A specific pattern of discrepancy between the measured and the calculated heads at the pipe ends is used to discern the occurrence, magnitude, location, and timing of a leak in real time.

6.2.2 Methods Ranking

In the limited analysis conducted to date Liou's method of leak detection is ranked first because it predicts leak location, magnitude, and timing in near real time. However, the analysis to date is not exhaustive and should be continued.

6.3 UNPLUGGING

To prevent pipeline plugging, cleaning is recommended. One method of pipe cleaning is to insert a plug into the line, termed a "pig". The plug is specially sized to negotiate pipe runs; a flexible polyurethane foam pig can traverse line size "tees" and short radius 90 degree elbows (Landis 1989).

The most convenient method of unplugging pipe blockages is to apply adequate pressure to dislodge the plug. This method will be tested extensively during the resuspension experiments discussed in Section 5.0. However, other methods both intrusive and nonintrusive can be used to remove flow blockages.

6.3.1 Methods Evaluation

Four methods are compared (Eyler, Lombardo and Barnhart 1982) and summarized here for Hanford application: vibration-augmented particle motion, friction-reducing surfactant injection, water jetting or auguring, and pulsed air injection.

Vibration-augmentation is a nonintrusive method that uses externally-applied vibration to shake the pipeline in the vicinity of the plug. The vibration disrupts any interlocking within the plug, freeing the particles to move relative to each other. Eventually a flow path is established over the full length of the plug and the pipeline can be restored to service.

Surfactant injection is an intrusive method in which friction reducing detergents or polymers are injected through a valved penetration near the plug. The reduction in friction allows particles to move more freely relative to one another and to the pipe, allowing liquid flow to eventually create a channel over the plug.

Pulsed air injection is an intrusive method that uses discrete pulses of air traveling through the water-filled pipeline to disrupt the partial plug by wave action.

Water jetting or auguring is an intrusive method that involves inserting a mechanical device into the pipeline to dislodge the plug. The device consists of a stationary water jet head or a rotating auger mounted on the end of a pipe. The device is inserted through a valved penetration near the plug and mines the particulate out of the plug via high-pressure water jetting or mechanical boring.

6.3.2 Methods Ranking and Limitations

For waste transfer applications nonintrusive methods rank above intrusive methods because of the radioactive and chemical hazards associated with the waste. However, intrusive methods are also considered because of the value of the pipeline and its importance to site operation.

Because it is nonintrusive, vibration is given priority over other methods described above. This method needs to be evaluated experimentally to refine application of the technique to slurry transfer to determine the optimal vibration amplitude and frequency, coordinate vibration and fluid flow, and determine proper vibrator position with respect to the plug for greatest effectiveness. In addition, it must be determined whether vibration increases or decreases the pressures required to unplug lines.

Air and surfactant injection are of equal but lessor priority than vibration. Both require valved penetrations for entry into the pipeline. Water jetting or auguring both require hardware insertion into the pipeline. These are the most aggressive methods of plug removal and also produce the most risk.

6.3.3 Recommendations

Nonintrusive methods are preferred to intrusive methods; continue to investigate additional nonintrusive methods for pipeline unplugging.

7.0 REFERENCES

- American Society of Heating Refrigeration and Air Conditioning (ASHRAE). 1989. ASHRAE Handbook of Fundamentals.
- Avallone, E. A., and T. Baumeister III, eds. 1978. Marks' Standard Handbook for Mechanical Engineers. 8th ed., McGraw-Hill Book Company, New York.
- Brandt, H. L., and B. M. Johnson. 1963. "Forces in a Moving Bed of Particulate Solids with Interstitial Fluid Flow." AICHE J. 9(6):771-777.
- Crane Co. 1988. Flow of Fluids through Valves, Fittings, and Pipe. Technical Paper No. 410, Crane Co., King of Prussia, Pennsylvania.
- Durrand, R. 1953. "Basic Relationships of the Transportation of Solids in Pipes - Experimental Research." In Proceedings Minnesota International Hydraulic Convention, September 1-4, Minneapolis, Minnesota.
- Eyler, L. L., N. J. Lombardo, and J. S. Barnhart. 1982. FY 1980 and 1981 Progress Report - Hydrotransport Plugging Study. PNL-3621, Pacific Northwest Laboratory, Richland, Washington.
- Fow, C. L., D. McCarthy, G. T. Thornton, P. A. Scott, and L. A. Bray. 1986. Rheological Evaluation of Simulated Neutralized Current Acid Waste - Transuranics. PNL-5902, Pacific Northwest Laboratory, Richland, Washington.
- Fox, R. W., and A. T. MacDonald. 1973. Introduction to Fluid Mechanics. 2nd ed. John Wiley & Sons, New York.
- Fox, R. W., and A. T. McDonald. 1978. Introduction to Fluid Mechanics. John Wiley and Sons, New York.
- Fromentin, A. 1989. Particle Resuspension from a Multi-Layer Deposit by Turbulent Flow. Paul Scherrer Institut, Wurenlingen und Villigen, Switzerland.
- Govier, G. W. and K. Aziz. 1972. The Flow of Complex Mixtures in Pipes. Robert Kreiger Publishing Co., Malabar, Florida.
- Hanks, K. W., and R. W. Hanks. 1986. "Accurate Pipeflow Pressure Drop Predictions from Bench Scale tests Require Correct Rheological Characterization." Departments of Civil and Chemical Engineering, Brigham Young University, Provo, Utah.
- Hanks, R. W. 1978. "Low Reynolds Number Turbulent Pipeline Flow of Pseudohomogeneous Slurries." In Hydrotransport 5, Fifth International Conference on Hydraulic Transport of Solids in Pipes, pp. C2-23 through C2-34. BHRA Fluid Engineering, Cranfield, Bedford, England.
- Hanks, R. W., and B. L. Ricks. 1975. "Transitional and Turbulent Pipeflow of Pseudoplastic Fluids." J. Hydronautics 9(1):39-48.

Hanks, R. W., and D. R. Pratt. 1967. "On the Flow of Bingham Plastic Slurries in Pipes and Between Parallel Plates." Soc. Pet Eng. J. 7(4):342-346.

Hooper, W. B. 1981. "The Two-K Method Predicts." Chemical Engineering pp. 96-100, August 24, 1981.

Ismail, H. M. 1951. "Turbulent Transfer Mechanisms and Suspended Sediment in Closed Channels." ASCE Transactions, Paper no. 2500, Vol. 117, pp. 409-434. American Society of Civil Engineers, New York.

Ito, H. and K. Imai. 1973. "Energy Losses at 90° Pipe Junctions." J. of the Hydraulic Division, Proceedings of the American Society of Civil Engineers 99(HY9):1353-1368.

Jamison, D. K., and J. R. Villemont. 1971. "Junction Losses in Laminar and Transitional Flows." J. of the Hydraulics Division, Proceedings of the American Society of Civil Engineers 97(HY7):1045-1063, July 1971.

Kittredge, C. P., and D. S. Rowley. 1957. "Resistance Coefficients for Laminar and Turbulent Flow Through One-Half-Inch Valves and Fittings." Presented at the ASME Annual Meeting, November 25-30, 1956, New York, New York. Paper No. 56--A-190, American Society of Mechanical Engineers, New York.

Landis, M. 1989. "Pipeline 'Pigging' - An Important Tail." Pollution Engineering, September, pp. 60-64.

Liou, C. P. 1990. "Pipeline Leak Detection and Location." Proceedings of the International Conference on Pipeline Design and Installation, K. K. Kienow ed, pp. 255-269, American Society of Civil Engineers, New York.

Mills, R. D. 1968. "Numerical Solutions of Viscous Flow through a Pipe Orifice at Low Reynolds Numbers." J. Mechanical Engineering Science 10(2):133-140.

Newitt, D. M., et al. 1955. Trans. Inst. Chem. Engrs. 33:93.

Olson, R. M. 1973. Essentials of Engineering Fluid Mechanics. Intext Educational Publishers, New York.

Perry, R. H., and C. H. Chilton. 1973. Chemical Engineers Handbook. McGraw Hill Book Co., New York.

Shook, C. A., and S. M. Daniel. 1965. Can. J. Chemistry (43)56.

Soo, S. L. 1987. Fundamentals of Multiphase Fluid Mechanics. Preliminary edition, S. L. Soo Associates, Urbana, Illinois.

Spells, K. E. 1955. "Correlations for Use in Transport of Aqueous Suspensions of Fine Solids Through Pipes." Trans Inst. Chem. Engrs 33:79-84.

Thomas, A. D. 1979. "The Role of Laminar/Turbulent Transition in Determining the Critical Deposit Velocity and the Operating Pressure Gradient for Long Distance Slurry Pipelines." In Hydrotransport 6, Sixth International Conference on the Hydraulic Transport of Solids in Pipes, Paper A2. BHRA Fluid Engineering, Cranfield, Bedford, England.

Wallis, G. B. 1969. One-Dimensional Two-Phase Flow. McGraw Hill, New York.

Wasp, E. J., et al. 1971. "Slurry Piping Systems: Trends, Design Methods, Guidelines." Chemical Engineering, p. 74, June 28.

Weissberg, H. L. 1962. "End Correction for Slow Viscous Flow through Long Tubes." The Physics of Fluids 5(9):1033-1036.

Weyl, W. A., and W. C. Ormsby. 1960. "Atomistic Approach to the Rheology of Sand-Water and Clay-Water Mixtures." Chapter 7 in Rheology, Vol. 3, ed. F. R. Eirich, pp. 249-297. Academic Press, New York.

Wicks, M. 1971. "Transport of Solids at Low Concentration in Horizontal Pipes" in Advances in Solid-Liquid Flow in Pipes and its Application, I. Zandi (comp.) Pergamon Press.

Williamson, J. V., and T. J. Rhone. 1973. "Dividing Flow in Branches and Wyes." J of the Hydraulics Division, Proceedings of the American Society of Civil Engineers 99(HY5):747-768.

APPENDIX

SAMPLE CALCULATION

APPENDIX

SAMPLE CALCULATION

This section includes a sample calculation showing the method that will be used to determine each dimensionless quantity measured in the transport experiment. A sample calculation will be shown for one Newtonian and one non-Newtonian case. In addition, the uncertainty in each experimentally determined dimensionless parameter will be determined.

Assume that the following data is collected during an experiment; these values are approximately equal to those that might be expected during an experiment.

- pipe diameter, $D = 3$ in. (0.076 m)
- pipe length, $L = 30$ ft (9.14 m)
- fluid viscosity, $\mu = 1$ cP (0.001 Pa s)
- fluid density, $\rho = 1000$ kg/m³
- pressure drop across the pipe, $dP = 120$ Pa (1.7 psid)
- fluid flow rate, $Q = 20$ gal/min (1.26×10^{-3} m³/s)

The bulk fluid velocity is defined as:

$$v = \frac{Q}{A} \tag{A.1}$$

where A is the pipe cross-sectional area.

For a circular pipe, the bulk fluid velocity is then

$$v = \frac{4Q}{\pi D^2} = \frac{4(1.26 \times 10^{-3} \text{ m}^3/\text{s})}{3.14159 \times (0.076 \text{ m})^2} = 0.277 \text{ m/s} \tag{A.2}$$

The experimentally determined friction factor is then:

$$f_{\text{exp}} = \frac{\frac{dP}{L}}{\frac{1}{2} \rho v^2 D} = \frac{(2)(35 \text{ kg/ms}^2) \left(\frac{0.076 \text{ m}}{9.14 \text{ m}}\right)}{(1000 \text{ kg/m}^3)(0.277 \text{ m/s})^2} = 0.026 \quad (\text{A.3})$$

This may be written in terms of the flow rate as

$$f_{\text{exp}} = \frac{\pi D_d P/L}{2 \rho Q^2} \quad (\text{A.4})$$

The Reynolds number for this case is:

$$\text{Re} = \frac{\rho v D}{\mu} = \frac{(1000 \text{ kg/m}^3)(0.277 \text{ m/s})(0.076 \text{ m})}{0.001 \text{ kg/m/s}} = 2.1 \times 10^4 \quad (\text{A.5})$$

This may be written in terms of the flow rate as

$$\text{Re} = \frac{4 \rho Q}{\pi D \mu} \quad (\text{A.6})$$

Uncertainty in the measurement of five factors can lead to error in the friction factor. These are

1. pipe diameter, D
2. distance between pressure taps, L
3. fluid density, ρ
4. pressure measurement, P
5. flow rate, Q.

The uncertainty in the friction factor measurement may be determined by applying differential error analysis, which results in the relation:

$$\left(\frac{\Delta f}{f}\right)^2 = \left[\left(\frac{\Delta P}{P}\right)^2 + 4\left(\frac{\Delta Q}{Q}\right)^2 + \left(\frac{\Delta \rho}{\rho}\right)^2 + \left(\frac{\Delta L}{L}\right)^2 + \left(\frac{\Delta D}{D}\right)^2\right] \quad (\text{A.7})$$

where ΔP = the uncertainty in P
 ΔQ = the uncertainty in Q
 $\Delta \rho$ = the uncertainty in ρ
 ΔL = the uncertainty in L
 ΔD = the uncertainty in D.

This may be evaluated numerically provided that the uncertainty in each of the five measurements is known. The uncertainty in the diameter and length measurement will be assumed to be 0.1% of the diameter and length measurement. The uncertainty in the determination of the fluid density will be assumed to be 2%; this uncertainty would result primarily from uncertainties in the determination of either the water temperature or from uncertainty in the determination of the fluid specific gravity in the non-Newtonian tests. The uncertainty in the pressure drop measurement depends on the instrument selected for measurement and will be 8.6 Pa (0.125 psid) or 7.21% of full-scale measurement. The uncertainty in the fluid flow rate measurement will be no greater than 2%. This results in an accuracy for the friction factor of:

$$\frac{\Delta f}{f} = \sqrt{(0.0721)^2 + 4(0.02)^2 + (0.02)^2 + 2(0.001)^2} = 8.5\%$$

In this case, the uncertainty in the friction factor is dominated by the uncertainty in the pressure drop measurement. It is interesting to note that the uncertainty that would be obtained by eliminating the uncertainty in the pressure transducer measurement would be:

$$\left(\frac{\Delta f}{f}\right)_{\min} = \sqrt{4(0.02)^2 + 2(0.001)^2 + (0.02)^2} = 4.5\%$$

The previous analysis described the method of determining the accuracy in the actual friction factor based on measured data. A similar procedure may be applied to determine the accuracy expected in a particular experiment. In this experiment, the pressure drop will be measured at some particular flow rate. The magnitude of the pressure drop expected prior to testing for

the test case above may be determined by reading the friction factor off the Moody diagram (Figure 3.8) and evaluating the relationship:

$$\Delta P = f_{\text{Moody}} \left(\frac{L}{D} \right) \left(\frac{1}{2} \rho v^2 \right) \quad (\text{A.8})$$

The friction factor in a smooth pipe at a Reynolds number of 2.1×10^4 is approximately 0.026. Calculations were performed using the friction factor for smooth pipe because this provides the maximum estimate of the possible uncertainty. Greater accuracy as a fraction of the full-scale measurement will be achieved for rough pipe. Consequently, the expected pressure drop is 1.2 Pa. The expected accuracy can then be evaluated in the same manner as the actual accuracy with the only distinction being that the predicted accuracy is based on the predicted pressure drop. (In the example shown, this happens to be numerically equal to the hypothetical "experimental" value.)

The uncertainty in the determination of the measured friction factor using the proposed pressure transducers was calculated for hypothetical flow rates ranging from 10 gal/min to 100 gal/min. It was assumed that in Newtonian flow the friction factors would be well represented using the Moody diagram. The expected accuracy of the measurements, which can be performed in a 54 ft pipe, is provided in the attached spreadsheet (Table A.1). The poorest accuracy is obtained for the case in which water flows through a 3-in pipe at 10 gal/min; in this case, the friction factor could be determined using the proposed equipment to 24.5% accuracy. This is not considered sufficiently accurate. Consequently, experiments will not be performed using water at a flow rate as low as 10 gal/min. Experiments will only be performed if the anticipated accuracy of a single friction factor measurement is better than 10%.

The calculation method for the experimental friction factor and for the accuracy in the determination of the friction factor is identical in both the Newtonian and non-Newtonian cases. However, in this case the non-Newtonian friction factor curves based on Hanks' correlation were used to estimate the expected pressure drop. The accuracy in the determination of the friction

TABLE A.1. Anticipated Accuracy for Newtonian Pipe Flow

Q gpm	Dp (in)	ro kg/m ³	mu Pa's (20C)	Re	Lsmooth (ft)	Ldeveloping (ft)	L(ft) measurement	Ltotal used	dP(Pa)	dP(psi)	Perr (psi)	Perr/dP	d(Re)/Re	dI/I
10	3	1000	0.001	1.1E+4	0.031	10.0	50.0	60	5.94E+1	8.61E-3	1.25E-3	14.52%	3.47%	15.2% Unacceptable
20	3	1000	0.001	2.1E+4	0.026	10.0	40.0	50	1.59E+2	2.31E-2	1.25E-3	5.41%	3.47%	7.0% acceptable
30	3	1000	0.001	3.2E+4	0.023	10.0	40.0	50	3.17E+2	4.60E-2	1.25E-3	2.72%	3.47%	5.2% acceptable
40	3	1000	0.001	4.2E+4	0.022	10.0	40.0	50	5.39E+2	7.82E-2	1.25E-3	1.60%	3.47%	4.8% acceptable
50	3	1000	0.001	5.3E+4	0.021	10.0	40.0	50	8.04E+2	1.17E-1	1.25E-3	1.07%	3.47%	4.6% acceptable
60	3	1000	0.001	6.3E+4	0.020	10.0	40.0	50	1.10E+3	1.60E-1	1.25E-3	0.78%	3.47%	4.5% acceptable
70	3	1000	0.001	7.4E+4	0.019	10.0	40.0	50	1.43E+3	2.07E-1	1.25E-3	0.60%	3.47%	4.5% acceptable
80	3	1000	0.001	8.4E+4	0.019	10.0	40.0	50	1.86E+3	2.70E-1	1.25E-3	0.46%	3.47%	4.5% acceptable
90	3	1000	0.001	9.5E+4	0.018	10.0	40.0	50	2.23E+3	3.24E-1	1.25E-3	0.39%	3.47%	4.5% acceptable
100	3	1000	0.001	1.1E+5	0.018	10.0	40.0	50	2.76E+3	4.00E-1	1.25E-3	0.31%	3.47%	4.5% acceptable
10	2	1000	0.001	1.6E+4	0.031	6.7	40.0	47	3.61E+2	5.23E-2	1.25E-3	2.39%	3.47%	5.1% acceptable
20	2	1000	0.001	3.2E+4	0.026	6.7	40.0	47	1.21E+3	1.75E-1	1.25E-3	0.71%	3.47%	4.5% acceptable
30	2	1000	0.001	4.7E+4	0.023	6.7	40.0	47	2.41E+3	3.49E-1	1.25E-3	0.36%	3.47%	4.5% acceptable
40	2	1000	0.001	6.3E+4	0.022	6.7	30.0	37	3.07E+3	4.45E-1	1.25E-3	0.28%	3.47%	4.5% acceptable
50	2	1000	0.001	7.9E+4	0.021	6.7	15.0	22	2.95E+3	3.32E-1	1.25E-3	0.38%	3.47%	4.5% acceptable
60	2	1000	0.001	9.5E+4	0.020	6.7	15.0	22	3.14E+3	4.56E-1	1.25E-3	0.27%	3.47%	4.5% acceptable
70	2	1000	0.001	1.1E+5	0.019	6.7	9.0	16	2.44E+3	3.53E-1	1.25E-3	0.35%	3.47%	4.5% acceptable
80	2	1000	0.001	1.3E+5	0.019	6.7	9.0	16	3.18E+3	4.62E-1	1.25E-3	0.27%	3.47%	4.5% acceptable
90	2	1000	0.001	1.4E+5	0.018	6.7	6.0	13	2.54E+3	3.69E-1	1.25E-3	0.34%	3.47%	4.5% acceptable
100	2	1000	0.001	1.6E+5	0.018	6.7	6.0	13	3.14E+3	4.56E-1	1.25E-3	0.27%	3.47%	4.5% acceptable
10	3	1181	0.0195	6.4E+2	0.100	9.6	40.0	50	1.81E+2	2.63E-2	1.25E-3	4.76%	3.47%	6.5% acceptable
20	3	1181	0.0195	1.3E+3	0.050	19.2	30.0	49	2.72E+2	3.94E-2	1.25E-3	3.17%	3.47%	5.5% acceptable
30	3	1181	0.0195	1.9E+3	0.033	28.8	20.0	49	2.72E+2	3.94E-2	1.25E-3	3.17%	3.47%	5.5% acceptable
40	3	1181	0.0195	2.6E+3	0.025	10.0	40.0	50	7.25E+2	1.05E-1	1.25E-3	1.19%	3.47%	4.6% acceptable
50	3	1181	0.0195	3.2E+3	0.044	10.0	40.0	50	1.99E+3	2.89E-1	1.25E-3	0.43%	3.47%	4.5% acceptable
60	3	1181	0.0195	3.8E+3	0.039	10.0	40.0	50	2.54E+3	3.68E-1	1.25E-3	0.34%	3.47%	4.5% acceptable
70	3	1181	0.0195	4.5E+3	0.038	10.0	40.0	50	3.37E+3	4.89E-1	1.25E-3	0.26%	3.47%	4.5% acceptable
80	3	1181	0.0195	5.1E+3	0.036	10.0	30.0	40	3.13E+3	4.53E-1	1.25E-3	0.28%	3.47%	4.5% acceptable
90	3	1181	0.0195	5.8E+3	0.035	10.0	20.0	30	2.56E+3	3.72E-1	1.25E-3	0.34%	3.47%	4.5% acceptable
100	3	1181	0.0195	6.4E+3	0.034	10.0	20.0	30	3.08E+3	4.46E-1	1.25E-3	0.28%	3.47%	4.5% acceptable
10	2	1181	0.0195	9.6E+2	0.067	9.6	40.0	50	9.17E+2	1.33E-1	1.25E-3	0.94%	3.47%	4.6% acceptable
20	2	1181	0.0195	1.9E+3	0.033	19.2	30.0	49	1.39E+3	2.00E-1	1.25E-3	0.63%	3.47%	4.5% acceptable
30	2	1181	0.0195	2.9E+3	0.044	6.7	20.0	27	2.72E+3	3.95E-1	1.25E-3	0.32%	3.47%	4.5% acceptable
40	2	1181	0.0195	3.8E+3	0.037	6.7	15.0	22	3.05E+3	4.42E-1	1.25E-3	0.28%	3.47%	4.5% acceptable
50	2	1181	0.0195	4.8E+3	0.037	6.7	9.0	16	2.86E+3	4.15E-1	1.25E-3	0.30%	3.47%	4.5% acceptable
60	2	1181	0.0195	5.8E+3	0.035	6.7	6.0	13	2.60E+3	3.77E-1	1.25E-3	0.33%	3.47%	4.5% acceptable
70	2	1181	0.0195	6.7E+3	0.032	6.7	6.0	13	3.23E+3	4.69E-1	1.25E-3	0.27%	3.47%	4.5% acceptable
80	2	1181	0.0195	7.7E+3	0.031	6.7	3.0	10	2.04E+3	2.97E-1	1.25E-3	0.42%	3.47%	4.5% acceptable
90	2	1181	0.0195	8.6E+3	0.030	6.7	3.0	10	2.50E+3	3.63E-1	1.25E-3	0.34%	3.47%	4.5% acceptable
100	2	1181	0.0195	9.6E+3	0.030	6.7	3.0	10	3.09E+3	4.48E-1	1.25E-3	0.28%	3.47%	4.5% acceptable

factors for flow rates between 10 gal/min and 100 gal/min are shown in Table A.2. (It should be noted that the friction factors could not be read with extreme accuracy from the available Hanks' correlation curves because they were published without grid lines. Obtaining numerically precise values of the friction factor would require actually evaluating Hanks' model. This procedure was described in Section 3. This was not considered necessary because in all cases, sufficient accuracy could be easily obtained.

The anticipated accuracy in the non-Newtonian friction factors, assuming no more than 24 ft are required for flow development and thus that at least 30 ft are available for measurement of the pressure drop, is shown in Table A.2. The actual accuracies achieved will depend on the developing lengths required in non-Newtonian flows. There is currently no method of determining the required length. Here, the maximum uncertainty occurs for the transport fluid with the lower consistency index. The maximum anticipated uncertainty is 3.8%, which is less than the uncertainty expected in the measurements of the Newtonian fluids. Greater uncertainty, expressed as a fraction of the measured friction factor, would occur if the friction factor was smaller than predicted on the basis of Hanks' model. Thus, for example, if the actual friction factor in pseudoplastic flow is half that predicted by Hanks, it is expected that measurement of the friction factor will be within 7.6% of the actual value.

Determination of the uncertainty in measuring the component loss coefficients is more complicated than that of the friction factors. This is because the loss coefficient accounts for only the excess portion of the measured pressure drop. The procedure for estimating the uncertainty in the measured loss coefficients is described below.

Proposed test conditions:

- pipe diameter, $D = 3$ in. (0.0762 m)
- distance between taps, $L = 10$ ft
- volume flow rate, $Q = 30$ gal/min (1.9×10^{-3} m³)
- fluid density, $\rho = 10^3$ kg/m³
- fluid viscosity, $\mu = 10^3$ Pa s

TABLE A.2. Anticipated Accuracy in Non-Newtonian Flow

Q	Dp	ro	K	Pa's ⁿ	Tauy/He	Pa	Rec	Hanks	fHanks	L(ft)	measurement	dP	dP	Perr	Perr/dP	dt/t
gpm	In	kg/m ³	Pa ⁿ	(20C)	Pa		Hanks				(Pa)	(psi)	(psi)	(psi)		
10	3	1200	0.07	.60	2	2.5E+5	4.8E+2	8.0E+3	0.400	30	5.5E+2	8.0E-2	1.3E-3	1.6%	5.1%	acceptable
20	3	1200	0.07	.60	2	2.5E+5	1.3E+3	8.0E+3	0.150	30	8.3E+2	1.2E-1	1.3E-3	1.0%	5.0%	acceptable
30	3	1200	0.07	.60	2	2.5E+5	2.2E+3	8.0E+3	0.100	30	1.2E+3	1.8E-1	1.3E-3	0.7%	4.9%	acceptable
40	3	1200	0.07	.60	2	2.5E+5	3.3E+3	8.0E+3	0.080	30	1.8E+3	2.6E-1	1.3E-3	0.5%	4.9%	acceptable
50	3	1200	0.07	.60	2	2.5E+5	4.6E+3	8.0E+3	0.060	30	2.1E+3	3.0E-1	1.3E-3	0.4%	4.9%	unacceptable
60	3	1200	0.07	.60	2	2.5E+5	5.9E+3	8.0E+3	0.050	30	2.5E+3	3.6E-1	1.3E-3	0.3%	4.9%	unacceptable
70	3	1200	0.07	.60	2	2.5E+5	7.3E+3	8.0E+3	0.040	30	2.7E+3	3.9E-1	1.3E-3	0.3%	4.9%	unacceptable
80	3	1200	0.07	.60	2	2.5E+5	8.8E+3	8.0E+3	0.030	30	2.6E+3	3.8E-1	1.3E-3	0.3%	4.9%	acceptable
90	3	1200	0.07	.60	2	2.5E+5	1.0E+4	8.0E+3	0.020	30	2.2E+3	3.2E-1	1.3E-3	0.4%	4.9%	acceptable
100	3	1200	0.07	.60	2	2.5E+5	1.2E+4	8.0E+3	0.010	30	1.4E+3	2.0E-1	1.3E-3	0.6%	4.9%	acceptable
10	2	1200	0.07	.60	2	1.1E+5	1.2E+3	8.0E+3	0.150	30	1.6E+3	2.3E-1	1.3E-3	0.5%	4.9%	acceptable
20	2	1200	0.07	.60	2	1.1E+5	3.1E+3	8.0E+3	0.100	30	4.2E+3	6.1E-1	1.3E-3	0.2%	4.9%	acceptable
30	2	1200	0.07	.60	2	1.1E+5	5.5E+3	8.0E+3	0.020	30	1.9E+3	2.7E-1	1.3E-3	0.5%	4.9%	acceptable
40	2	1200	0.07	.60	2	1.1E+5	8.2E+3	8.0E+3	0.020	30	3.4E+3	4.9E-1	1.3E-3	0.3%	4.9%	acceptable
50	2	1200	0.07	.60	2	1.1E+5	1.1E+4	8.0E+3	0.015	15	2.0E+3	2.8E-1	1.3E-3	0.4%	4.9%	acceptable
60	2	1200	0.07	.60	2	1.1E+5	1.4E+4	8.0E+3	0.015	15	2.8E+3	4.1E-1	1.3E-3	0.3%	4.9%	acceptable
70	2	1200	0.07	.60	2	1.1E+5	1.8E+4	8.0E+3	0.012	15	3.1E+3	4.5E-1	1.3E-3	0.3%	4.9%	acceptable
80	2	1200	0.07	.60	2	1.1E+5	2.2E+4	8.0E+3	0.009	15	3.0E+3	4.4E-1	1.3E-3	0.3%	4.9%	acceptable
90	2	1200	0.07	.60	2	1.1E+5	2.5E+4	8.0E+3	0.009	12	3.1E+3	4.4E-1	1.3E-3	0.3%	4.9%	acceptable
100	2	1200	0.07	.60	2	1.1E+5	2.9E+4	8.0E+3	0.008	12	3.4E+3	4.9E-1	1.3E-3	0.3%	4.9%	acceptable
10	3	1600	0.035	.90	10	2.7E+5	6.1E+2	8.0E+3	0.600	30	1.1E+3	1.6E-1	1.3E-3	0.8%	5.0%	acceptable
20	3	1600	0.035	.90	10	2.7E+5	1.3E+3	8.0E+3	0.200	30	1.5E+3	2.1E-1	1.3E-3	0.6%	4.9%	acceptable
30	3	1600	0.035	.90	10	2.7E+5	2.1E+3	8.0E+3	0.090	30	1.5E+3	2.2E-1	1.3E-3	0.6%	4.9%	acceptable
40	3	1600	0.035	.90	10	2.7E+5	2.8E+3	8.0E+3	0.052	30	1.5E+3	2.2E-1	1.3E-3	0.6%	4.9%	acceptable
50	3	1600	0.035	.90	10	2.7E+5	3.6E+3	8.0E+3	0.034	30	1.6E+3	2.3E-1	1.3E-3	0.6%	4.9%	acceptable
60	3	1600	0.035	.90	10	2.7E+5	4.4E+3	8.0E+3	0.024	30	1.6E+3	2.3E-1	1.3E-3	0.5%	4.9%	unacceptable
70	3	1600	0.035	.90	10	2.7E+5	5.2E+3	8.0E+3	0.017	30	1.5E+3	2.2E-1	1.3E-3	0.6%	4.9%	unacceptable
80	3	1600	0.035	.90	10	2.7E+5	6.1E+3	8.0E+3	0.013	30	1.5E+3	2.2E-1	1.3E-3	0.6%	4.9%	unacceptable
90	3	1600	0.035	.90	10	2.7E+5	6.9E+3	8.0E+3	0.011	30	1.6E+3	2.4E-1	1.3E-3	0.5%	4.9%	unacceptable
100	3	1600	0.035	.90	10	2.7E+5	7.7E+3	8.0E+3	0.009	30	1.7E+3	2.4E-1	1.3E-3	0.5%	4.9%	unacceptable
10	2	1600	0.035	.90	10	1.2E+5	1.0E+3	8.0E+3	0.250	20	2.3E+3	3.4E-1	1.3E-3	0.4%	4.9%	acceptable
20	2	1600	0.035	.90	10	1.2E+5	2.2E+3	8.0E+3	0.070	20	2.6E+3	3.8E-1	1.3E-3	0.3%	4.9%	acceptable
30	2	1600	0.035	.90	10	1.2E+5	3.5E+3	8.0E+3	0.032	20	2.7E+3	3.9E-1	1.3E-3	0.3%	4.9%	acceptable
40	2	1600	0.035	.90	10	1.2E+5	4.8E+3	8.0E+3	0.023	20	3.4E+3	5.0E-1	1.3E-3	0.3%	4.9%	acceptable
50	2	1600	0.035	.90	10	1.2E+5	6.1E+3	8.0E+3	0.012	15	2.1E+3	3.0E-1	1.3E-3	0.4%	4.9%	unacceptable
60	2	1600	0.035	.90	10	1.2E+5	7.5E+3	8.0E+3	0.009	15	2.3E+3	3.3E-1	1.3E-3	0.4%	4.9%	unacceptable
70	2	1600	0.035	.90	10	1.2E+5	8.9E+3	8.0E+3	0.008	15	2.7E+3	4.0E-1	1.3E-3	0.3%	4.9%	acceptable
80	2	1600	0.035	.90	10	1.2E+5	1.0E+4	8.0E+3	0.007	15	3.1E+3	4.5E-1	1.3E-3	0.3%	4.9%	acceptable
90	2	1600	0.035	.90	10	1.2E+5	1.2E+4	8.0E+3	0.006	15	3.4E+3	4.9E-1	1.3E-3	0.3%	4.9%	acceptable
100	2	1600	0.035	.90	10	1.2E+5	1.3E+4	8.0E+3	0.005	12	2.8E+3	4.0E-1	1.3E-3	0.3%	4.9%	acceptable

- fluid velocity, $V = 0.41$ m/s
- Reynolds number, $Re = 3.2 \times 10^4$
- expected loss coefficients, $K = 0.9$

The excess pressure drop caused by the elbow may be found using

$$\Delta P_{\text{excess}} = K \frac{1}{2} \rho V^2 = \left(\frac{0.9}{2}\right) \left(10^3 \text{ kg/m}^3\right) \left(0.41 \text{ m/s}\right)^2 = 7.76 \times 10^1 \text{ Pa} \quad (\text{A.9})$$

$$= 1.12 \times 10^{-2} \text{ psi}$$

The total pressure drop expected across 10 ft of pipe in fully-developed flow is

$$f = 0.023 \text{ at } Re = 3.16 \times 10^4$$

$$\Delta P_L = \left(\frac{1}{2} \rho V^2\right) \left(f \frac{L}{D}\right) = \left(\frac{1}{2}\right) \left(10^3 \text{ kg/m}^3\right) \left(0.41 \text{ m/s}\right)^2 \left(0.023\right) \left[\frac{10 \text{ ft}}{(3\text{-in.}) \left(\frac{1 \text{ ft}}{12 \text{ in.}}\right)}\right]$$

$$= 7.93 \times 10^1 \text{ Pa} \quad (1.15 \times 10^{-2} \text{ psi})$$

Thus, the total pressure drop between taps is expected to be

$$\Delta P_L + \Delta P_{\text{excess}} = 2.27 \times 10^{-2} \text{ psi}$$

The pressure transducer selected must be able to measure a differential pressure of 2.27×10^{-2} psi. In this case a transducer with a full-scale reading of 0.5 psi would be adequate. The resolution of the proposed pressure transducer is 1.25×10^{-3} psi. The accuracy for the measurement of the excess pressure drop is

$$\frac{\Delta P_{\text{err}}}{\Delta P_{\text{excess}}} = \frac{1.25 \times 10^{-3}}{1.12 \times 10^{-2}} = 11.1\% \quad (\text{A.10})$$

The accuracy in the measurement of the component loss coefficients is

$$\begin{aligned} \left(\frac{\Delta K}{K}\right)^2 &= \left(\frac{\Delta P}{P}\right)^2 + 4\left(\frac{\Delta V}{V}\right)^2 + \left(\frac{\Delta \rho}{\rho}\right)^2 \\ &= (0.111)^2 + 4(0.02)^2 + (0.02)^2 \end{aligned} \tag{A.11}$$

$$\frac{\Delta K}{K} = 12\%$$

Because measurement of component loss coefficients is inherently less accurate than the measurement of friction factors, an accuracy of 15% was deemed acceptable for the purposes of characterizing the loss coefficients. The cases in which acceptable accuracy may be anticipated for the loss coefficient are noted in Table A.3. In general, better accuracy is anticipated for components such as ball valves, which have large loss coefficients. Less accuracy is expected for components with very low loss coefficients. However, because the losses associated with such components are often low, it is not important to be able to predict the loss with a high degree of accuracy.

It should be noted that the estimated uncertainty in the component loss coefficients assumes that flow has reached the fully developed state at the downstream pressure tap. It is expected that this will have occurred. However, there is currently no way to estimate the developing length in non-Newtonian flows and the developing length may exceed that measured in Newtonian flows.

TABLE A.3. Anticipated Accuracy for the Measurement of Loss Coefficients for Elbows

Q	Dp	ρ	μ	Re	K	f _{smooth}	L(1)	d _{excess}	d _{pipe}	dP _{tot}	P _f	P _{err}	P _{err/dP}	dK/K
gpm	(in)	kg/m ³	Pa·s		elbow		(ft)	(Pa)	(Pa)	(psi)	psi	(psi)		
10	3	1000	.001	1.05E+4	0.9	0.031	10	8.62E+0	1.19E+1	2.97E-3	0.5	.00125	100.0%	unacceptable
20	3	1000	.001	2.11E+4	0.9	0.026	10	3.45E+1	3.98E+1	1.08E-2	0.5	.00125	25.0%	unacceptable
30	3	1000	.001	3.16E+4	0.9	0.023	10	7.76E+1	7.93E+1	2.27E-2	0.5	.00125	11.1%	acceptable
40	3	1000	.001	4.22E+4	0.9	0.022	10	1.38E+2	1.35E+2	3.95E-2	0.5	.00125	6.3%	acceptable
50	3	1000	.001	5.27E+4	0.9	0.021	10	2.15E+2	2.01E+2	6.04E-2	0.5	.00125	4.0%	acceptable
60	3	1000	.001	6.33E+4	0.9	0.020	10	3.10E+2	2.76E+2	8.50E-2	0.5	.00125	2.8%	acceptable
70	3	1000	.001	7.38E+4	0.9	0.019	10	4.22E+2	3.57E+2	1.13E-1	0.5	.00125	2.0%	acceptable
80	3	1000	.001	8.44E+4	0.9	0.019	10	5.51E+2	4.66E+2	1.48E-1	0.5	.00125	1.6%	acceptable
90	3	1000	.001	9.49E+4	0.9	0.018	10	6.98E+2	5.88E+2	1.82E-1	0.5	.00125	1.2%	acceptable
100	3	1000	.001	1.05E+5	0.9	0.018	10	8.62E+2	6.89E+2	2.25E-1	0.5	.00125	1.0%	acceptable
10	2	1000	.001	1.58E+4	0.9	0.031	6.7	4.36E+1	6.01E+1	1.50E-2	0.5	.00125	19.8%	unacceptable
20	2	1000	.001	3.16E+4	0.9	0.026	6.7	1.74E+2	2.02E+2	5.46E-2	0.5	.00125	4.9%	acceptable
30	2	1000	.001	4.75E+4	0.9	0.023	6.7	3.93E+2	4.01E+2	1.15E-1	0.5	.00125	2.2%	acceptable
40	2	1000	.001	6.33E+4	0.9	0.022	6.7	6.98E+2	6.82E+2	2.00E-1	0.5	.00125	1.2%	acceptable
50	2	1000	.001	7.91E+4	0.9	0.021	6.7	1.09E+3	1.02E+3	3.06E-1	0.5	.00125	0.8%	acceptable
60	2	1000	.001	9.49E+4	0.9	0.020	6.7	1.57E+3	1.40E+3	4.30E-1	0.5	.00125	0.5%	acceptable
70	2	1000	.001	1.11E+5	0.9	0.019	6.7	2.14E+3	1.81E+3	5.72E-1	1	.00250	0.8%	acceptable
80	2	1000	.001	1.27E+5	0.9	0.019	6.7	2.79E+3	2.36E+3	7.47E-1	1	.00250	0.6%	acceptable
90	2	1000	.001	1.42E+5	0.9	0.018	6.7	3.53E+3	2.83E+3	9.22E-1	1	.00250	0.5%	acceptable
100	2	1000	.001	1.58E+5	0.9	0.018	6.7	4.36E+3	3.49E+3	1.14E+0	2	.00500	0.8%	acceptable
10	3	1264	.018	7.40E+2	0.9	0.100	10	1.09E+1	4.85E+1	8.61E-3	0.5	.00125	79.1%	unacceptable
20	3	1264	.018	1.48E+3	0.9	0.050	10	4.36E+1	9.70E+1	2.04E-2	0.5	.00125	19.8%	unacceptable
30	3	1264	.018	2.22E+3	0.9	0.033	10	9.80E+1	1.45E+2	3.53E-2	0.5	.00125	8.8%	acceptable
40	3	1264	.018	2.96E+3	0.9	0.025	10	1.74E+2	1.94E+2	5.34E-2	1	.00250	9.9%	acceptable
50	3	1264	.018	3.70E+3	0.9	0.044	10	2.72E+2	5.32E+2	1.17E-1	2	.00500	12.7%	acceptable
60	3	1264	.018	4.44E+3	0.9	0.039	10	3.92E+2	6.80E+2	1.55E-1	2	.00500	8.8%	acceptable
70	3	1264	.018	5.18E+3	0.9	0.038	10	5.34E+2	9.01E+2	2.08E-1	5	.01250	16.1%	unacceptable
80	3	1264	.018	5.92E+3	0.9	0.036	10	6.97E+2	1.12E+3	2.63E-1	5	.01250	12.4%	acceptable
90	3	1264	.018	6.66E+3	0.9	0.035	10	8.82E+2	1.37E+3	3.27E-1	5	.01250	9.8%	acceptable
100	3	1264	.018	7.40E+3	0.9	0.034	10	1.09E+3	1.65E+3	3.97E-1	5	.01250	7.9%	acceptable
10	2	1264	.018	1.11E+3	0.9	0.067	6.7	5.51E+1	1.64E+2	3.17E-2	0.5	.00125	15.6%	unacceptable
20	2	1264	.018	2.22E+3	0.9	0.033	6.7	2.21E+2	3.27E+2	7.95E-2	0.5	.00125	3.9%	acceptable
30	2	1264	.018	3.33E+3	0.9	0.044	6.7	4.96E+2	9.70E+2	2.13E-1	0.5	.00125	1.7%	acceptable
40	2	1264	.018	4.44E+3	0.9	0.037	6.7	8.82E+2	1.45E+3	3.38E-1	0.5	.00125	1.0%	acceptable
50	2	1264	.018	5.55E+3	0.9	0.037	6.7	1.38E+3	2.27E+3	5.29E-1	1	.00250	1.3%	acceptable
60	2	1264	.018	6.66E+3	0.9	0.035	6.7	1.99E+3	3.09E+3	7.36E-1	1	.00250	0.9%	acceptable
70	2	1264	.018	7.77E+3	0.9	0.032	6.7	2.70E+3	3.84E+3	9.49E-1	1	.00250	0.6%	acceptable
80	2	1264	.018	8.89E+3	0.9	0.031	6.7	3.53E+3	4.86E+3	1.22E+0	2	.00500	1.0%	acceptable
90	2	1264	.018	1.00E+4	0.9	0.030	6.7	4.47E+3	5.96E+3	1.51E+0	2	.00500	0.8%	acceptable
100	2	1264	.018	1.11E+4	0.9	0.030	6.7	5.51E+3	7.35E+3	1.87E+0	2	.00500	0.6%	acceptable

DISTRIBUTION

<u>No. of Copies</u>		<u>No. of Copies</u>	
12	DOE/Office of Scientific and Technical Information	28	<u>Pacific Northwest Laboratory</u>
			J. A. Bamberger, K7-15 (10)
			J. M. Bates, K7-15
			I. G. Choi, K7-15
			L. L. Eyler, K7-15
			J. R. Gaskill, P7-19
			L. M. Liljegren, K7-15
			N. J. Lombardo, K7-02
			R. L. McKay, P7-19
			E. W. Pearson, K7-15
			J. R. Phillips, K7-15
			M. R. Powell, P7-19
			P. A. Scott, P7-19
			G. Terrones, K7-15
			Publishing Coordination
			Technical Report Files (5)
	<u>ONSITE</u>		
4	<u>DOE Richland Operations Office</u>		
	J. J. Davis, A5-16		
	W. R. Wrzesinski, A5-16		
	R. E. Gerton, A4-02		
	G. W. Rosenwald, A4-02		
10	<u>Westinghouse Hanford Company</u>		
	T. M. Burke, S4-58		
	D. T. Heimberger, R2-07		
	W. C. Miller, S4-55		
	E. J. Shen, S4-58		
	L. C. Stegen, S4-58		
	E. D. Waters, S4-58		
	Document Clearance Adm. (2)		
	Project WE14 Files (2)		

**DATE
FILMED**

8 / 26 / 93

END

